THE UNIVERSITY *of* EDINBURGH

Co-factors of LIM-HD transcription factors in neural development and axon pathfinding in zebrafish

Zhen Zhong

PhD Thesis

Submitted in accordance with the regulations for the degree of PhD

University of Edinburgh

May 2011

Abstract

The zebrafish neuromuscular system is an elegant model to study neural development.

To reveal a specific programme for zebrafish motor axon pathfinding I established a method to selectively block motor axon pathfinding by interfering with LIM domain transcription factor signaling. LIM homeodomain proteins (LIM-HDs) are an important class of transcriptional regulators and involved in neural development as well as neuron fate decision in vertebrates. DD domain dimerization of CLIM (cofactor of LIM-HDs) can activate LIM-HDs and downstream gene transcription while over-expression of dominant-negative CLIM (DN-CLIM), which lacks the DD domain, blocks LIM-HD activity. Motor neurons fluoresce in HB9:GFP transgenic zebrafish as the promoter of the motor neuron specific gene *Hb9* drives expression of GFP. Motor axons in DN-CLIM injected HB9:GFP zebrafish are unable to exit the spinal cord, instead they grow inside the spinal cord. Thus axon pathfinding, but not general growth appears to be impaired in these neurons. This provides an excellent research model to find genes involved in motor axon pathfinding downstream of LIM-HDs. Gene array expression profiling was carried out on GFP^+ motor neurons by fluorescence-activated flow sorting (FACS) with and without prior injection of DN-CLIM mRNA to elucidate the potential genes relevant to motor axon pathfinding. Genes that were most strongly down-regulated in DN-CLIM injected embryos were considered to belong to a motor axon specific guidance programme. *Calca*, *tac-1* and *chodl* genes, retrieved from the gene array data, showed specific expression pattern in motor neuron and obvious down-regulation after DN-CLIM injection by in situ hybridization. This validated the array results. Chodl contains a C-type lectin domain representing a potential cell surface receptor for guidance factors. Gene knock-down experiments with two independent morpholinos led to stalling of CaP motor axons at the horizontal myoseptum, a pivotal choice point for axon pathfinding. This suggests that this novel gene specifically affects motor axon pathfinding in zebrafish.

Single stranded DNA binding protein 1 (SSDP1) functions as an activator of SSDP1/CLIM/LIM-HD complex which involved in the transcriptional control of embryonic development. To verify how SSDP1 function in neural development in zebrafish, I have cloned Zebrafish SSDP1a and SSDP1b, which are most closely related to mouse and human SSDP1. SSDP1a is widely expressed during zebrafish development while SSDP1b is specifically expressed in sensory trigeminal and Rohon-Beard neurons. Over-expression of the N-terminal portion of SSDP1 (N-SSDP1) increases endogenous CLIM protein levels in vivo and impairs the formation of eyes and midbrain-hindbrain boundary. In addition, SSDP1b knock down impairs trigeminal and Rohon-Beard sensory axon growth. N-SSDP1 can partially rescue the inhibition of axon growth induced by DN-CLIM. These results reveal specific functions of SSDP1 in neural patterning and sensory axon growth which are in part due to the stabilization of LIM-HD/CLIM complexes.

In summary, co-factors of LIM-HDs play important roles in neural development, cell fate specification as well as axon pathfinding.

List of abbreviations

AChR	acetylcholine receptor
ALS	amyotrophic lateral sclerosis
AP	Apterous
BCIP/NBT	5-bromo-4-chloro-3-indolyl phosphate/nitro blue tetrazolium
bLHL	basic helix-loop-helix
BTX	bungarotoxin
Calca	calcitonin/calcitonin-related polypeptide, alpha
CaP	caudal primary motor neuron
CGRP	calcitonin-related polypeptide, alpha
ChAT	choline acetyltransferase
Chodl	chondrolectin
CLIM	co-factor of LIM-HD
Col	Collagen
CNS	central nervous system
CoPA	commissural primary ascending interneuron
C-SSDP	C-terminus of SSDP
DAB	diaminobenzidine
DD	dimerization domain
DLF	dorsal longitudinal fasciculus
DN-CLIM	dominant-negative CLIM
D-V	dorso-ventral
FACS	fluorescence activated cell sorting
GFP	green fluorescent protein
HD	homeodomain
HM	horizontal myoseptum
HMC	hypaxial motor column
HTS	high-throughput screening
LCCD	Ldb/Chip conserved *domain*
LID	LIM-interacting domain
LIM-HD	LIM homeodomain proteins
LMC	lateral motor column
MHB	midbrain hindbrain boundary
MiP	middle primary motor neuron

MMC	medium motor column
MO	morpholino
NLI	nuclear LIM interactor
Nrp	Neuropilin
N-SSDP	N-terminus of SSDP
PI	propidium iodide
pMN	motor neuron progenitor domain
PMN	primary motor neuron
RBs	Rohon-Beard neurons
RISC	RNA-induced silencing complex
RoP	rostral primary motor neuron
RT	room temperature
RT-PCR	reverse transcription polymerase chain reaction
Shh	Sonic hedgehog
SMA	spinal muscular atrophy
SMN	secondary motor neuron
SSDP	single-stranded DNA binding protein
Tac1	tachykinin1
TAE	Tris-acetate buffer
TILLING	Targeting Induced Local Lesions IN Genomes
UAS	upstream activating sequence
VCMap	virtual comparative map
ZFN	zinc finger nuclease

Statement of original contribution

The work in this thesis has been performed by the candidate, Zhen Zhong, unless specifically stated otherwise.

Zhen Zhong

01/05/2011

Co-author statement

The work presented in Chaper two of this thesis has been previously published.

Zhen Zhong, Hong Ma, Naoko Taniguchi-Ishigaki, Lalitha Nagarajan, Catherina G. Becker, Ingolf Bach, and Thomas Becker. SSDP cofactors regulate neural patterning and differentiation of specific axonal projections. ***Dev Biol,*** 2011, 349(2):213-24

The thesis author Zhen Zhong was the primary researcher for all the results presented in chapter two under the guidance of Dr. Catherina G. Becker and Dr Thomas Becker.

Hong Ma, Naoko Taniguchi-Ishigaki and Lalitha Nagarajan conducted the *in vitro* experiments including Western blot, cell culture and qRT-PCR, which are presented in Fig.4.5 C, D and F. Dr. Ingolf Bach assisted in the preparation of the manuscript.

Table of contents

1. Introduction

1.1 The Zebrafish

Zebrafish or zebra danio, *Danio rerio*, is a tropical sweet water fish belonging to the minnow family of Cyprinidae.

Zebrafish is an elegant research model organism to study genetics and development. Large numbers of embryos can be obtained from an individual female on a regular basis. Zebrafish embryos are accessible at all stages of development because of external fertilization. Furthermore, embryos and larvae are optically transparent and develop rapidly enough to follow individual cell movement and differentiation. These embryos are also amenable to a variety of experimental embryological approaches. Many kinds of transgenic and mutant zebrafish are available to reveal the functions of individual neuron or neural circuit (Lewis K.E., 2003).

The ninth assembly of the zebrafish genome (Zv9) was published on 10 Nov 2010. This provides an estimate of ~ 24,818 genes, including 14,607 protein coding genes (http://www.sanger.ac.uk/Projects/D_rerio). In addition, a project is underway to incorporate the zebrafish sequences into the human–mouse–rat virtual comparative map (VCMap), with the aim of defining conserved syntenic regions between the four genomes (Alestrom et al., 2006). This would become the theory basis for developing zebrafish not only as a genetic developmental model, but also as a human disease model in order to elucidate the pathogenesis of human disease as well as the therapeutic approaches.

All the excellent characteristics of zebrafish as a model organism combined with multiple experimental technologies (microarray, immunohistochemistry, in situ hybridization as well as confocal microscope approaches) enable us to rapidly study from gene discovery to gene expression and finally to gene function. Zebrafish is an effective tool for assessing gene functions in the neuron system through gain- and

loss-of function experiments by using microinjection mRNA, plasmid DNA or anti-sense morpholinos (MOs). Time-lapse studies in whole zebrafish embryos by confocal microscope offer an insight into the dynamic nature of *in vivo* interaction between the neurons and their environment, which especially provide us with a detailed understanding of cell-cell communication in axon pathfinding as well as in neuron-muscular junction formation (Key and Devine, 2003).

Transgenic zebrafish lines, in which fluorescent reporter genes are expressed in tissue-restricted patterns or under the control of inducible promoters, supply direct imaging reporter or indicator of interest gene with fluorescence in the developing embryo. By combining the time-lapse imaging and transgenic zebrafish, analysis of cell migration as well as axon pathfinding can be conducted on single cell level during development. For example, HB9:GFP transgenic zebrafish line is in use in this study as green fluorescent protein (GFP) is specifically expressed in motor neurons under the *Hb9* promoter (Flanagan-Steet et al., 2005). Transgenic zebrafish is also an important approach to study the gene function in development by misexpression. The Gal4/UAS (upstream activating sequence) transcriptional activation system was adopted in zebrafish to realize this aim. In this system, the activator line expressing yeast transcription factor Gal4 under particular tissue-specific or stage-specific promoter, was crossed with the effector line, which can express the gene of interest under the regulation of UAS activated by Gal4 (Halpern et al., 2008). Several approaches have been developed for introducing transgenes into the zebrafish germline, from the injection of naked DNA to transposon-mediated integration. Tol2 transposition, in particular, has dramatically increased the frequency of chromosomal integration of exogenous DNA, allowing the recovery of single-copy transgenic insertions and improving germ-line transmission of transgenes (Urasaki et al., 2008).

Morpholino technology:

Morpholino phosphorodiamidate oligonucleotides (morpholinos; MOs) are synthetic 25-base anti-sense DNA analogues with a morpholino ring, which can specifically bind to a complementary RNA sequence as a gene targeting tool. In particular, morpholinos are resistant to nucleases and therefore remarkably stable. The

fact that Morpholinos do not carry a negatively charged backbone means they have high affinity to RNA as well as low toxicity as they are less likely to interact non-specifically with other cell components (Summerton and Weller 1997; Eisen and Smith 2008a). Comparing with other antisense technology, MOs do not act through the recruitment of an RNA-induced silencing complex (RISC) or RNAseH but function solely by steric block mechanism, which renders a MO/RNA heteroduplex unable interact with RNA-binding proteins. Antisense RNA has been shown to have widespread effects that are sequence independent, preventing the practical application of this approach in zebrafish (Oates et al., 2000). At the same time, the power of MOs in gene targeting studies was quickly recognized and applied to other organisms, including *X. tropicalis* (Nutt et al., 2001), the chick *Gallus gallus* (Kos et al., 2001), oocytes of the mouse Mus musculus (Coonrod et al., 2001). Because of their exquisite sequence specificity, complete stability in biological systems, and highly predictable targeting, MOs are the most commonly used antisense reagents in zebrafish model. Translation-blocking MOs directly hybridize to the start site of translation and sterically inhibit scanning of the mRNA by 40S ribosomal complex (Summerton, 1999). The effect of translation blocking is not complete as MOs can not alter the activity once translation is initiated, therefore the effect is only referred to as a knock-down (Summerton, 1999). Splice-inhibiting morpholinos are designed to inhibit pre-mRNA splicing or even to cause exon skipping by targeting the exon-intron junction, so its advantage is that one can quantify the efficacy of the MO by RT-PCR (Draper et al., 2001). Considering the potential problems existing in morpholino technology, such as off-target effects and incomplete effectiveness of gene knock-down, proper control experiments should be performed for specificity of the MOs, which are: 1) Use of mismatch morpholinos. 2) Use of different morpholinos to the same genes. 3) Rescue experiments. To rescue the phenotype by introducing the gene product of interest that is immune to the MOs is the most reliable control(Eisen and Smith, 2008). We therefore need to compare the embryos from the same batch that have been injected by morpholino alone with by MO plus mRNA of its targeting gene.

Targeting Induced Local Lesions IN Genomes (TILLING) and zinc finger nuclease (ZFN)

The disadvantage of MOs is the transient effect, which makes it only suitable for early developmental stages. The incomplete knockdown and off-set effects of MOs also prompted scientists to generate permanent knockout methods. Target-selected mutagenesis in zebrafish has been developed recently through Targeting Induced Local Lesions IN Genomes (TILLING) technology, a method based on enzymatic cleavage of heteroduplex DNA using the plant endonuclease CEL-I (McCallum et al., 2000; Wienholds et al., 2003). Engineered zinc finger nuclease (ZFN) is another highly effective genome manipulation technology. ZFNs consist of a non-specific cleavage domain fused to a zinc finger domain, which can bind to the specific DNA sequence, introducing mutations in the specified locus. ZFNs reduce the collateral genetic damage compared with TILLING, but it is still not sure if all the genes will be accessible by ZFNs (Ekker, 2008).

The application of zebrafish as a disease model in human medicine has been expanded recently (Fishman, 2001), from inherited diseases, infectious diseases to regenerative and tissue repair models (Alestrom et al., 2006). Because of its well-characterized nervous system and relatively simple neuromuscular junction organization, zebrafish has developed to be a model for neuromuscular disease, such as spinal muscular atrophy (SMA) (McWhorter et al., 2003b) as well as neurodegenerative diseases, such as amyotrophic lateral sclerosis (ALS) (Ramesh et al. 2010; Sager et al. 2010). Especially, zebrafish show an impressive tissue regeneration capacity at the adult stage (Bernhardt, 1999; Becker et al., 2004) and are capable of regenerating motor neurons lost after spinal cord lesion (Reimer et al., 2008), which make it an excellent neuron regeneration model. Meanwhile, the zebrafish's characteristics which include small-size embryos, high embryo production and consuming smaller quantities of expensive drugs make it amenable for high-throughput screening (HTS) in the drug discovery process (Zon and Peterson, 2005).

1.2 Neuronal development in spinal cord

1.2.1 Neuron patterning in ventral neural tube in spinal cord development

In the developing spinal cord, distinct classes of motor neurons as well as interneurons are produced in specific dorso-ventral, rostro-caudal and medio-lateral positions. It is important to understand how these different neurons acquire their positional information and identity, which also decides their migration routes, settling positions as well as axonal projections.

The “French Flag Model” (reviewed in Wolpert, 1996) provides a theoretical frame work describing how progenitor domains can arise from an initially homogenous cell population. The model assumes a signaling centre, the organizer, at one end of the tissue that releases a chemical signal that diffuses over the tissue in a gradient. Cells in the tissue read out the concentration of the signal and assume a fate appropriate for a given concentration range. In analogy to the Franch flag, higher signal concentrations induce “blue” cells, lower concentrations activate the “white” cells, while “red” cells differentiate to the default state in the area that is most distant to the source of the signal, where little or no signal is present. Such signals are termed morphogens.

In the developing neural tube, Sonic Hedgehog (Shh) is such a morphogen (Placzek et al., 1991). Shh is produced by the floor plate and notochord at the ventral midline of neural tube. It spreads dorsally, establishing a ventro-dorsal concentration gradient and patterns progenitor domains in the ventral spinal cord (Ericson et al. 1996; Ericson et al. 1997; Jessell 2000). Briscoe and his colleagues extended this ventral neural tube patterning model by proposing three developmental stages (Ericson 1997; Ericson et al. 1997; Briscoe 1999; Briscoe et al. 2000; Sander 2000; Briscoe et al. 2001; Novitch et al. 2001b; Vallstedt 2001): Firstly, the gradient of Shh signaling activity establishes the dorso-ventral domains by repressing one class of homeodomain transcription factors (class I, including Pax7, Dbx1, Dbx2, Irx3 and Pax6) and activating another class of homeodomain transcription factors (class II,

including Nkx6.2, Nkx6.1, Olig2, Nkx2.2). Class I genes are generally more dorsally expressed than class II genes.

However, this does not explain the sharp boundaries between expression domains of class I and class II genes along the dorso-ventral axis of the neural tube. Thus, the second step of progenitor domain development is cross-repression between class I and class II genes. For example, Pax6 is cross-repressive with Nkx2.2 and Dbx2 is cross-repressive with Nkx6.1. These interactions lead to the establishment of five ventral progenitor domains, p0, p1, p2, pMN, p3, from dorsal to ventral.

Thirdly, the combinatorial expression of homeodomain (HD) as well as basic-helix-loop-helix (bHLH) proteins further defines the distinct classes of post-mitotic motor neurons or interneurons that are generated from these progenitor domains.

There is substantial data on how the Shh signal is received and transmitted in responding cells. Shh binds the Patched1 (Ptc1) receptor, which releases the repression of the trans-membrane factor Smoothened (Smo), and allows intracellular signal transduction (Ingham and McMahon 2001; Varjosalo and Taipale 2008). Further studies discovered that downstream of Shh/Ptc1/Smo a family of zinc-finger transcription factors, known as Gli proteins (Gli1, Gli2 and Gli3) control the ventral patterning in the neural tube (Jacob and Briscoe, 2003; Lei et al., 2004). A gradient of Gli transcriptional activity is established inside the cells, which mirrors the extracellular Shh signal gradient. With the exception of Gli1, which acts as an activator in most circumstances, Glis are post-translationally regulated. Both N-terminal and C-terminal part of Gli2 and Gli3 have been identified. The C-terminal part acts as a transcriptional activator domain, whereas the N-terminal part acts as a transcriptional repressor domain (Dai et al., 1999; Ruiz i Altaba, 1999; Sasaki et al., 1999). The ventral to dorsal gradient of Shh activity induces a parallel gradient of Gli activator function. At the same time, the Shh gradient progressively inhibits the Gli repressor activity, which is orientated in the opposite direction of the Shh gradient (Persson et al., 2002).

Recent research suggests that there are additional signals involved in the

neuronal patterning in the spinal cord that are independent of Shh. For example, the ventral patterning defects in $Shh^{-/-}$ or $Smo^{-/-}$ mice can be partially restored by additionally deleting the Gli3 gene (Litingtung and Chiang, 2000; Persson et al., 2002; Wijgerde et al., 2002). This indicates that some Shh-independent positional information may exist in the neural tube to regulate ventral neurons as well as motor neuron differentiation. Several lines of evidence show that Bone Morphogenetic Proteins (BMPs) from the dorsal neural tube (Lee and Jessell, 1999) functions as morphogens that are oriented opposite to Shh. In the absence of Shh signaling, BMPs might be sufficient to supply positional information throughout neural tube in $Shh^{-/-}$ /$Gli3^{-/-}$ double mutant embryos (Barth et al., 1999; Liem et al., 2000). Other potential morphogen signals helping to pattern the neural tube could be fibroblast growth factors and retinoic acid (Kudoh et al., 2002; Melton et al., 2004; Mason, 2007).

1.2.2 Motor neuron patterning and neurongenesis

In developing mouse and chicken embryos (generally applies to higher vertebrates), the motor neuron progenitor domain (pMN) is delimited by the dorsal V2 interneuron progenitor domain and ventral V3 interneuron progenitor domain. The combinatorial actions of the activated factors and the repressor factors define the boundary of the pMN domain, resulting in the specific expression of transcription factors (Nkx6.1, Nkx6.2, Pax6 and Olig2) within this domain. After the early D-V patterning of spinal cord by Shh, additional signals are involved in the generation of more specified neuronal subtypes at later stage as development proceeds. Motor neurons in spinal cord can be subtyped by their cell body localization as well as axon projection pattern. In higher vertebrates, based on the localization along rostral-caudal spinal cord, each discontinued longitudinal motor column is comprised of specific motor neuron subtypes, which innervate the same muscle targets. Hoxc belongs to a homeodomain transcription factor family with a homeobox sequence which specifically binds with DNA and activates its transcription. Hoxc, expressed in discrete rostral-caudal domains of spinal cord, are involved in establishing the

longitudinal columnar motor neuron identities (Guthrie, 2004). The patterned expressions of Hoxc6 in rostral and Hoxc9 in caudal, in response to the FGF signal, control the lateral motor column (LMC) and preganglionic motor column (PGC; column of Terni in chick) identities, respectively (Dasen et al., 2003; Dasen et al., 2005).

The development of motor neurons and oligodendrocytes are closely linked, Both arise from the pMN domain of the ventral spinal cord (Kimmel et al., 1994; Lewis K.E., 2003). Shh signaling activates Nkx6, which then induces Olig2 expression in the pMN domain (Novitch et al., 2001; Park et al., 2002). Olig2 interacts with E-box elements of *Hb9* gene to repress its expression, thus to maintain pMN identity, then Olig2 is abruptly down-regulated during pMNs developing to motor neurons (Mizuguchi, 2001). Ngn2, a basic bHLH transcription factor which is regulated by Olig2 and Pax6 (Novitch et al., 2001; Scardigli et al., 2003), promotes cells in the the pMN zone to differentiate into post-mitotic $HB9^{+}$ motor neurons. So Olig2 and Ngn2 function antagonistically to either suppress or activate the motor neuron gene expression programme, respectively (Lee and Pfaff, 2003; Lee et al., 2005). During motor neuron development, different bHLH transcription factors express sequentially and combine with LIM-HDs to activate the promoter of *Hb9* (Lee and Pfaff, 2003). Ngn2 in the progenitor cells and neuroM in the postmitotic motor neurons can activate the $Hb9^{+}$ motor neuron differentiation while NeuroD contribute to maintenance of *Hb9* expression in the mature motor neurons (see Fig. 1.1) (Sommer et al., 1996; Roztocil et al., 1997). Meanwhile, in neighboring non-motor neurons, Nkx2.2 and Irx3 can repress the expression of Hb9 transcription factor as well as the motor neuron differentiation, which is the de-repression model of gene regulation and fate specification in the neural tube (Lee et al., 2004). Once the progenitor cells exit the cell cycle, different LIM-HD transcription factor combinations start expressing in motor neurons or interneurons and specify the neuron fates within each segments of spinal cord.

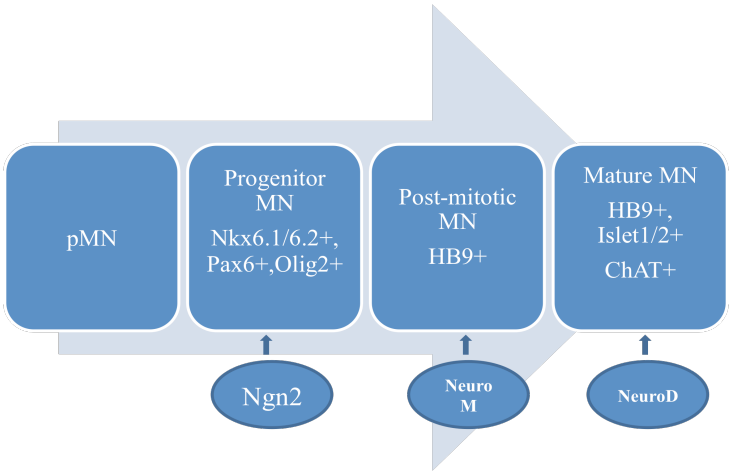

Fig.1.1 Diagram detailing the hierarchy of motor neuron development in higher vertebrates

1.3 LIM homeodomain proteins (LIM-HDs) and the LIM-HD interaction protein complex

LIM homeodomain proteins (LIM-HDs) constitute an important class of transcriptional regulators that determine the specific neuronal fates in vertebrates (Thor et al., 1999). LIM homeodomain proteins are characterized by an N-terminal tandem repeat of two cysteine-rich metal binding domains (LIM) and a homeodomain (HD) in the C-terminal, which mediate the assembly of protein complex necessary for regulating of gene expression (Dawid et al., 1998). CLIM (co-factor of LIM-HD) (Bach et al., 1997); also known as Ldb (LIM domain binding protein) (Agulnick et al., 1996) or NLI (nuclear LIM interactor) (Jurata et al., 1996) and CHIP in Drosophila ((Morcillo et al., 1997), a widely expressed nuclear protein, binds with high affinity to the LIM domain through C-terminal LIM-interacting domain (LID). The N-terminal dimerization domain (DD) mediates homeodimerization of CLIM and promotes the formation of $(LIM\text{-}HD)_2$-$(CLIM)_2$ tetramers and triggers the transcriptional activator function of LIM-HD proteins in vivo (Jurata and Gill, 1997; Thaler et al., 2002; Hiratani et al., 2003). Another important domain located in the middle of CLIM, the Ldb/Chip conserved domain (LCCD) domain, is responsible for interaction with single-stranded DNA binding proteins (SSDPs) (Torigoi et al., 2000). These three

domains of CLIM are involved in three types of interaction (SSDP binding, LIM binding and dimerization), which form diverse complexes and serve multiple functions in development (Fig. 1.2A). CLIM, bound to LIM-HDs, plays an important role in eye, midbrain–hindbrain boundary (MHB) and anterior midline development in zebrafish (Fig. 1.2 C, D) (Segawa et al., 2001; Becker et al., 2002). CLIM also serves as a docking site for additional cofactors involved in neuronal development and specification (Thaler et al., 2002). One of the important CLIM/LIM-HD complexes in *Drosophila* is the CHIP/Apterous complex. CHIP, recruiting Apterous (AP) and SSDP, triggers a signaling cascade that specifies wing development in fly (Milan et al., 1998). CHIP can also form an additional complex (CHIP/PNR) with LIM-only (dLIM) protein, the GATA family transcription factor, and the bHLH transcription factors and function in thoracic macrochaete (sensory bristles) differentiation (Zenvirt et al., 2008).

1.3.1 LIM-HD in neuron specification in spinal cord

Different LIM-HD combinations expressed in different neurons regulate cell fate decisions and neuronal differentiation. For example, in the spinal cord, loss-of-function studies show that Lhx3 is required for the generation of V2 interneurons and Islet1 is necessary for motor neuron development (Shirasaki and Pfaff, 2002). Hexamer complexes of (CLIM)2(Islet1)2(Lhx3)2 directly bind to the *Hb9* promoter and induce motor neuron formation. In contrast, V2 interneurons are induced by V2-specific Lhx3:CLIM tetramers (Thaler et al., 2002). So Islet1 plays a key role in deciding the cell fate between motor neurons and V2 interneurons. In Islet1 Morpholino injected zebrafish, primary motor neurons are missing and develop into a not fully characterized type of ventral interneuron (Hutchinson and Eisen, 2006). Reduced Islet1 expression in mice leads to a conversion of MNs to V2 interneurons. Islet1 also plays an essential role in motor column formation as well as axon pathfinding (Liang et al., 2011).

Other transcription factors interact with LIM-dependent differentiation of

neurons, for example in the cross repression of motor neuron and V2 interneuron fates. The homeodomain protein Hb9 is one of the first motor neuron markers in the postmitotic MNs after exiting the cell cycle. Hb9 can repress V2 interneuron differentiation by binding directly to the V2-tetramer response elements for LIM-HD complexes. Moreover, MNs express the LIM-only protein 4 (LMO4) to block V2-tetramer assembly. Conversely, the V2 interneuron transcription factor Chox10 binds the MN-hexamer response elements and inhibits their activity in V2 interneurons. Thus, multiple complementary feedback mechanisms are active to stabilize neuronal identities of motor neurons and interneurons (Lee et al., 2008). For example, the homeodomain protein Hb9 is critical in consolidation of motor neuron identity: in mice lacking Hb9, MNs aquire the V2 interneuron molecular marker Chox10, and display disorganization of motor columns and axon pathfinding defects (Arber, 1999; Thaler, 1999).

1.3.2 LIM-HD functions in motor column formation as well as axon pathfinding

The LIM-homeodomain (LIM-HD) protein family is an important transcription factor family which is expressed in all vertebrate motor neurons, involved in the control of motor neuron identity as well as in axon navigation (Tsuchida, 1994; Tanabe and Jessell, 1996; Eisen, 1999; Sockanathan, 2003). Different classes of motor neurons as well as interneurons, express unique combinations of LIM-HD transcription factors and innervate distinct targets. This suggests that LIM-HD proteins may be involved in controlling axon pathfinding. Studies in *Drosophila* have shown that LIM-HD proteins can direct motor axon projections without influencing the neuron's fate (Thor and Thomas, 1997; Thor et al., 1999). The LIM-HD proteins Lhx9 and Lhx1 are expressed in the dorsal spinal interneuron population dI1 and dI2 in chicken, respectively. Axon pathfinding of dI1 and dI2 is controlled by Lhx9 and Lhx1, which determine the rostral and caudal turn of the axons of dI1 and dI2, respectively (Avraham et al., 2009).

The topographic and functional organization of the spinal cord motor axon

projections is a consequence of the generation of subtypes of motor neurons during development. In higher vertebrates, motor neurons that project to specific target muscles in the periphery are clustered together in specific rostrocaudal, mediolateral, and dorsoventral positions of motor columns and pools. The combinatorial expression of LIM-HD transcription factors defines the subtype of motor neurons that occupy the different columns in spinal cord, and consequently decides their specific axon pathways in the periphery.

The first step of motor axonogenesis is the exit of motor neuron axons. All motor axons exit the spinal cord in the ventral spinal roots, while at the hindbrain level, motor neurons arise from two progenitor domains that can be distinguished by ventral-exiting and dorsal-exiting of their motor axons. One of the distinctions of these two groups of motor neurons is the LIM-HD transcription code: the motor neurons with ventral-exiting axons express Islet1/2 and Lhx3/4, while the neurons with dorsal-exiting axons lack the Lhx3/4 expression during their initial axon growth. In mice deficient for Lhx3/4 expression, some of the axons that exit ventrally in wildtype animals grow out of the neural tube dorsally (Sharma, 1998).

In the spinal cord there are four motor columns, the Median Motor Column (MMC, formerly MMCm), which spans the entire raustral-caudal extent of the spinal cord, the lateral motor column (LMC), the preganglionic motor column (PGC), and the Hypaxial motor column (HMC). HMC and PGC motor neurons only occupy the thoracic level of spinal cord. HMC neurons project axons to body wall muscles. PGC neurons innervate sympathetic ganglia. The lateral motor column (LMC) neurons, spanning brachial and lumbar spinal cord levels, contain lateral (LMCl) and medial (LMCm) neuron pools. The axons from these LMCl innervate the dorsal limb and the axons from the LMCm innervate the ventral limb. The MMC projects dorsally to the axial musculature and is the only motor column, in which motor neurons retain Lhx3/4 expression after their axons have emerged from the neural tube. Motor neurons in other columns (PGC, HMC and LMC) down-regulate the expression quickly. Ectopic expression of Lhx3 in motor neurons of the PGC, HMC and LMC redirects axons of these motor neurons towards to dorsal muscle targets of $Lhx3^{+}$

MMC motor neurons (Sharma et al., 2000).

Motor axon pathfinding has been studied extensively in the vertebrate limb, and differentially expressed dorsal and ventral cues are essential for proper motor axon navigation (Eberhart et al., 2002). Specific lateral Motor Column (LMC) neurons, targeting to limb, make a pathway decision after they emerge from the plexus region. Axons from neurons in the lateral LMC (LMCl) grow dorsally and axons from neurons in the medial LMC (LMCm) grow ventrally. In the LMCl, down-regulation of the LIM-HD Islet1 is accompanied by activation of the LIM-HDs Islet2 and Lim1, which control their dorsal projection. Combined expression of Islet1 and Islet2 is a marker for medial LMC (LMCm) motor neurons, and controls navigation of axons to the ventral limb (Kania et al., 2000).

LIM-HDs may exert their function by controlling expression of recognition molecules, such as those of the ephrin:Eph cell surface signaling system, which is involved in pathfinding of LMC motor axons. Expression of EphA4 in the lateral LMC (LMCl) and correct axon pathfinding to the dorsal limb require the LIM-HD transcriptional factor Lim-1. Knockout of EphA4 in mouse embryos redirects LMCl axons aberrantly into the ventral half of the hindlimb, similar to Lim-1 knockout (Kania and Jessell, 2003). Conversely, ectopic expression of EphA4 in the LMCm in chick induces errors in pathway selection, misguiding axons to the dorsal nerve (Eberhart et al., 2002). In parallel, EphB1 expression requires Islet1, which is only expressed in the LMCm and directs a ventral trajectory of axons. LMCm axons project aberrantly to dorsal limb in ephrin-B2 or EphB mutant mice (Luria et al., 2008).

Sema3F: Neuropilin (Nrp) signaling also contributes to LMC navigation in parallel with ephrin:Eph signal. Sema3F in the dorsal limb acts as a repulsive ligand for Nrp2, which is expressed in LMCm and leads axons of the LMCm to the ventral limb. In the absence of Nrp2 or Sema3F in mouse embryos, a significantly higher number of LMCm axons project into dorsal limb. Nrp1 is expressed by both LMC at the brachial level. Accordingly, in $Nrp1^{-/-}$ or $Sema3A^{-/-}$ (Nrp1 ligand) mutant embryos, LMCl and LMCm both prematurely project into the limb and are defasciculated. The

specific trajectories of both LMCl and LMCm axons are also disrupted (Huber et al., 2005). Thus, Sema3F:Nrp2 and Sema3A:Nrp1 play distinct roles in guiding LMC axons. Although the binding of LIM-HDs to specific promoters of axon guidance factors has not been established yet, we know from the above that Lim-1 regulates the expression of EphA4 and that Islet1 controls expression of EphB1. In addition, the promoter of the *Hb9* gene in LMC, HMC and MMC is directly targeted by LIM-HDs (Lee et al., 2004; Nakano et al., 2005), which suggests that LIM-HDs regulate motor neuron differentiation and control specific axon pathfinding of different motor neuron types.

1.3.3 Co-factors of LIM-HDs in head and spinal cord development

Single stranded DNA binding protein 1 (SSDP1, also known as SSBP3) was originally identified by its ability to bind to single-stranded poly-pyrimidine sequences (Bayarsaihan et al., 1998). SSDP1 can function as an activator component of a Lim1-Ldb1-SSDP1 complex that plays an essential role in head development and body growth in mouse embryos (Nishioka et al., 2005). Depletion of any component in this complex results in a headless phenotype. The role of the proline-rich domain of SSDP1 is critical for embryo head development, as deletion of proline-rich domain results in head truncation in mouse embryos (Enkhmandakh et al., 2006). Another functional domain is the N-terminal end of SSDP1(Wu, 2006), which is responsible for protein interaction with CLIM (Torigoi et al., 2000). SSDP proteins do not contain a nuclear localization signal and depend on binding to Ldb-LIM to enter the nucleus (van Meyel et al., 2003). Güngor *et al.* (Gungor et al., 2007) identified a cascade of specific protein interactions protecting LIM-HD from proteosomal degradation. In the cascade, CLIM stabilizes LIM-HDs and occupies the LIM domain, which inhibits the binding of destabilizing enzyme D1 to LIM-HD. The N-terminus of SSDP1 prevents binding of another destabilizing enzyme, D2/RLIM, to CLIM by occupying the LCCD domain, thereby protecting the LIM-HD/CLIM protein complex (Fig.1.2 B). It has also been demonstrated that the SSDP1/CLIM/LIM-HD protection cascade is

unidirectional, as over-expression CLIM or LIM-HD did not lead to an increase of SSDP1 or CLIM levels, respectively. Apart from the classic SSDP1/CLIM/LIM-HD complex, SSDPs also direct the SSDP/CHIP/PNR complex in scutellar bristle formation in Dropsophila. SSDP/CHIP/PNR complex, which prevents CHIP from forming homodimers, antagonizes the classical SSDP/CHIP/Apterous complex (Bronstein et al., 2010). SSDP genes are well conserved in evolution from invertebrates to human (Chen et al., 2002). Here we apply zebrafish as a research model to further understand the specific function of SSDP1 in development in their interaction with LIM-HDs complex.

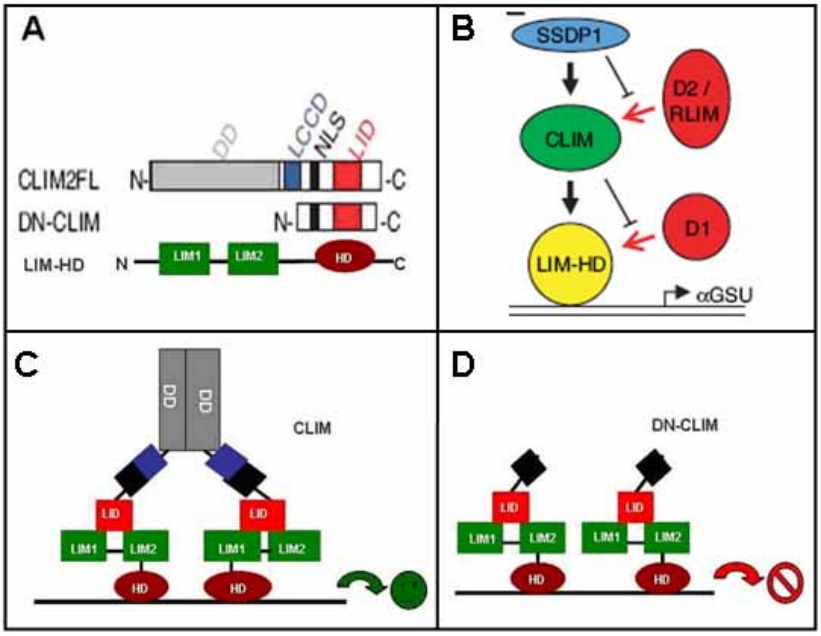

Fig.1.2 A. Schematic representations of CLIM full length and the dominant-negative CLIM molecule (DN-CLIM) which contains the nuclear localization sequence (NLS, in black) and the LIM interaction domain (LID, in red) of CLIM (upper). The general structure of LIM-homeodomain (LIM-HD) proteins is depicted at the bottom. Two N-terminal LIM domains (LIM1 and LIM2, in green) are associated with a homeodomain (HD). B. Model of a cascade of protein interactions that protects LIM-HDs from proteasomal degradation. In the presence of CLIM (green), the binding of D1 to LIM domains is inhibited, resulting in stabilization of LIM-HDs. The presence of SSDP1 (blue) prevents binding of D2/RLIM to CLIM thereby protecting the LIM-HD/CLIM protein complex. C. CLIM dimerization can activate

the LIM-HDs, controlling gene transcription. D. DN-CLIM can bind LIM-HDs, but cannot activate LIM-HD without dimerization. Adapted from *(Retaux and Bachy, 2002)* and *(Gungor et al., 2007)*.

Summary

Zebrafish provide an excellent research model to study neuron development as well as axon pathfinding. SSDP/CLIM/LIM-HD transcription factors play an important role in neuron specification in vertebrates. In this study, expression profiling by gene chip analysis was used to discover the genes downstream of the CLIM/LIM-HD complex, which control motor axon pathfinding in zebrafish. I used fluorescence activated cell sorted (FACS) HB9:GFP^{+} motor neurons from zebrafish embryos in which axon pathfinding had been blocked by DN-CLIM injection and compared their expression profile with that of motor neuorns in an uninjected control group. Gene knock-down and rescue studies indicate that one of the retrieved genes, *chondrolectin* (*chodl*), plays an important role in leading motor axons past the choice point: the horizontal myoseptum (HM). Further, SSDP/CLIM/LIM-HD transcription factors play an important role in neuronal specification in vertebrates. In this study, I cloned the SSDP1a and SSDP1b genes in zebrafish for the first time, and I show that these genes are involved in trigeminal and RBs sensory axon outgrowth, as well as in midbrain-hindbrain boundary and eye formation. Evidence is provided that SSDP1 plays an important role in neuronal patterning and sensory axon outgrowth by stabilizing the CLIM/LIM-HD complex. These finding provide insights into the mechanisms by which co-factors of transcription factors shape the nervous system by regulating neuronal development as well as axon pathfinding.

2. Material and methods

2.1 Materials

2.1.1 Enzymes and reaction kits

DNA polymerases	
Taq DNA Polymerase with standard buffer	NEB
Go Taq	Promega
Moltaq Polymerase	Molzym
Phusion™	Finnzymes
Restriction endonucleases	
Various (5-20 U/µl)	NEB
Reverse transcriptase (RT), (RNA-dependent) DNA polymerases	
SuperScript®III (RT)	Invitrogen
RNaseOUT™ Recombinant Ribonuclease Inhibitor	Invitrogen
RNase-Free DNase Set	Qiagen
Random primer (500ug/ml)	Promega
RNaseZAP®R2020	Sigma-Aldrich
DNA-dependent RNA polymerases	
mMessage mMachine™SP6, T7 Kit	Ambion
Megascript™Kit SP6, T7, T3	Ambion
Poly(A) Tailing Kit	Ambion
FACs sorting	
Trypsin-EDTA	Invitrogen
Penicillin-Streptomycin, liquid	Invitrogen

Trypan Blue Stain	Invitrogen
Pronase	Roche
Leibovitz medium L15 without phenol red	Invitrogen
Fetal calf serum	Invitrogen
Others	
Proteinase K	Roche

2.1.2 Bacterial strain and media

NEB Turbo Competent *E. coli* (High Efficiency)	NEB
XL1-Blue competent cells	Stratagene
LB medium capsules (25capsules/litre)	Qbiogene, Fisher scientific
Agar (20g/litre)	Qbiogene, Fisher scientific

All media were autoclaved prior to use. Antibiotics were added when needed.

Ampicilin (50mg/ml in H_2O stock, 100µg/ml working solution)

Kanamycin (50mg/ml in H_2O stock, 30µg/ml working solution)

2.1.3 Gene cloning kits:

HiSpeed Plasmid Midi Kit	Qiagen
Illustra plasmidPrep Mini Spin Kit	GE Healthcare
QIAquick Gel extraction Kit	Qiagen
QIAquick PCR Purification Kit	Qiagen
MiniElute™ Gel Extraction Kit	Qiagen
MiniElute™ PCR Purification Kit	Qiagen
MiniElute™ Reaction Clearup Kit	Qiagen
RNeasy Mini Kit	Qiagen
pGEM®-T Easy Vector System I	Promega
T4 DNA Ligase and standard buffer	NEB

2.1.4 Vectors

pGEM®-T easy	Promega	TA cloning vector
pCS2+MT	(Rupp et al., 1994)	mRNA overexpression vector
pBlueScript® II	Stratagene (UK)	

2.1.5 Morpholinos

Morpholino-based antisense oligonucleotides were synthesized by Gene Tools LLC (Philomath, OR, USA). Morpholino sequences are listed.

Table1: Morpholino sequence designed to knock down the gene expression.

SSDP1a	CTAGAATGAGCTTCTTACCTCTGAC
SSDP1b	GGATAAATATGCAACACACCTCTGA
SSDP 5 mm	GGTCCCTTTACCTTTGGCGAACATG
Chodl MO1	TATGAAACTCCTCATCTCACCTGAA
Chodl MO2	CTGACCTGGAGAGACAAAATTCACA
Chodl MO3	CGCATCCTCGTGTTTCCCTTGAGTC
ColXIX MO (Hilario et al., 2010).	TGCGGAGAAAGTTTATTATTCCAGC
Standard control	CCTCTTACCTCAGTTACAATTTATA

2.1.6 Oligonucleotides

DNA primer oligonucleotides were designed by primer3 online and were synthesized by VHbio or integrated DNA Technologies, Inc. (Leuven, Belgium)

Table 2: Primers

gene name	size	primer pair
SSDP1a	1057bp	F:5’- CATGTTTCCTAAAGGCAAAAGC -3’ R: 5’- TCAGACGCTCATGGTCATGG -3’
SSDP1b	1068bp	F: 5’- ATGTTCGCCAAAGGTAAAGGG -3’ R: 5’- TCACACACTCATTGTCATTGTTG-3
Chodl (probe)	730 bp	F: 5'-AGTCGTGTTGCGTTCTGGGA -3' R: 5'-CTGTCTATCTTTGGCGTCTTGG-3'
Chodl (MO test)	1010bp 673bp	F: 5' GTGTAAGCCCAGCTCGTTG 3' R: 5' CTATCTTTGGCGTCTTGGAG 3'
FL- Chodl	1061bp	F: 5'-CTCTCTCCGCATTTCAGAGG-3’ R: 5'-GCTAGCAGGAAGGTGCAGAC-3’
Calca	863 bp	L: 5'- CCT ACG CTC TGA TTA TTT GCC -3' R: 5'- TTC CTC CCT CCT TCG GTT C -3'
Tac1	401bp	F:5'- AAGGGAAAGTTACTGGGAGC -3' R: 5'- GGGAGCGAATGTGAAGATGA -3'
PCBP3	628bp	F: 5'- GGCTAAATGTCACCCTCACC -3' R: 5'- AGCAGGACGAACACTCACG -3'
Nkx1.2lb	978bp	L:5'- ATCACACGATCGAGCACAAG-3' R:5'- TTAGCACGTATTGCCGAATG-3'

2.1.7 Antibodies

Primary antibody

All primary antibodies used in this study are listed in table 3. Specifically, for Chodl antibody production, peptides (aa 282-296: C+ LWISKTPKIDSGMEV; aa 105-120: GLTREEGDNAQEPGAF) derived from the zebrafish Chodl protein sequence (NP_001017578.1http://www.ncbi.nlm.nih.gov/protein/62955133?report=genbank&log$=prottop&blast_rank=2&RID=JC9S5PZY01S) were synthesized and conjugated to the carrier protein KLH (Eurogentic, Liège, Belgium). The immunization of 2 rats (A and B) was performed by injection of conjugated peptides (mix of two peptides) with 3 subsequent booster injections as speedy 28-day immunization protocol. Scheduled (preimmune, medium and final) bleeds were collected and the specificity of bleeds was evaluated by indirect Elisa analysis.

Secondary antibody:

All Cy2-, Cy3-, Cy5 and HRP conjugated anti-rabbit, anti-rat and anti-mouse secondary antibodies were purchased from Jackson ImmunoResearch Laboratories Inc. (Newmarket, UK; 1:200). Goat Serum (ab7481, Abcam,Cambridge,UK) was used for blocking in immunohistochemistry, and heat inactivated prior to use for 30min at 60°C.

Table 3: Primary antibodies

Antibody	**host**	**source**	**Catalogue number/Clone**	**Dilution**
Acetylated Tubulin	mouse	Sigma	C-9891/6-11B-1	1:1000
CholineAcetyltransferase (ChAT)	goat	Chemicon	AB144P	1:500
c-Myc	mouse	Santa Cruz Biotechnology	G2806	1:600
c-Myc-FITC	mouse	Santa Cruz Biotechnology	E3007	1:1000
engrailed, 4D9	mouse	DSHB	concentrate	1:100
GABA	rabbit	Sigma	A 2052	1:1000
GFP	rabbit	Invitrogen	A 11122	1:200
HB9	mouse	DSHB	81.5C10-a	1:400
Islet	mouse	DSHB	40.2 D6	1:1000
Pax2	Rabbit	Covance	PRB-276P	1:300
SV2(synaptic vesicle)	mouse	DSHB	supernatant	1:20
znp-1	mouse	DSHB	concentrate	1:400
Zn5 (DM-GRASP)	mouse	DSHB	Ascites	1:2000
BTX (Alexa Fluor594)		Molecular probe	B-13423	1:400
Clim	rabbit	(Ostendorff et al., 2002)		1:3000
SSDP1	rabbit	Abnova		1:200
HNK1	rat	(Becker et al., 2001)		1:200
3A10 (neurofilament)	mouse	DSHB		1:50

2.1.8 Buffers and stock solutions

Blocking buffer	whole mount immunohistochemistry
1 %(v/v)	DMSO
1 %(v/v)	normal goat serum
1 %(v/v)	BSA
0.7 %(v/v)	Triton-X 100
Danieau H_2O pH=7.6	
58 mM	NaCl
0.7 mM	KCl
0.4 mM	MgSO4
0.6 mM	Ca(NO3)2
5 mM	HEPES
Hybridization buffer	(all solutions in RNA free H2O)
5 ml	formamide
2.5 ml	20xSSC
10 µl	Tween
100 µl	100mg/ml yeast RNA
2.38 ml	RNA free-H2O
10 µl	50mg/ml heparin
Phosphate buffered saline (10×PBS)	pH=7.4
1.36 M	NaCl
0.1 M	Na2HPO4
27 mM	KCl
18 mM	KH2PO4
PBST	
0.1 %(v/v)	Tween 20 in 1×PBS

Tris-acetate-EDTA buffer (TAE)(50x) pH 8.5

2 M Tris-acetate

100 mM EDTA

Citrate buffer pH=7.4

0.3 M tri-sodium citrate

Saline sodium citrate buffer (SSC) (20x stock) pH 7.4

3 M NaCl

0.3 M tri-sodium citrate

DIG blocking stock

10 g Blocking reagent (Roche)

100 ml PBST

PFA PH7.2

4% paraformaldehyde (w/v) in 1 xPBS

DAB stock solution

6% (w/v) diaminobenzidine (DAB)

E3 medium 1L

5 mM NaCl

0.17 mM KCl

0.33 mM CaCl2

0.33 mM MgSO4

500 ul 0.2% methylene blue (Sigma)

Lysis buffer (WB)

20 mM Tris pH7

150 mM NaCl

5 mM EGTA

1% Triton

0.10% SDS

1% Protease inhibitor

Blocking buffer (WB)

0.10%	Tween20
4%	BSA
in 1X TBS	

Extraction buffer (Genomic DNA)

10 mM	Tris pH 8
2 mM	EDTA
0.20%	Triton X-100
200 µg/ml	Proteinase K

2.1.9 Chemicals

Chemicals were purchased as *pro analysis* quality from Sigma-Aldrich (UK) and Fisher Scientific (UK).

2.1.10 Zebrafish

Zebrafish (*Danio rerio*) were kept at 26.5°C in an automated fish holding system (Aqua Schwarz Goettingen, Germany), at a 14-hour light and 10-hour dark cycle. They were fed two times a day, with dry flakes, ZM pellets (ZM Ltd., UK) and *Artemia salina* larvae. The fish were breed and raised according to standard protocols (Westerfield, 1989; Nusslein-Volhard) and all experimental procedures were approved by the British Home Office. We used wild-type (*wik*) and *Tg(hb9:gfp)* (Flanagan-Steet et al., 2005) embryos.

2.2 Experimental procedures

2.2.1 Molecular Biology Methods

2.2.1.1 DNA, RNA qualification and quantification

Nucleic acid concentration DNA, cDNA and RNA were measured directly by NanoDrop (NanoDrop ND1000, Thermo Scientific, USA).

DNA agarose gel electrophoresis To analyze restriction digests, quality of nucleic acid preparations, etc. horizontal agarose gel electrophoresis was performed. Gels were prepared by heating 0.8%-2.5% (w/v) agarose (molbiol grade, Fisher) with (7µl/100ml) ethidium bromide (Fisher Scientific, UK) in Tris-acetate buffer (TAE), depending on the size of fragments to be separated. DNA samples were adjusted to 1×DNA sample buffer and were subjected to electrophoresis at 10 V/cm in BIO-Rad gel chambers in 1×TAE running buffer. Pictures were taken in an E.A.S.Y. UV-light documentation system or bands were made visible on an UV-screen (λ=360nm) and desired fragments were cut out with a scalpel. To extract DNA from agarose gels, the QIAquick™ Gel Extraction or MiniElute™ Gel Extraction Kit from Quiagen, UK was used according to the manufacturer´s protocol.

DNA sequencing Sequence determination of dsDNA or PCR product was performed by DNA sequencing services™ (University of Dundee, UK).

2.2.1.2 Molecular Cloning

Preparation / enzymatic manipulation of insert DNA DNA primer oligonucleotides were designed by primer3 online and were produced by Integrated DNA technologies, Inc. (Leuven, Belgium.) Different kinds of insert DNA fragments were cloned (see item list below).

Plasmid DNA fragments For cloning of distinct regions of plasmid DNA, donor molecules were digested with appropriate restriction enzymes. Completed digests

were applied to agarose gel electrophoresis and appropriate bands were cut out and DNA was eluted by QIAquick Gel Extraction Kit (Qiagen).

Taq DNA polymerase-derived products PCR products amplified with DNA polymerase were directly subjected to TA cloning. PCR-purification kit ((MiniElute™ PCR Purification Kit, QIAquick™ PCR Purification, Qiagen) was used to purify DNA fragments from PCR products according to the manufacturer's protocol. The fragment was eluted from the column with 50ul DNA-free water and concentration was determined by Nano-drop.

PCR products with introduced restriction sites Frequently, the ends of the insert DNA did not contain suitable restriction enzyme sites, i.e. when a donor cDNA was designated for cloning into a certain reading frame of an expression vector. Restriction enzyme sites were generated by PCR at the desired location. For this technique, restriction sites were designed at the 5' end of the PCR primers. Because certain restriction enzymes inefficiently cleave recognition sites located at the end of a DNA fragment, usually four additional bases were introduced 5' to the restriction site. PCR products were gel-purified, digested with the appropriate restriction enzymes, and purified with spin columns.

Standard Polymerase chain reaction (PCR) The standard PCR (Saiki et al., 1985), an amplification of DNA by *in vitro* enzymatic replication, was performed in an MJ mini-gradient thermal cycler (Biorad, UK).

Reagents:

Template (cDNA, gDNA, Plasmid DNA)	10pg – 1ng
dNTPs	200 µM (each dNTP)
Primer (forward)	0.1 – 1 µM
Primer (reverse)	0.1 – 1 µM
Reaction buffer (10x)	1x
DNA polymerase	2.5U

Add ddH2O to final volume 50 µl

Program:

cycles	time	temperature
1	5 min	94 ˚C
25 – 35	30 s	94 ˚C
	45 s	Tm – 1 ˚C
	1 min per kb	72 ˚C
1	10 min	72 ˚C
	forever	4 ˚C

Usually the reaction was carried out in a 0.2 ml PCR reaction tube. Moltaq polymerase was routinely used for the amplification of up to 2 kb long DNA fragments. Proof reading PfuUltra™ HF DNA Polymerase was used to amplify DNA for overexpression and full-length constructs. After the PCR reaction was finished, 5 µl of the product was analysed by agarose gel electrophoresis.

Nested PCR The nested PCR approach was used to amplify sequences from genomic DNA (gDNA), which contains a very low number of copies of a specific DNA template. This approach prevents the amplification of the wrong product by sequentially using two primer pairs for the same sequence. The first primer pair includes the sequence of the second primer pair and the first PCR reaction is used as a template of the second (1:40 dilution). The reaction mix is equal to the standard PCR.

Enzymatic manipulation of vector DNA prior to cloning

Plasmid was digested at one locus either by a single restriction enzyme or by two at a multi-cloning site to achieve insertion of target DNA in a defined orientation. Digestion reaction was carried out by NEB restriction endonucleases according to the manufacturer´s protocols. Complete digested bands, which were verified by agarose gel electrophoresis, were cut out and extracted by QIAquick Gel Extraction Kit (Qiagen)

Ligation of plasmid vector and insert DNA

Ligation of DNA fragments was performed by mixing 50 ng vector DNA with over

3-times insert DNA. 1 µl of T4-Ligase and 2 ul of ligation buffer (NEB) were added to a final volumn of 20ul. The reaction was incubated either for 2h at room temperature or overnight at 16 ℃. The final reaction mixture was used directly for transformation without any further purification.

TA cloning TA Cloning exploits the terminal transferase activity of Taq polymerase. This enzyme adds a single, 3'-A overhang to each end of the PCR product. This makes it possible to clone this PCR product directly into a linearized cloning vector with single 3'-T overhangs. The PCR products with 3'-A overhang, are mixed with this vector in high proportion. The complementary overhangs of "T" vector and PCR product were ligated under the action of T4 DNA ligase. All procedures were performed with the pGEM-T easy vector following the manufacturer's instruction.

DNA transformation into bacteria

10ng of plasmid DNA or 5ul of ligation mixture were added to NEB Turbo competent cells and incubated for 30mins on ice. After a heat shock (30 seconds, 42℃) and successive incubation on ice (5 minutes), 500 ul of SOC-medium were added to the bacteria and incubated at 37℃ with 200 rpm shaking for 1 hour. Cells then were plated on LB plates containing the appropriate antibiotics overnight.

Plasmid DNA extraction from bacterial cultures

Mini-scale plasmid extraction

3 ml LB/Amp-Medium (100 ug/ml ampicillin) were incubated with bacteria from single colony at 37℃ overnight with constant agitation. Cultures were transferred into 1.5 ml Eppendorf tubes and cells were pelleted by centrifugation (13,000 rpm, 1min, RT). Plasmid extraction was processed by illustra plasmidPrep Mini Spin Kit (GE Healthcare) according to the manufacturer's protocol. Finally, DNA was eluted from the columns with 50ul DNA-free water and concentration was determined by Nano-drop.

Midi-scale plasmid extraction

50ml LB/Amp-Medium (100 ug/ml ampiciline) were incubated with bacteria from

single colony at 37℃ overnight with 200 rpm in a shaker. Cultures were transferred into 50 ml Falcon and plasmid extraction was processed by HiSpeed® Plasmid Midi Kit (Qiagen, UK), according to the manufacturer´s protocol.

Finally, DNA was eluted from the columns by 500ul DNA-free water and concentration was determined by Nano-drop.

Genomic DNA extraction (Large sample number, very quick and dirty, adequate for PCR) Embryos were incubated with extraction buffer at 50-56°C for 2-3 hrs (longer is ok) and boiled in waterbath for 5-10 min to inactivate Proteinase K. gDNA was spined down and resolved with 50 ul dd H2O.

2.2.1.3 RNA extraction and cDNA transcription

Total RNA extraction from zebrafish tissue

To extract total RNA from brain and spinal cord tissue or whole embryos, the animals were killed via a schedule 1 method (Home Office, UK). 24 hpf zebrafish embryos were dechorionation and 30 embryos were homogenized in 600ul buffer RLT with 10% β-ME. Total RNA was obtained by RNeasy® mini Kit (Qiagen, Crawley, UK), according to the manufacturer´s protocol. Finally the total RNA was eluted in 50 ul RNA-free water. Quantity and quality of total RNA was determined by Nano-drop. Total RNA samples were stored at -80℃.

First strand cDNA synthesis

First strand synthesis was carried out using the SuperScript III™ RT and the RNaseOUT™ Recombinant Ribonuclease Inhibitor (Invitrogen Ltd., Paisley,UK) according to the manufacturer´s protocols. The reaction steps were performed in a MJ mini-gradient thermal cycler (Biorad, UK).

Condition for cDNA synthesis

Random primer (500 ug/ml)	0.5 ul
dNTPmix (10mM)	1 ul
Total RNA	10 pg – 5 ug
H2O	top up to 13 ul
65 °C for 5 mins	
Ice at least 1 min	
Product from above	13 ul
5 ×First strand beffer	4 ul
DTT (0.1M)	1 ul
RNase Inhibitor	1 ul
SuperScript Ⅲ RT (200U/ ul)	1 ul
	20 ul
25 °C 5 mins	
50°C 60mins	
70°C 15mins	
Store at -20 ˚C	

In-vitro RNA transcription

To generate DIG labeled probes for *in situ* hybridization: an *in vitro* transcription was performed using the MEGAscript™ Kit (Ambion, Cambridge, UK). 10 μg of plasmid DNA containing the desired insert, flanked by a T3, T7 or SP6 promoter were digested with restriction endonucleases overnight. Thereby, only the promoter sequence and the desired DNA insert were transcribed. The digested plasmid DNA was precipitated as described in Precipitation of DNA (see above). For the generation of DIG labelled RNAs, DIG-11-dUTP (Roche, UK) was used.

Conditions for probe making:

10 mM ATP

10 mM CTP

10 mM GTP

6.5 mM UTP

3.5 mM DIG-11-dUTP

2 μL 10X Reaction Buffer

0.1–1 μg linear template DNA

2 μL Enzyme Mix

Up to 20 μL with Nuclease-free Water

37°C, 3 hr

Table 4: Strategy for making probes of candidate genes Genes were cloned by using the specific primer pair from zebrafish 24hpf whole embryo cDNA and ligated with T-vector. Plasmids containing specific genes were linearized and probes were synthesized by RNA polymerase based on the linearized plasmid template.

Gene	Insert length	Vector	endonuclease /polymerase	Anti-biotics
SSDP1a	1057	T-vector	SpeI/T7	Amp^R
SSDP1b	1068	T-vector	SpeI/T7	Amp^R
Chodl	730	T-vector	SpeI/T7	Amp^R
Calca	863	T-vector	SpeI/T7	Amp^R
Tac1	401bp	T-vector	SphI/Sp6	Amp^R
PCBP3	628bp	T-vector	ApaI/SP6	Amp^R
Nkx1.2lb	978bp	T-vector	SpeI/T7	Amp^R

To generate mRNA for overexpression studies, Ambion's mMESSAGE mMACHINE™ Kit (Ambion, Cambridge, UK) was used. *In vitro* transcription was performed according to the manufacturer's protocol. After 2h incubation, the template DNA was degradated by adding 1 µl DNase and RNA was incubated with polyA buffer at 37°C for another 1h. PolyA tailed RNAs were purified by lithium chloride precipitation (part of the kit) and stored at –80°C.

Conditions for synthesizing RNA:

Final concentrations/amounts for a 20 ul reaction:

0.1–1 µg linear template DNA

10 µL 2X NTP/CAP

2 µL 10X Reaction Buffer

2 µL SP6/T7 polymerase

To 20 µL Nuclease-free Water

37°C, 2 hr

Table5: RNA expression constructs for mRNA synthesis. Manipulated gene sequences were inserted into specific RNA expression vectors. mRNA was synthesized by RNA polymerase based on the linearized templates.

RNA transcripts	**Inserted gene**	**linearization-polymerase**
pCS2-NLS-MT-NSSDP1	(mSSBP3: BC003430.1 1-92aa)	Not Ⅰ - SP6
pCS2-NLS-MT-SSDP1b	(zSSDP1bFL: GQ903696.1:1-1095bp)	Not Ⅰ - SP6
pCS2-MT-Chodl	(z*chodl* FL:zgc:110088**:**891bp)	Not Ⅰ - SP6
pCS2-MT-DNCLIM	(m*Ldb2*: NM_010698:888bp-1242bp)	Not Ⅰ - SP6
pCDA3-Chodl-Ires-GFP	(z*chodl* FL:zgc:110088**:**891bp)	Xba Ⅰ - T7

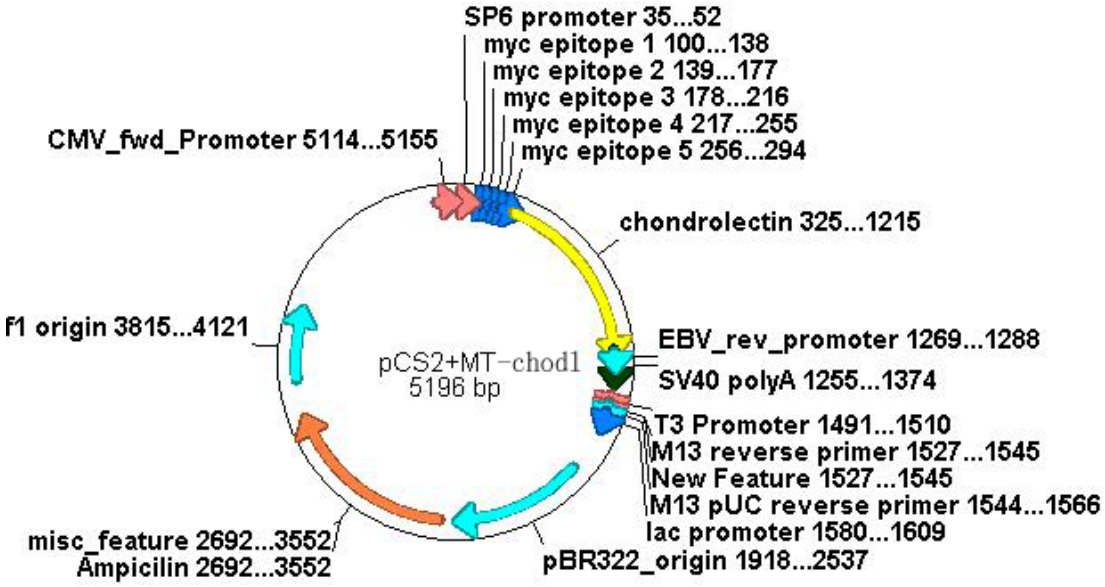

Fig. 2.1 The Chodl over-expression construct was made by insertion of the *chodl* full-length sequence into pCS2-MT RNA expression vector with 5'myc tag.

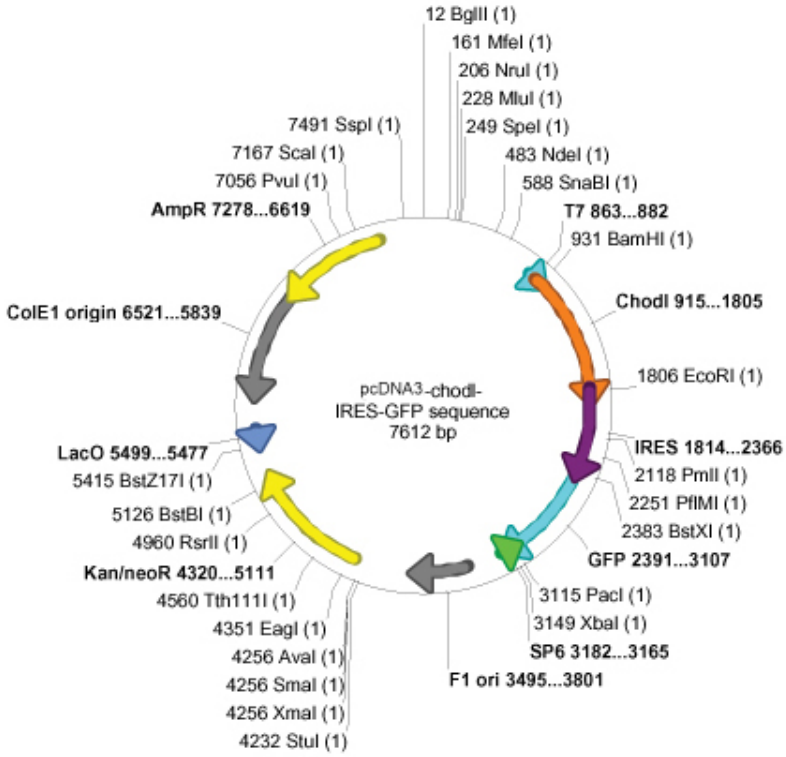

Fig. 2.2 The Chodl over-expression construct was made by insertion of *chodl* gene into the pCDNA3-IRES-GFP RNA expression vector.

2.2.2 Histological Methods

2.2.2.1 Whole mount RNA in situ hybridization

Whole mount RNA in situ hybridization was performed to detect the mRNA expression patterns in 24 hpf zebrafish embryos. Embryos were dechorionated and fixed overnight in 4% PFA at 4℃. The following day, the embryos were washed with PBST and stored in 100% methanol at -20℃ for 30 minutes (until a few months). Methanol was removed by a descending methanol series (75%, 50%, 25% methanol in PBST). After washing with PBST, embryos were digested with 10ug/ml ProteinaseK (Roche) for 10 minutes at RT, followed by neutralization step with 2mg/ml glycine in PBST. Embryos were post-fixed with 4% PFA for 20 mins at room temperature and washed by PBST. After pre-hybridized with hybridization buffer at 55°C for 3 hours, whole embryos were incubated with the probe at 55°C overnight and washed extensively at 55°C. The hybridized probe was detected using an alkaline phosphatase–coupled anti-digoxigenin antibody (Roche, Mannheim, Germany). The signal was developed using *FAST* 5-bromo-4-chloro-3-indolyl phosphate/nitro blue tetrazolium (BCIP/NBT) (Sigma-Aldrich, Deisenhofen, Germany), resulting in a brownish reaction product. The sense probes, developed in parallel under the same conditions as the anti-sense probes, did not show any specific labeling, which can work as a negative control.

2.2.2.2 Whole mount immunohistochemistry

To detect the protein expression patterns in 24 hpf embryos, whole-mount immunohistochemistry was performed. Animals were dechorionated and yolks were poked with fine forceps and metal needles. Embryos were fixed in 4% PFA containing 1% (v/v) DMSO for 45 minutes at RT and washed with 1×PBS. Embryos were incubated with blocking buffer to prevent unspecific binding of the primary antibody for 30 minutes at RT. Older animals (33 hpf) were digested with 1mg/ml

collagenase for 5 minutes at RT and washed by PBS before adding the blocking buffer. Primary antibodies were diluted in blocking buffer and applied to embryos overnight at 4 ℃. Unbound primary antibody was removed by three washing steps with PBS. Fluorescence or HRP conjugated secondary antibody were diluted 1:200 in blocking buffer and applied to embryos overnight at 4℃. Unbound secondary antibody was removed by washing step with PBS. To visualize the HRP signals, embryos were incubated in 0.5mg/ml diaminobenzidine (DAB) in 1×PBS for 20 min at 4℃. The brownish precipitate was developed in 5-10 min by 0.035% H2O2 in 1×PBS. Finally embryos were washed by PBS and cleared in an ascending glycerol series (30, 50, 70% glycerol in 1×PBS). Embryos were mounted in 70% glycerol and observed with microscope. (Fluorescence microscope was specific for fluorescence signals).

2.2.2.3 In situ hybridization double labeling with immunohistochemistry

For whole-mount embryos double labeling with immunohistochemistry, Whole-mount NBT/BCIP stained embryos were re-fixed in 4% paraformaldehyde with 1%DMSO for 45 mins and washed by PBS. Embryos were incubated with primary antibodies against GFP overnight, and stained by cy2 conjugated secondary antibodies overnight at 4 ℃.

For embryos section double labeling with immunohistochemistry, whole-mount NBT/BCIP/alkaline phosphate-stained embryos were cryoprotected in 30% sucrose buffer, and embedded in Tissue Tek OCT Compound (Agar Scientific Ltd, UK) to freeze slowly in liquid nitrogen. 10 μm sections were cut using CM3050 cryostat (Leica), mounted onto glass slides and incubated with polyclonal antibody against GFP overnight at 4 ℃, and with the appropriate secondary antibody for another three hours at room temperature. Specimens were photographed by confocal microscopy

(LSM710, Zeiss, Oberkochen, Germany). Structure identification was aided by the embryonic atlas posted on the ZFIN website. (http://zfin.org/zf_info/anatomy.html).

2.2.3 Microinjection into zebrafish eggs

Freshly fertilized eggs were harvested and arranged in a line in a petri dish with 2% agarose. For injections, rhodamine dextran (5%, MW = 10000, Invitrogen, Molecular Probes, USA) was added to either mRNA or MO solutions. A glass micropipette (3um, GB 150F-8P, Sciences Products GmbH, Hofheim, D) was filled with the mRNA (1–2 μg/μl) or MO solutions (up to 2 mM) by capillary force and attached to a micromanipulator. A volume of 0.5 to 1 nl per egg (one- to four-cell stage) was injected using a IM 300 Mircroinjector (Intracel, UK). Finally, injected eggs were incubated in E3 medium at 28.5℃ until the desired developmental stage was reached for phenotype analyses. Control MO injections were carried out with every experiment on embryos taken from the same clutch or pool as embryos receiving specific MO, to avoid developmental differences between clutches. For rescue and synergy experiments, the total morpholino load per egg was kept constant between groups by supplementing

2.2.4 Fluorescence activated cell sorting and gene array

All fish embryos (26 hpf) were dechorionated and washed with calcium free Ringer buffer for 15 min. Embryos were then mechanically dissociated in EDTA-trypsin (0.25% trypsin and 1 mM EDTA in PBS) and incubated for 30 -60 min at 28.5 °C. Embryo digestion was stopped by adding equal volume of 2 mM $CaCl_2$ with 20% fetal calf serum and centrifuged at 300g for 5 min at RT. The tissue was re-suspended in 500 μl of L-15 medium, and all cell suspensions were sorted by a BD FACSAria™ II Flow Cytometer (BD Biosciences, San Jose, California, USA) in Institute for Stem cell Research (University of Edinburgh). Viability was tested by propidium iodide (PI) staining. Sorted cells were immediately frozen in lysis buffer at the concentration of

1000 cells/µl. Samples were then sent to Miltenyi Biotech (Bergisch Gladbach, Germany) for RNA isolation and gene profiling by Chip hybridization Agilent Technology (Wokingham, UK) arrays which cover ~ 21'000 genes.

2.2.5 Live imaging

Dechorionated 18 hpf embryos were mounted on cover-slips with 2% low-melting agarose prepared in E3 embryo medium with 0.02% （w/v）tricaine (MS-222). Image stacks were taken every 10 mins by confocal microscopy (LSM710, Zeiss, Oberkochen, Germany) with a 20 ×lens at 28℃. Confocal time-lapse imaging was performed to observe axon outgrowth from 18hpf to 27hpf. CaP axon growth speed (axon length quantification) was analyzed based on time-lapse still picture series with the ZEN2009 software (Zeiss, Oberkochen, Germany).

2.2.6 Western blots

Total extracts of embryonic zebrafish (24 hpf) tissue was collected in ice cold lysis buffer. After centrifugation at 6000 rpm for 5min, the supernatant was taken for protein quantification (Micro BCA Protein Assay Kit - PIERCE Biotechnology, Rockford, IL, USA). The homogenised tissue samples were diluted with loading buffer (NuPAGE 4X SDS Sample buffer, Invitrogen, Paisley, UK) and boiled at 95°C for 5min. After loading the samples onto Precise TM protein gels 4-20% (Thermo Scientific, UK), they were run at 100 V for 1-1.5 hours in HEPES running buffer (Thermo Scientific, UK). The bands were then transferred onto a PVDF membrane (Millipore, UK), which was fixed in methanol and distilled water for 15 seconds prior to the transfer, at 400 mA for 2 hours. Following the transfer, blot was hybridized with a 1:2000 dilution of Chodl antiserum A and B in blocking buffer overnight. Protein A horseradish peroxidase (HRP; BioRad) was used to visualize specific bands. They were then developed in developing spray (Calbiochem, Nottingham, UK), and exposed to film in the dark room for 5-15 min.

2.2.7 Quantitative analysis and statistics

2.2.7.1 Quantitative analysis of motor neuron identity

GFP^+, $CHAT^+$, $HB9^+$ and $Islet^+$ neurons: Embryos were fixed at 24 hpf and their trunk region was scanned with a 20x objective by confocal microscopy (LSM710, Zeiss, Oberkochen, Germany). All fluorescent neurons in trunk segments 7, 8 and 9 were counted in z-projections of confocal image stacks of the upper half of the laterally mounted spinal cord to avoid the overlapping of cells in the two hemi-segments. At least two independent experiments were performed per treatment and the experimenter was blind to the treatment for the analysis.

2.2.7.2 Quantitative analysis of axon outgrowth

Axons were counted as previously described (Becker et al., 2002). Briefly, axon fascicles, axons or branches were counted within one cell diameter away from the upper ganglion in laterally mounted, anti-tubulin immuno-labeled embryos. Rohon-Beard axons or branches were counted in the most dorsal aspect of the upper epidermis. Primary motor axons were counted on both sides of the embryos in segments 7-14. Control and treatment groups were always processed in parallel from the same clutch of eggs to avoid differences in overall development. The observer was blinded to the treatments. Motor axons numbers also expressed as percentage to the total axons counted per embryos (16). Other counts are collectively expressed as number of axons, comprising single axons, fascicles of axons and axonal branches.
To classify stalled growth of CaP axons and ventral motor nerves as shorter or longer than the position of the horizontal myoseptum (HM), which were either identified by 4D9 immunoreactivity (znp-1 labeled preparations) or by the characteristic thickening of the CaP axon at the horizontal myoseptum (HB9:GFP transgenic embryos).

Table6: Axons were classified to the following standard to determine morpholino knock-down effects on axon growth.

Classification	Histological morphology
unaffected	CaP axon arrived at edge of ventral myotome with branches at 24&33hpf
HM+	truncated CaP axons extend beyond HM but do not reach the edge of the ventral myotome
HM	Cap axon stalled at HM
HM-	CaP axons are absent or do not reach the HM.

2.2.7.3 Statistics

Data are presented as mean and error bars represent the standard error of the mean. Groups were compared using one-way ANOVA (≥2 groups). Two-way ANOVA was applied to analyze CaP axon growth in time-lapse studies. A p value of less than 0.05 represented a significant difference between groups (Sigma Stat 3.5).

3. Chapter one: Discovering novel genes that are downstream of LIM-HDs and are involved in motor axon pathfinding in zebrafish

3.1 Introduction

3.1.1 Neuron system in Zebrafish

The zebrafish is an excellent research model for neuron development as neurons can be individually identified and traced over time in living embryos. The zebrafish spinal cord contains early-born primary neuron, which includes sensory neurons, interneurons and motor neurons, and late-born secondary neuron including only interneurons and motor neurons. The primary motor neurons and interneurons persist until the adults, while primary sensory neurons called Rohon-Beard neurons (RBs) die during the larval stage. Later sensory reception is regulated by neural crest-derived dorsal root ganglion sensory neurons. RBs are multi-polar neurons that extend their central axons longitudinally to pioneer the dorsal longitudinal fasciculus (DLF) within the spinal cord and also extend their peripheral axons under the skin (Bernhardt et al., 1990).

There are only three primary motor neurons (PMNs) per spinal hemi-segment. These are the rostral (RoP), middle (MiP), and caudal PMN (CaP). PMNs have large somata, located relatively dorsally, above the ventral third of spinal cord. These three primary motor neurons located differently relative to the somite boundary: Rop is just located rostrally to the boundary, Mip is caudal to the boundary and rostral to CaP which is almost in the central somites. These neurons grow axons out of the spinal cord following a common path in the middle of each segment to the horizontal myoseptum. At this point, all the primary motor neuron growth cones pause before they diverge to their cell-specific pathway. The CaP axon grows towards the ventral

somite, pioneering the ventral motor nerve, which is the only primary motor neuron which grows ventrally beyond the horizontal myoseptum. The axon of MiP follows the CaP axon up to the horizontal myoseptum where it retracts and grows towards the dorsal somite. The RoP axon takes a lateral direction from the horizontal myoseptum (Fig. 3.1). Secondary motor neurons are born 5-6 hours later than the primary motor neurons. Compared with PMNs, secondary motor neurons have smaller, rounder somata and are typically found in the ventral edge of the spinal cord. Secondary motor neurons initiated axonal outgrowth later than primary motor neurons and progressively add axons along the paths of axons of PMNs during development (Myers et al., 1986). The primary and secondary motor neurons have distinct and overlapping functions in adults (Kimmel and Westerfield, 1990; Williams et al., 2000). Primary motor neurons innervate fast muscles, involved in startle response and fast swimming, while the secondary motor neurons innervate fast and slow myotomal muscles as well as pectoral fins, involved in fast and slow swim (Liu and Westerfield, 1988; Devoto et al., 1996).

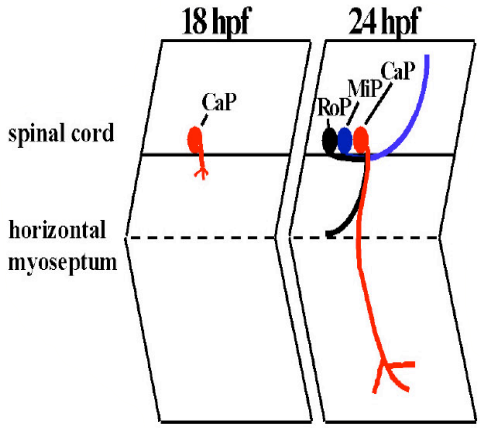

Fig.3.1 Between 18 and 24 hours post-fertilisation (hpf) the CaP axon pioneers the ventral pathway and the MiP axon pioneers the dorsal pathway (lateral view of individual trunk hemisegments). Adapted from (Feldner et al.,

Mauthner neurons, located in the hindbrain, play an important role in escape reaction from brain to spinal cord motor neurons. Its relatively large axon crosses the midline in the brain and extends down the length of the spinal cord, contacting motor neurons and interneurons along the way. Mauthner neurons are a pair of large reticulospinal neurons that initiate the escape response fish use to avoid predators

(Korn and Faber, 2005). The Mauthner axon's growth cone enters the spinal cord after all the primary motoneurons of the trunk spinal cord have begun axonal outgrowth (Myers et al., 1986). The neuronal network in the spinal cord functions in regulating the reflexive motor response to touch stimuli: the trigeminal primary sensory neurons input the touch information indirectly to the primary motor neuron by Mauthner neurons, which act as a bridge between the brain and the spinal cord (Metcalfe et al., 1990). The Commissural Posterior Ascending (CoPA) cell, a class of large excitatory interneuron, receives input from ipsilateral primary sensory Rohon Beard neurons and relays that excitation to the other side of the body (Fetcho, 2007).

3.1.2 Motor neuron differentiation and axon pathfinding in zebrafish

During embryonic development, spinal cord motor axons precisely project along specific pathways, under the control of guidance cues, to reach their final peripheral muscle targets and form synapses. There are different steps during this stereotypical projection of motor axons: 1) motor neurons acquire their identity; 2) axons grow within the spinal cord and make an exit point decision; 3) axons grow along their initial trajectory out of spinal cord; 4) axons interact with different choice points during the specific pathway and neuromuscular junction formation occurs simultaneously; 5) target muscles are innervated and axons branch. Varied transcription factors combinations specifically contribute to different phases and choice point decision during axon pathfinding.

The zebrafish is an excellent model organism to study axon guidance since embryonic zebrafish have individually identifiable primary motor neurons (PMNs), facilitating the analysis of mechanisms of motor axon pathfinding at the level of single axon. There are only three primary motor neurons in each spinal hemisegment and their axons exit the spinal cord on a joint pathway in midsegmental position to grow towards the horizontal myoseptum at around 17-18 hour post-fertilization (hpf) (Myers et al., 1986). The horizontal myoseptum acts as an intermediate target for

primary motor axons, where the growth cones of all primary motor neurons pause for up to 2 hours (Eisen et al., 1986; Melancon et al., 1997), then the CaP extends its growth cone ventrally, the MiP axon grows dorsally to innervate dorsal musculature and the RoP axon extends laterally. About half of the hemisegments contain a fourth motor neuron-VaP, which is initially equivalent to CaP, but dies by 36hpf (Eisen et al., 1990). Eisen et al. raised the issue that primary motor neuron survival in zebrafish requires trophic support from muscle to explain the VaP death (Eisen and Melancon, 2001). Only these three primary motor neurons innervate the axial muscle between 18 hpf and 24 hpf. After that the axon of secondary motor neurons (SMN) (around 26 hpf) will extend along the paths of the primary motor axons following a general rostral-to-caudal sequence of trunk segment differentiation (Beattie, 2000). Both types of motor axons reach the HM, but the SMN axon can not extend as far as PMN ventrally, as they were never observed to make a loop and grow laterally over the muscle surface, as PMN axons did (Myers et al., 1986).

Axon pathfinding is accomplished through the interaction between growth cones and the guidance (attractive or repulsive) cues in the environment. Identifying these cues is important for the understanding of the mechanism of neuromuscular development and motor neuron diseases, such as amyotrophic lateral sclerosis (ALS), as aberrant expression or function of axon guidance proteins may be involved in the pathologic changes and mechanisms (Schmidt et al., 2009). During the last two decades many classes of molecules have been identified that function as motor axon guidance cues, including Netrin and its receptor DCC; Ephrins and their Eph receptors; Slits and their Robo receptors as well as Semaphorins and their co-receptors Neuropilins and Plexins (Colamarino and Tessier-Lavigne, 1995; Brose et al., 1999; Zou et al., 2000; Hammond et al., 2005; Murray et al., 2010). Mapping of optic axons onto the tectum is regulated by gradients of ephrin-As and ephrin-Bs on the tectum and corresponding gradients of receptor expression in retinal ganglion cells (Stuermer and Bastmeyer, 2000). Pathfinding of optic axons along the optic pathway

is controlled by robo2 receptor expression in retinal ganglion cells (RGC), which recognizes the repellent slit guidance molecules in the brain environment. Moreover, the repellent extracellular matrix molecule tenascin-R forms boundaries at the edge of the optic pathway (Fricke et al., 2001; Becker et al., 2003). Over-expression of semaphorin 3A1 or semaphorin 3A2 impaired ventral motor axon outgrowth, suggesting that these molecules are involved in motor axon pathfinding in zebrafish (Roos et al., 1999; Halloran et al., 2000). Anti-sense MO knockdown of plexinA3 or Nrp1a leads to additional exit points from the spinal cord for axons of primary motor neurons and to aberrant branching of motor axons, indicating the importance of the semaphorin guidance system for motor axons. Synergistic effects in combined MO knock-down experiments of *plexinA3* with *sema3A* or *nrp1a* with *sema3A* suggest that PlexinA3 or Nrp1a interact with Sema3A in guiding axon pathfinding (Julia Feldner, 2005; Feldner et al., 2007). A recently published paper found that Netrin, secreted by the muscle pioneers at the horizontal myoseptum, can direct the axon pathfinding of DCC-expressing RoPs (Lim et al., 2011). Several motor axon guidance cues have been identified through mutagenesis screens: *diwanka* (*lh3*) (Zeller and Granato, 1999; Schneider and Granato, 2006) and *unplugged*（Musk）(Zhang and Granato, 2000; Zhang et al., 2001; Zhang et al., 2004; Jing et al., 2010) guide the motor axons along the common path, while *topped* and *stumpy*, revealed as zebrafish collagenXIXa1 (colXIX a1) (Beattie et al., 2000; Rodino-Klapac and Beattie, 2004; Hilario et al., 2010) appear to guide the axons past the first intermediate target, the horizontal myoseptum.

How is motor neuron identity regulated in zebrafish? During spinal cord development in zebrafish, Hh signaling induces the motor neuron progenitor (pMN) domain (defined by expression of olig2), where the first primary and secondary motor neurons and then oligodendrocytes develop (Kimmel et al., 1994; Park et al., 2004). Once motor neurons have formed, different combinations of LIM-homeodomain transcription factors (LIM-HDs) are expressed in motor neurons.

Initially, all PMNs start expressing *islet1*. Later, CaPs downregulate *islet1* expression and start expressing *islet2* instead. MiPs transiently down-regulate *islet1* and continue expressing *islet1* afterwards (Appel et al., 1995; Tokumoto et al., 1995) (Fig.3.2). Thus, primary motoneurons in zebrafish express particular LIM-HD transcription factor codes consisting of different combination of *lim3, islet1* and *islet2* (RoP and MiP express *islet1/lim3,* while CaP and VaP express *islet2/lim3*) during motor axonogenesis (Appel et al., 1995). Islet1 is required for formation of all PMNs as well as neuron specification. In *islet1* MO injected embryos, all the PMN cell bodies are still present even without axonal projections out of the spinal cord. However, some cells co-expressed the interneuron marker GABA together with the motor neuron marker zn-1 after MO injection, indicating that motor neurons partially transdifferentiated (Hutchinson and Eisen, 2006). *Islet2* knock-down by morpholino specifically results in aberrant CaP axon growth, leaving the axon extension of MiP/RoP unaffected (Segawa et al., 2001). Nkx6 controls MiP specification partly by regulating the second phase of *islet1* expression (Hutchinson et al., 2007) (summary in **Table 7**). These data suggest that LIM-HDs contribute to the specification of motor neuron fates, which in turn may control their specific axon pathfinding.

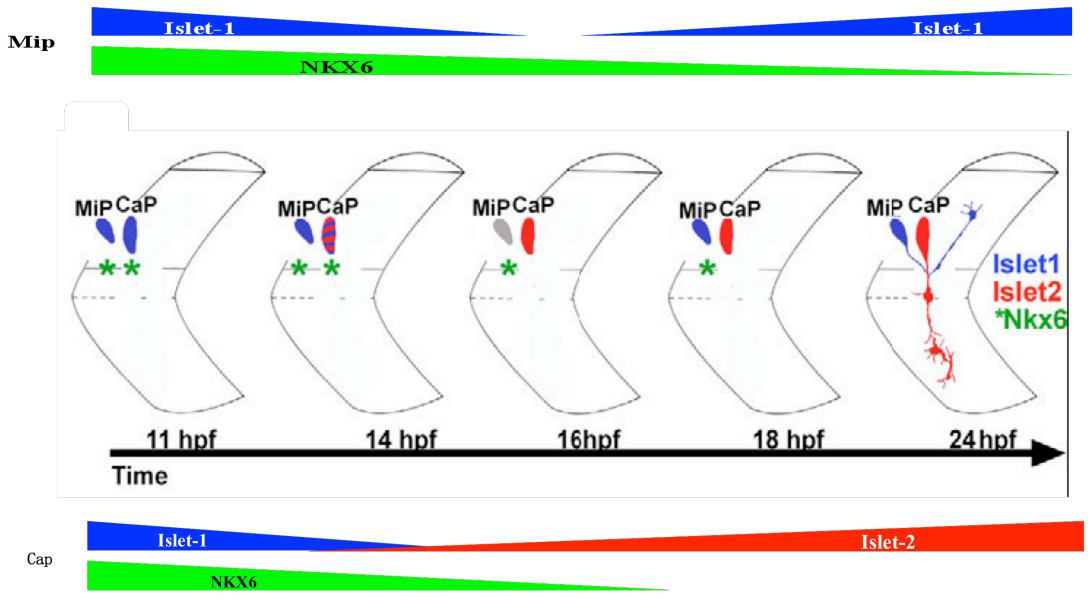

Fig. 3.2 Schematic of Islet1/2 and Nkx6 expression in MiP and CaP neurons between 11hpf and 24hpf. (modified after Hutchinson et al., 2006)

Table 7 *Islet*1/2 and *Nkx6* function in PMN specification and axonal differentiation. (Summarized from Segawa et al. 2001; Hutchinson and Eisen 2006 and Hutchinson et al. 2007)

Islet1	MO	All the PMNs were missing & ventral interneurons increased.
	Function	PMN formation and partially supress interneuron fate
Islet2	MO	CaP axons misbranched or shorter
	Function	CaP axons pathfinding but not for CaP specification;
Nkx6	MO	MiP axons were abnormal and became interneuron-like
	Function	Regulate MiP development by maintaining *islet1* expression

In the sensory nervous system of zebrafish, over-expression of the LIM domain of Islet2 prevents the binding of Islet2 to CLIM, which causes defects in outgrowth of Rohon-Beard (RB) and trigeminal peripheral axons (Segawa et al., 2001). Islet2 is essential for mediating Slit signaling to induce axonal branching of the trigeminal sensory ganglion neurons (Yeo et al., 2004). In parallel, Islet1 is required for the peripheral axon outgrowth of RB neurons (Tanaka et al., 2011). A critical role for CLIM has also been established in axonal outgrowth of peripheral sensory axons of trigeminal and RB neurons by DN-CLIM over-expression (Becker et al., 2002). Thus the LIM-HD signaling pathway is involved in peripheral sensory axon outgrowth.

The data presented above suggest that LIM-HDs can play an important role in axon pathfinding without changing the cell fate. On the other hand, LIM-HDs show specific combinatorial expression in the three PMNs of each hemisegment in zebrafish (Appel et al., 1995). The expression patterns of LIM-HDs in the LMC as well as the corresponding motor axon pathfinding in limb is well studied in amniotes (see chapter 1), but the guidance cues of MMC to axial muscles and hypaxial motor column (HMC) to ventral body wall muscle is still not very clear. All three PMNs in each hemisegment in zebrafish innervate the body wall along specific pathway; therefore the zebrafish provides a good model to study body wall innervation as well as motor axon pathfinding. Moreover, the down-stream genes of LIM-HD transcription complexes that control the motor axon pathway selection as well as the corresponding axon guidance cues are poorly known (Shirasaki and Pfaff, 2002). It is

important to further investigate downstream targets of LIM-HDs, which control motor neuron specification as well as axon pathfinding in zebrafish, in order to gain insight into how LIM-HDs transcription factors act in neuron development as well as axon guidance.

3.1.3 DN-CLIM injected embryos provide us with an excellent research model to find genes involved in motor axon growth and pathfinding

The dominant negative CLIM construct (DN-CLIM) which contains the LIM interaction domain (LID) without the N-terminal dimerization domain (DD), was designed to displace full-length CLIM from LIM-HDs and cause defects in neuron specification and development. When DN-CLIM competes with the endogenous CLIM *in vivo* to bind LIM-HD, neither LIM-HDs nor the down-stream gene transcription can be activated (Fig. 1.2 D). We and other laboratories have found that blocking the activity of LIM-HDs, by over-expressing the dominant-negative co-factor DN-CLIM, prevents motor axon growth out of the spinal cord. DN-CLIM over-expression inhibits transcription of LIM-HD target genes in vitro (Segawa et al., 2001; Becker et al., 2002; Gungor et al., 2007). Overexpression of the LIM interaction domain of CLIM (LID^{CLIM}) and the LIM domain of Islet2 (LIM^{Isl2}) both inhibit Islet2 binding to CLIM *in vitro*. In LID^{CLIM} overexpression embryos, peripheral axons of sensory neurons (Rohon-Beard and Trigeminal neurons) as well as ventral projections of motor neuron are all absent, which shows the same phenotype as overexpression of LIM^{Isl2}. This also reproduces the defects induced by Islet2 MO. These data indirectly suggest that the dominant negative effects of LID^{CLIM} act by interrupting the function of LIM-HDs (Segawa et al., 2001). The analysis in a transgenic fish, in which GFP is expressed under the control of the motor neuron specific promoter *Hb9* (Flanagan-Steet et al., 2005), indicated that motor neurons still differentiated and grew axons after DN-CLIM injection, however, motor axons simply failed to leave the spinal cord, instead they grew caudally along the ventral edge of the spinal cord

(Zhong et al., 2011). We reasoned that the gene expression profile of DN-CLIM treated motor neurons should differ from controls in the expression of genes involved in motor axon pathfinding, while leaving expression of genes involved in motor neuron differentiation (more evidence shown in results in cell identities) and general axon growth less affected. Thus we designed a gene profiling experiment of DN-CLIM treated motor neurons with the aim to find novel guidance receptors of motor axons. A few different tissues have now been successfully Fluorescence-Activated Cell Sorting (FACS) from zebrafish embryos (Covassin et al., 2006; Takizawa et al., 2007; Fan et al., 2008). The FAC sorting procedure (trunk dissection, cells dissociation etc.) does not grossly change the gene expression profile in embryos per se (Cerda et al., 2009). So FAC sorted GFP expressing zebrafish motor neurons for RNA-profiling was used for our aim. This screening procedure is potentially much quicker than more established chemical mutation screens (Birely et al., 2005), because no crossing and raising of fish is required and no positional cloning is needed to identify genes of interest.

In conclusion, gene profiling on isolated GFP^{+} motor neurons by fluorescence-activated flow cell sorting (FACS) with and without prior injection of DN-CLIM mRNA provides us with a promising research tool to retrieve more genes specific for motor axon pathfinding.

3.1.4 Zebrafish as a disease model

The application of zebrafish as a disease model in human medicine has been expanded recently (Fishman, 2001), from inherited diseases, infectious diseases to regenerative and tissue repair models (Alestrom et al., 2006). Because of its well-characterized nervous system and relatively simple neuron-muscular junction organization, zebrafish has developed to be a model for neuronmuscular diseases, such as spinal muscular atrophy (SMA) (McWhorter et al., 2003b) as well as neurodegenerative diseases, such as amyotrophic lateral sclerosis (ALS) (Ramesh et

al. 2010; Sager et al. 2010). Especially, zebrafish have an impressive tissue regeneration capacity at the adult stage (Bernhardt, 1999; Becker et al., 2004) and are capable of regenerating motor neurons after spinal cord lesion (Reimer et al., 2008), which made it an excellent neuron regeneration model. Meanwhile, its small-size embryo, high embryo production and low consumption of expensive drugs make it amenable for high-throughput screening (HTS) in the drug discovery process (Zon and Peterson, 2005).

3.2 Results

3.2.1 Motor neuron identity in DN-CLIM injected zebrafish

We already know that the motor axons of DN-CLIM injected zebrafish did not exit the spinal cord, as DN-CLIM disrupted the function of LIM-HDs, which are important transcription factors for motor neuron development. This provides us with an excellent research model to uncover a gene expression programme that is specific for motor axon pathfinding by comparing gene expression with and without DN-CLIM injection.

We need to test if motor neurons still keep their motor identity even if they only extend axons within the spinal cord after DN-CLIM injection. Therefore, immunohistochemistry was performed to show that HB9:GFP$^+$ cells expressed motor neuron specific proteins (Hb9 and Islet) but not interneuron markers (Pax2 and GABA). Cell quantification in DN-CLIM injected embryos shows 29% fewer HB9:GFP$^+$ cells ($p<0.05$, $n=6$) and 37% fewer HB9$^+$ cells ($p=0.005$, $n=3$) compared with controls, which is accordance with the theory that LIM-HDs can activate *Hb9* expression by binding with the enhancer in vertebrates (Lee et al., 2004) and DN-CLIM may inhibit this activation through interacting with the LIM domain (Fig. 1.2). This indicates that these motor neurons at least in part keep their motor neuron identity even though they cannot grow axons out of the spinal cord under the

influence of DN-CLIM over-expression.

To find out whether these motor neurons are mature, we labelled motor neurons with an antibody to choline acetyltransferase (ChAT), the acetylcholine (ACh)-synthesizing enzyme, which is a mature motor neuron marker (Arvidsson et al., 1997). In DN-CLIM injected embryos without motor axons growing out of the ventral spinal cord, only 21% of the hemi-segments contained ChAT immuno-positive motor neurons, whereas ChAT was expressed in PMNs of all segments in control embryos. Thus, motor neurons in more than half of the hemi-segments without peripheral motor axons fail to express ChAT, which suggests that most PMNs in DN-CLIM injected embryos do not mature and DN-CLIM not only inhibited axon extension out of the spinal cord but also impaired full motor neuron differentiation. ($p<0.001$; PMNs were analysed in 6 embryos for each group, 13 hemi-segments were examined per embryo on average) (Fig. 3.3)

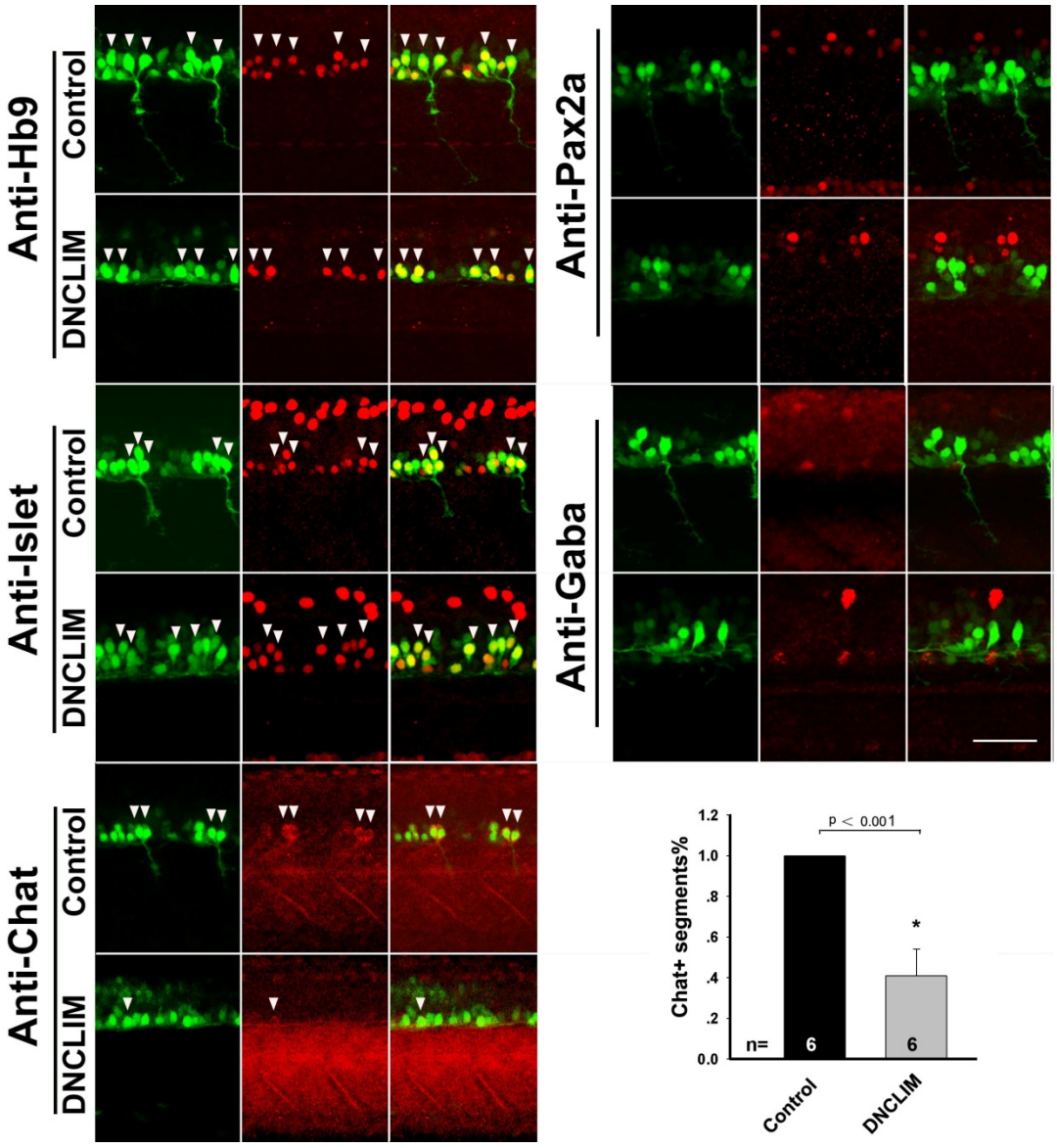

Fig. 3.3 Dominant-negative CLIM (DN-CLIM) abrogates the pathfinding of PMN (primary motor neuron) axons by interfering with LIM transcription factor signalling, while not altering their motor neuron fate. We can see the motor neurons readily grow their axons within the spinal cord after DN-CLIM injection in HB9:GFP transgenic fish. All the motor neurons without axons retain their motor neuron markers (Hb9 & Islet) (white arrowhead) and did not express interneuron markers (Pax2a & GABA). Around 56% less ChAT positive PMN (white arrowhead) without axon extension in DN-CLIM injected embryos compared with uninjected embryos.
Scale bar=50μm. PMNs were analyzed in 6 embryos for each group,
13 hemi-segments were examined per embryos on average.
Rostral is to left and dorsal is up in all the figures unless it is indicated.

3.2.2 Gene expression profiling of FAC-Sorted GFP+ motor neurons in DN-CLIM injected zebrafish.

We hypothesized that receptors for axon guidance molecules involved in correct pathfinding of motor axons may not be expressed in DN-CLIM treated motor neurons that do not manage to navigate the normal motor axon pathway. Indeed we find that DN-CLIM over-expression prevented expression of the functionally important axon guidance receptors Neuropilin-1a (Nrp1a) (Feldner et al., 2005) and PlexinA3 (Feldner et al., 2007) in HB9:GFP transgenic motor neurons. *PlexinA3* and *nrp1a* mRNAs both co-localized with GFP^+ motor neurons in HB9:GFP transgenic zebrafish, but the GFP^+ motor neurons, which only extended their axons within the spinal cord after DN-CLIM injection did not express *plexinA3* and *nrp1a*, as indicated by in situ hybridization. Thus Nrp1a and PlexinA3 are under the control of LIM-HDs. Moreover, this suggests that gene expression profiling of motor neurons in DN-CLIM injected embryos could lead to the identification of additional axon pathfinding receptors by virtue of their reduced expression levels. (Fig. 3.2)

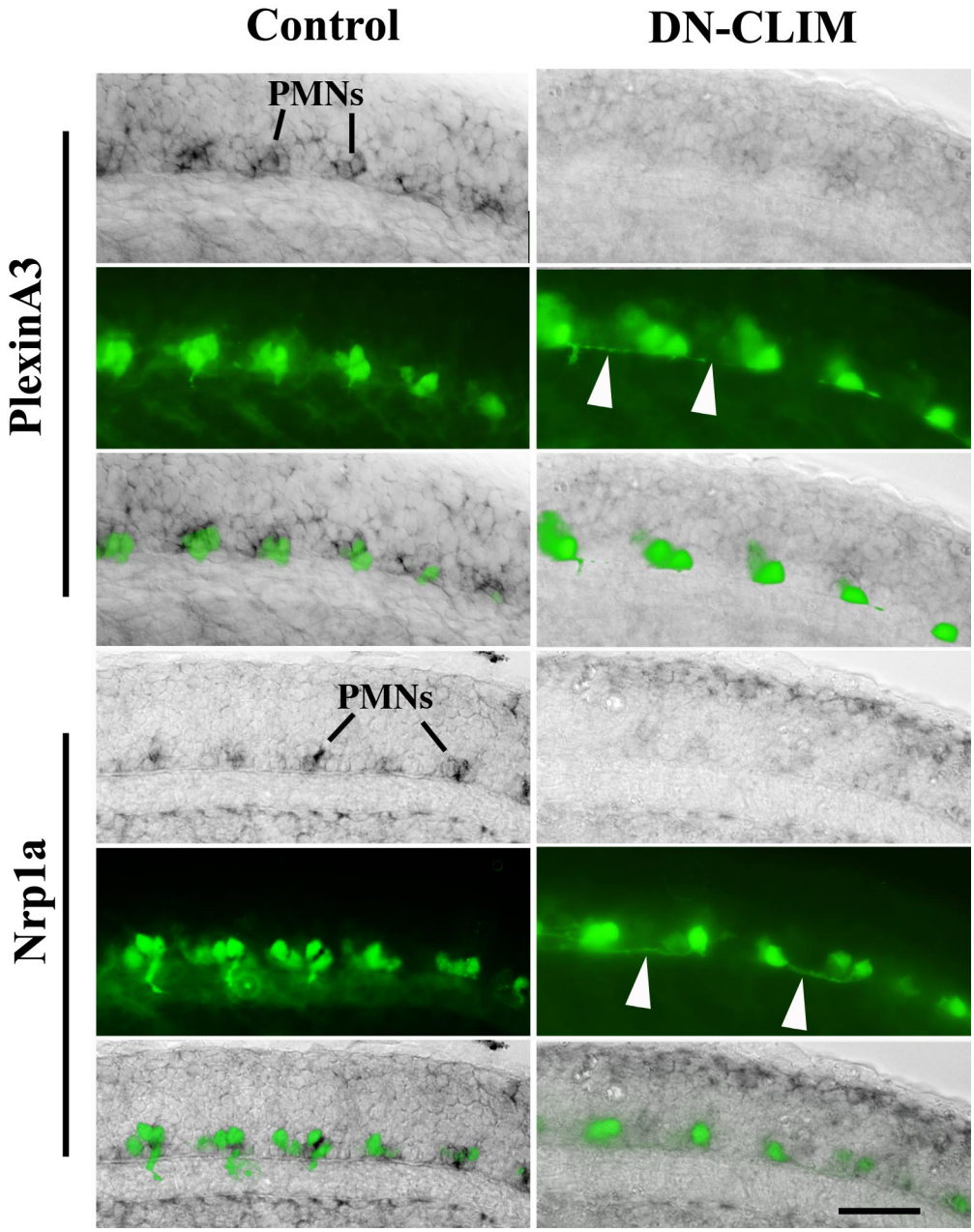

Fig. 3.2 *PlexinA3* and *nrp1a* are down-regulated after DN-CLIM injection, which can work as the internal control in gene array of GFP^{+} cells sorted from DN-CLIM injected HB9:GFP transgenic zebrafish compared with uninjected control. Arrowheads indicate that axons grow within the spinal cord after DN-CLIM injection. PMN: Pirmary motor neuron. Scale bar=50μm

To purify motor neurons in DN-CLIM mRNA injected and uninjected HB9:GFP transgenic embryos (150 embryos per group) at 26 hpf, we dechorionated and dissociated embryos by EDTA-trypsin treatment into single cells at 26 hpf and

subjected the resulting cell suspension to FACS. In my pilot screen I used 150 DN-CLIM mRNA injected embryos, which were pre-sorted embryos without axon extension out of the spinal cord. Embryo dissociation yielded 1 x 10^6 cells, of which 20% were GFP^+ cells. The purity of the GFP^+ fraction was >96%. RNA extracted from these cells (0.4ug) was sufficient for Miltenyi Biotech to produce the present data in two technical replicates (Fig. 3.4). This indicated that 158 genes were significantly down-regulated in GFP+ cells after DN-CLIM injection (**Table 9**). (Fig. 3.3 A)

Unexpectedly, there were many eye specific genes in the list of down-regulated genes. This might have resulted from transgene expression in the eyes, which are completely lost after DN-CLIM injection, hence the strong under-representation of these gene transcripts in DN-CLIM injected embryos. As HB9:GFP transgenic zebrafish express GFP also in a minority of cells in the hindbrain region, I further enriched spinal motor neurons by FAC sorting only cells dissociated from tail tissue (Fig. 3.3B). 600 embryos dissected at the level of hindbrain and tail tissue were processed for FACS, from which 250 000 GFP^+ and 650 000 GFP^- cells were collected and sent for gene array analysis. A gene chip comparing GFP^+ with GFP^- cells in uninjected embryos represents a motor neuron expression profile consisting of 2120 over-represented genes (fold change >2) (data not shown). We cross-correlated the list of genes (158 genes) down-regulated after DN-CLIM injection with this motor neuron expression profile (2120 genes, GFP^+ vs. GFP^- cells) and found that 28 genes down-regulated by DN-CLIM are also enriched in the GFP+ motor neuron expression profile (**Table 8**). Finally, we cross-referenced our gene list with the online expression pattern database (zfin.org).Thus we retrieved 4 down-regulated genes (*calca, nkx1.2lb, tac1, chodl*) with exclusive ventral expression in the spinal cord as potential motor neuron-specific genes.

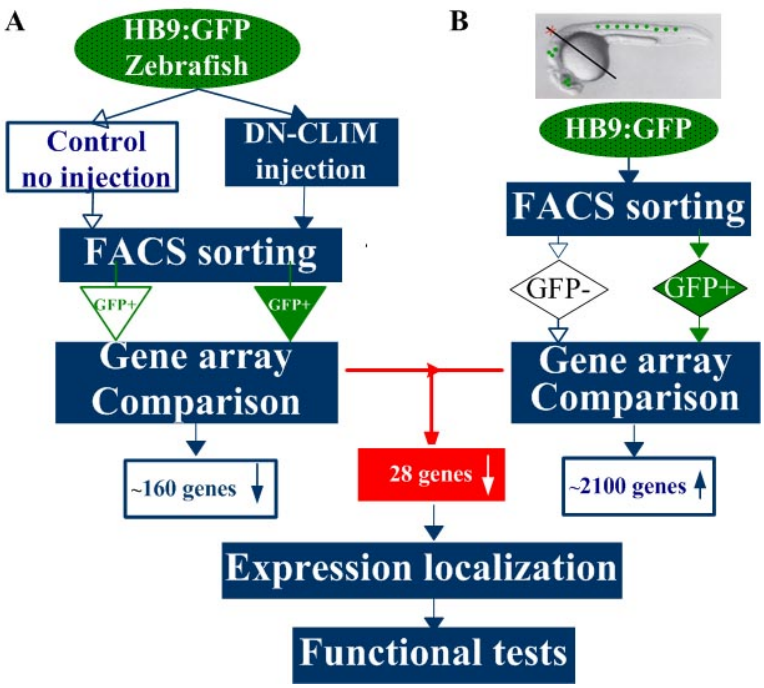

Fig. 3.3 Schematic procedure of gene expression profiling of GFP^+ motor neurons sorted from HB9:GFP transgenic zebrafish. Gene array data from chip A) DN-CLIM injected versus control embryos and chip B) GFP^+ versus GFP^- group in control embryos were cross-correlated and 28 genes, which are potential motor axon guidance genes, were processed for further analysis.

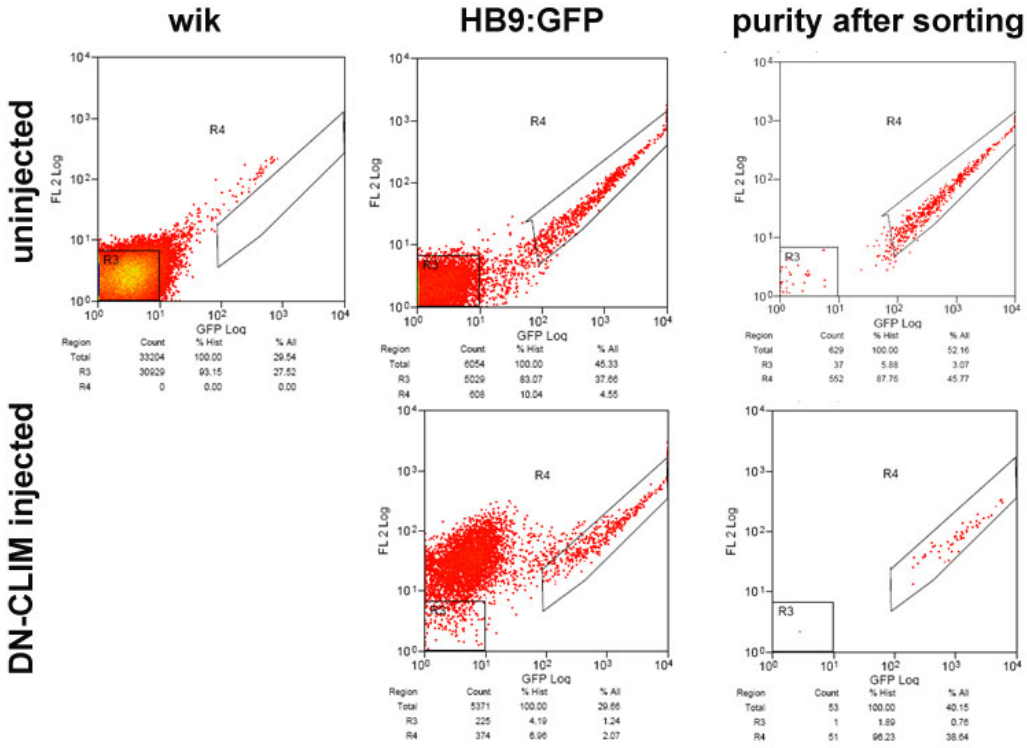

Fig. 3.4 Fluorescence activated cell sorting: GFP^+ motor neurons (indicated as wedge R4 in each box) sorted out of DN-CLIM injected HB9:EGFP zebrafish (purity 96% in bottom right) and uninjected control fish (purity 88% in upper right). The squares (R3) in each box indicate GFP^- cells and rhodamine dextran mixed with DN-CLIM injection leads to a shift of fluorescent cells in middle bottom box. Control in left column is GFP negative cells sorted with wik embryos to equalize the FACS sorting system.

3.2.3 Chodl, Calca and Tac1 are down-stream of LIM-HDs

In situ hybridization was performed in HB9:GFP transgenic zebrafish to verify expression of *chodl, calca, tac1*, and *nkx1.2lb* in motor neurons. *chodl*, *calca* and *tac1* mRNA expression overlapped with HB9:GFP^+ motor neurons of 24hpf embryos (Fig. 3.6). However, *nkx1.2lb* was found in interneurons dorsal to the motor neurons (data not shown) and was therefore excluded from further analysis. *Chodl* and *tac1* appeared to be expressed in the majority of spinal cord motor neurons while *calca* was expressed in only one or two motor neurons per segment. *chodl*, *calca* and *tac1* were all down-regulated after DN-CLIM injection as determined by *in situ* hybridization (Fig. 3.5). This result validates the gene array paradigm and also suggests that *chodl, calca* and *tac1* may play important roles in motor neuron development down-stream of LIM-HD signaling.

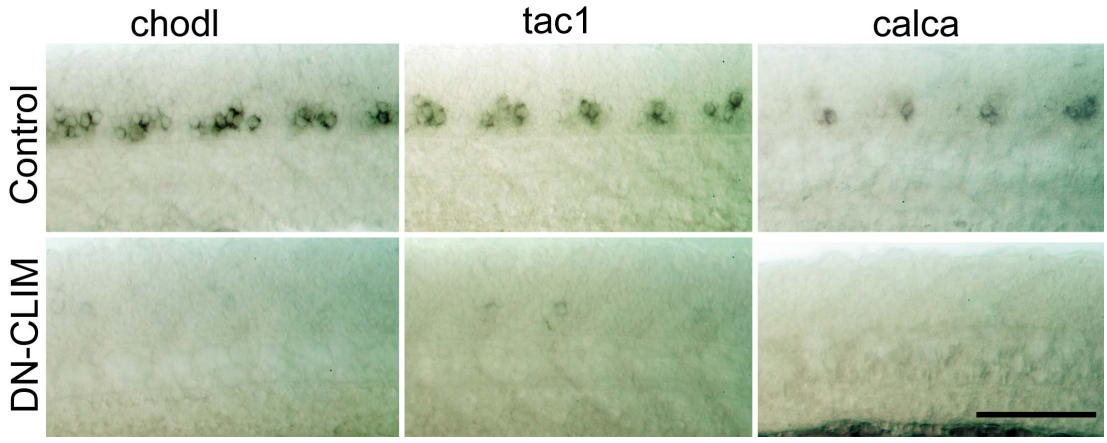

Fig. 3.5 Chondrolectin (*chodl*), tachykinin1 (*tac1*) and calcitonin (*calca*) are three of the most down-regulated genes recovered by the gene screen. We confirmed their

specific expression pattern in spinal cord of 24 hpf embryos and obvious down-regulation after DN-CLIM injection by *in situ* hybridization.
Scale bar= 100μm

Motor neurons in the rostral trunk were developmentally more advanced than those in the tail, corresponding to the developmental gradient of trunk somite formation. We can see motor axon outgrowth of CaP axons in more rostral, older spinal cord segment while in more caudal, younger segments axons have not grown out in 22hpf zebrafish. RNA expression patterns in 22hpf embryos suggest different developmental timing of expression onset of the three genes: *chodl* is the only gene expressed before motor neurons start growing their axons, as its mRNA is expressed in the caudal new-born motor neurons without axons. *tac-1* is expressed just when motor axons grow out of the spinal cord, as mRNA expression is found in the caudal-most segments showing motor axon outgrowth. The last gene to be expressed is *calca,* which is expressed in the more rostral spinal cord, with no expression in the more caudal, younger segments with shorter motor axons. I quantified five embryos (10 segments with CaP axons per animal) for each group and calculated the ratio of motor neurons with mRNA expression to the segments with CaP axons in rostral mature spinal cord. *tac-1* is expressed in 96% of segments with CaP axons and only 66% segments containing CaP axons express *calca*. c*hodl* is expressed in all segments with and without axons (Fig. 3.6). These expression patterns indicate that *chodl* expression, but not *tac-1* or *calca* expression, is initiated before motor axons leave the spinal cord. Thus muscle contact could play a role for the initiation of *tac-1* and *calca* expression, but not for *chodl*.

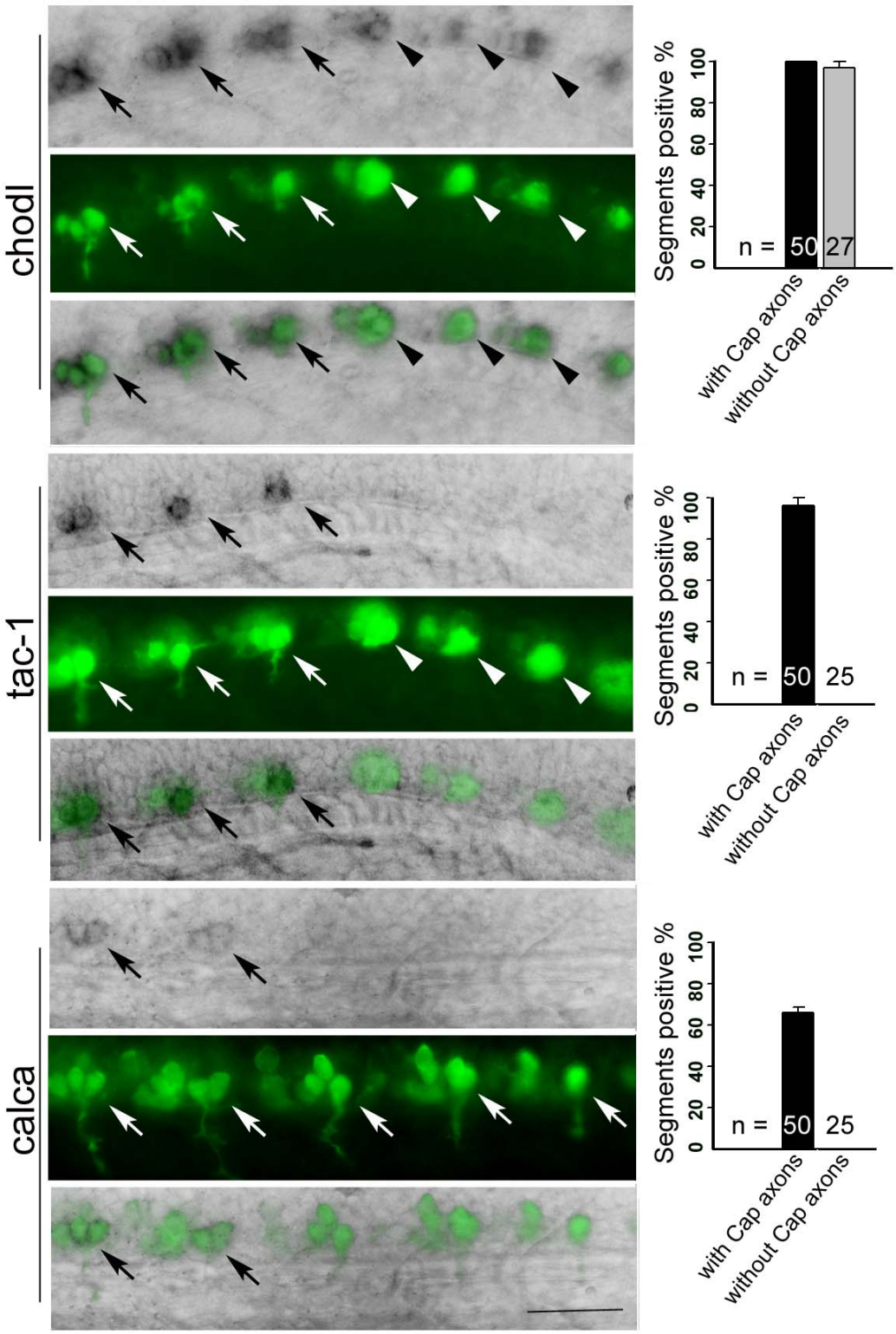

Fig. 3.6 Expression patterns of three novel genes recovered from the gene array. *Chodl* RNA expressed in both rostral (old) and caudal (new-born) spinal cord motor neurons before they started out-growing their axons, while *tac-1* RNA expressed only

after motor axons grew out. The last gene to be expressed was *calca* which was expressed in around half of rostral motor neurons with axons. Graphs show cell in situ hybridization quantification of *chodl, tac-1* and *calca* in MNs (motor neurons) with axons (arrow) compared with MNs without axons (arrowhead). *Chodl, tac-1* and *calca* all co-localized with GFP in 24hpf HB9:GFP transgenic zebrafish. White axons indicate mature motor neurons with CaP axons, while white arrowhead shows the new-born MNs without CaP axons. Black arrows and arrowheads suggest that RNA signals are co-localized with GFP^+ fluorescent signals in HB9:GFP transgenic zebrafish. n=number of segments. Scale bar=50μm.

3.2.4 Chodl is one of the potential axon guidance molecules

We retrieved *chodl* with exclusive expression in motor neurons, as determined by *in situ* hybridisation in HB9:GFP transgenic animals. This expression was lost when DN-CLIM was over-expressed, in turn validating the screening result. Chodl contains a C-type lectin domain, a common recognition motif in adhesion molecules, a signal peptide and a transmembrane domain, thus representing a potential cell surface receptor for guidance factors (Fig. 3.7A). Chodl is highly conserved in vertebrates and protein homology shows 94% identity with chicken and *Xenopus*, and 92% with mouse and human Chodl (Fig. 3.7 B).

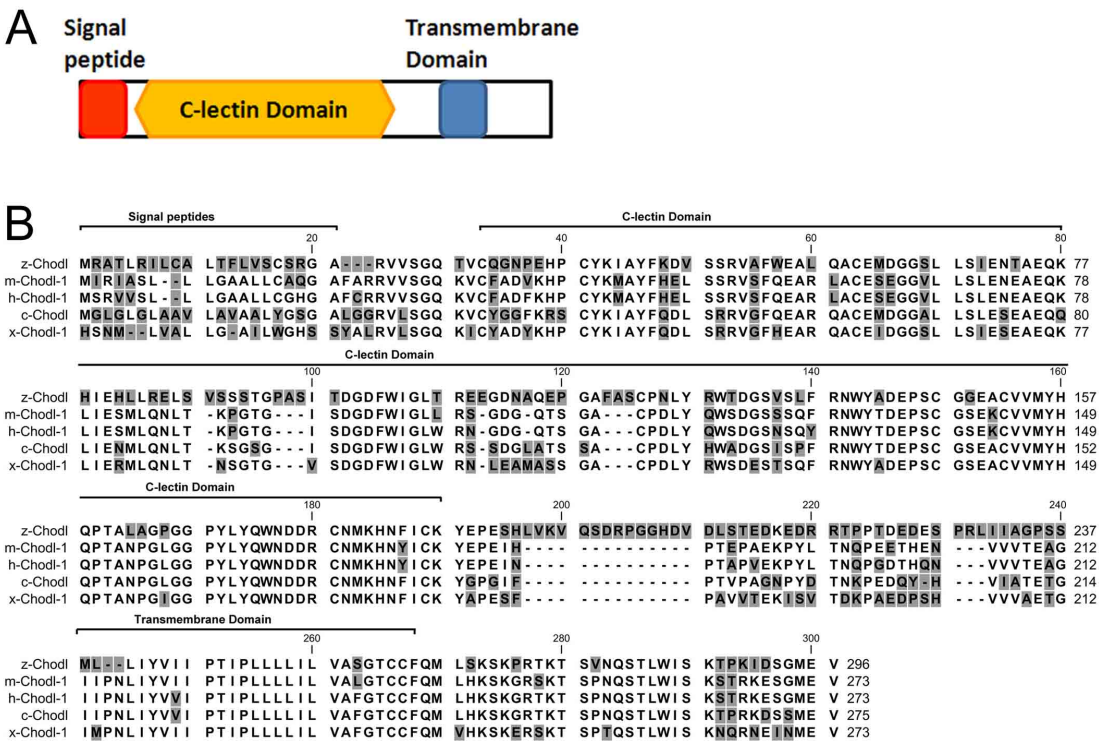

Fig. 3.7 Chondrolectin, a C-type lectin family member, contains a signal peptide and a transmembrane domain and represents a potential cell surface receptor for guidance factors. **A).** Model of Chodl protein contains a signal peptide, a C-lectin Domain and transmembrane domain. **B)**. C-type lectin domain is highly conserved in vertebrates. Sequence comparisons reveal that zebrafish Chodl (zChodl) shares 92% total a.a. identity with mouse (mChodl) or human (hChodl) and 94% with chick (cChodl) or *Xenopus* (xChodl) protein.

3.2.4.1 Chodl functions in CaP axon guidance

Chodl is expressed in motor neurons from 12hpf, 2-3 hours after primary motor neurons were born and embryo retained the *chodl* expression until 24hpf when PMN almost finished their axon projection, which suggests that chodl functions during PMN axon pathfinding. We also noticed *chodl* expressed in trigeminal ganglion cell and transiently in the dorsal spinal cord from 12hpf to 20hpf. (Fig. 3.8)

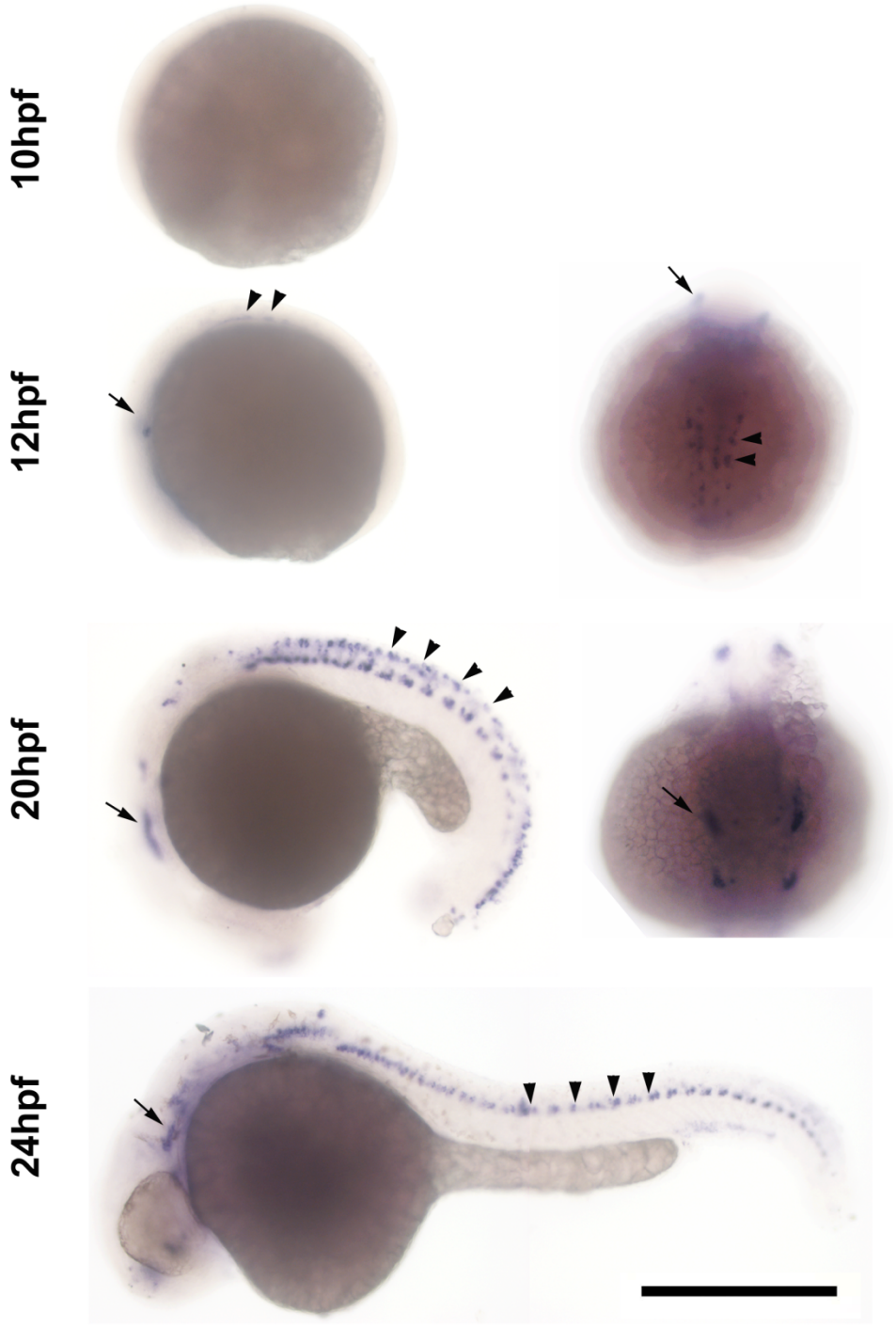

Fig.3.8 *Chodl* expression pattern during zebrafish development. *Chodl* starts expressing in motor neurons (arrowhead) from 12hpf when motor neurons are born and expression is retained until 24hpf when primary motor neurons almost finish their axon projection. *chodl* is also expressed in trigeminal ganglion cells as indicated by black arrow.
Scale bar=500μm

I performed morpholino (MO) knock down studies using two kinds of morpholinos (two splice-inhibiting MOs: MO1 and MO2, one translation-blocking MO: MO3), which show identical phenotypes, namely shorter CaP axons (Fig. 3.9). A single splice-inhibiting MO (1mM) elicits a weak phenotype (6.4% or 13% of shorter CaP axons by MO1 or MO2, respectively), while the two splice-inhibiting MOs co-injected at an intermediate dose (0.5 mM for each) induces significant synergistic effects ($p<0.05$, 34% of truncated CaP axons). We found that 95% of all CaP motor axons were shorter after MO3 injection (1mM) compared with control MO injection (Con MO). MO knockdown effects are dosage dependent, as 54.3% CaP axons are shorter with 0.5mM MO3 injection. The lateral line nerve primordium, generally used to stage embryos (Kimmel et al., 1995), grows unaltered in MO-injected embryos, indicating that MO injections do not retard overall development of embryos (trunk segment 4.8±0.18 was reached in control morpholino treated embryos and trunk segment 4.4 ±0.15 in Chodl morphants; $n > 40$; $P = 0.1$; Fig. 3.9).

I also verified the efficacy of splice-inhibiting MOs by RT-PCR (Fig. 3.9). The two splice-inhibiting MOs are designed to bind e2i2 and i1e2 separately and both target to exon2 from the transcript, resulting in a non-functional protein with a translational frame shift. Injection of combined MO1 with MO2 resulted in an ectopic band compared with control MO injection, while the single MO (MO1 or MO2) injection only produces a weaker wild-type band without a shorter band.

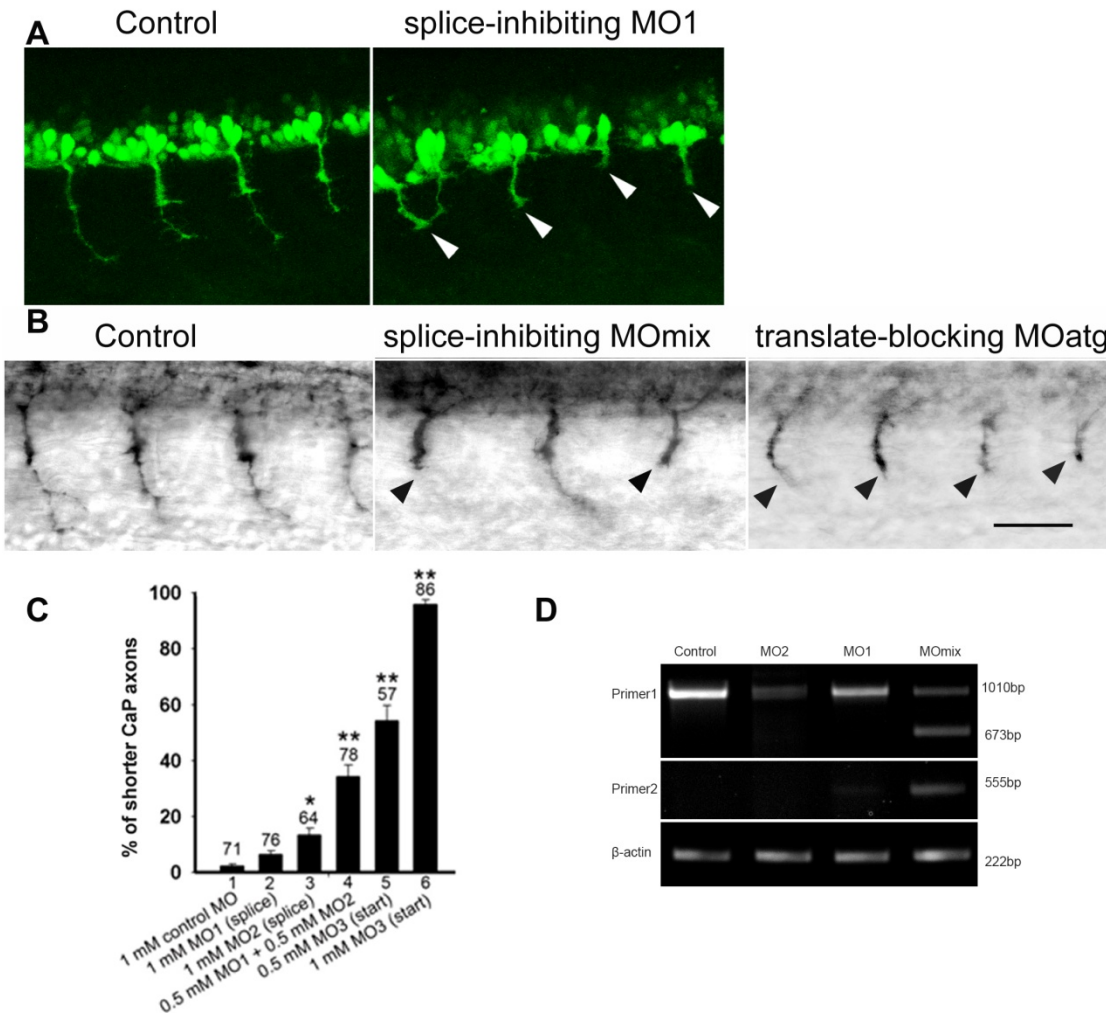

Fig. 3.9 Morpholino knock-down results in shorter CaP axons in 24hpf zebrafish. **A**. Lateral views at mid-trunk level of 24hpf HB9:GFP transgenic zebrafish. CaP motor axons (arrows) grow ventrally out of the spinal cord in control morpholino injected embryos. Most of the CaP axons were shorter in Chodl morphants (white arrowhead). **B**. We performed morpholino (MO) knock down studies using two splice-inhibiting MO1 & MO2 and a translate-blocking MO3. Lateral views at mid-trunk level of zebrafish Cap axons stained by Znp1 antibody. Arrowhead indicates short axons in morphants. **C**. Quantification of short Cap axons shows effects of splice-inhibiting MO (column2,3,4) and translation-blocking MO (column5&6), indicating a synergism and a dose-dependency effect. *P < 0.05; **P < 0.01; ANOVA **D**. Verification of the efficacy of splice-inhibiting MOs by RT-PCR. Both splice-inhibiting MOs are designed to target exon2 of the transcript and both can reduce levels of correctly spliced *chodl* (data not shown), but only combining MO1 with MO2 resulted in an ectopic band. Beta-actin was used to equalize cDNA concentrations. Scale bar=50μm

A single MO can sometimes produce a population of different mRNAs including intron insertion due to activation of a cryptic splice site (Draper et al., 2001). While intron2 is over 2000bp, which is too long to amplify with primers in exon1&exon3, so we cannot detect extra bands apart from weaker wild-type band. I designed primer in intron2/exon7 to test if there is intron2 insertion and RT-PCR shows there is a band with single splice-inhibiting MO1 knock-down, which suggest MO1 (e2i2) results in a fully or partially intron2 insertion. The synergistic effect of MO1 and MO2 results in an ectopic shorter band because of the exclusion of exon2, while the intron2 insertion still happens, as indicated by amplification of a band when using primers located in intron2/exon7 (Fig. 3.9), which further verified the varied effects of splice-inhibiting morpholinos. This is not unexpected, since a morpholino oligonucleotide directed against any splice junction is expected to generate either a complete or partial single exon deletion or a complete or partial single intron insertion (gene-tools.com). (Fig. 3.10)

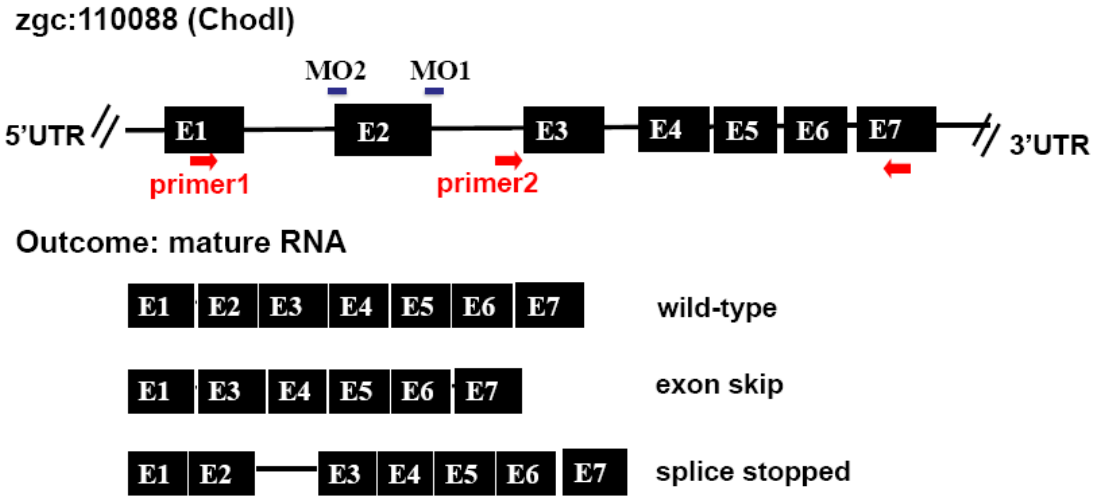

Fig. 3.10 Splice-inhibiting MOs (MO1 and MO2) are designed to exclude exon2 (E2: 337bp) by binding with e2i2 and i1e2 separately. Variable effects were identified when splice-inhibiting MOs were applied. Intron2 was partially or completely inserted in the transcript RNA after splice-inhibiting MO knock-down as we can see a band amplified with a pair of primers located in intron2 and exon7 compared with control. The primer pair in exon1 and exon7 did not produce a band presumably, because the sequence with the intron insertion (over 2000bp) was too big to be amplified.

Western blot (hybridized with antiserum A) shows the whole Chodl protein full-length (32.7kDa) as well as different isoforms (between 26kDa and 20 kDa) are all down regulated by MO injection. There are at least another 3 in-frame ATG translational start sites downstream of the first start codon, which can translate alternative isoforms (Fig. 3.11). The preimmunio serum shows the same pattern as the antibody pattern in western blot (data not shown), combined with that these two custom antibodies both cannot recognize specific antigen in zebrafish by immunofluorescence except these unspecific signal in dorsal spinal cord which did not show intensity change after MO knock down (data not shown), we can make a conclusion that these two custom antibodies cannot work specifically.

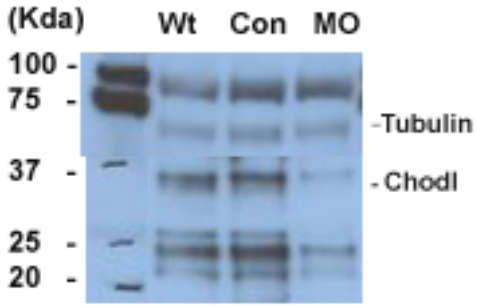

Fig. 3.11 Western blot hybridized with whole protein from 24hpf embryos. The full length Chodl protein (32.7 kDa) as well as alternative isoforms (from around 20kDa to 26kDa) are all downregulated in Morphant compared with control. Tubulin (55kDa) is used to equalize whole protein quantity among different group. Wt: HB:GFP embryos without injection. Con: control MO injected embryos. MO: Chodl MO injected embryos. (Translation-blocking and splice- inhibiting MOs mixture).

3.2.4.2 Chodl is necessary for the CaP axon to grow past the horizontal myoseptum through the ventral pathway

To trace CaP axon pathfinding over time following MO knock-down, I labeled CaPs in wildtype and morphant at 24 and 33 hpf with znp-1 antibody. A prominent varicosity is present when CaP axons pass the horizontal myoseptum (HM) and remains there during further axon growth. The position of the HM can also be traced

by muscle pioneer cells which are 4D9 positive. This thickening of the axon and 4D9 antibody staining both can be used as a visual landmark for HM position. CaP axons were classified by their position relative to the horizontal myoseptum (HM) as unaffected, HM-, HM and HM+ (**Table 6**).

To determine which of the different phases of axon growth were affected by the knock down resulting in shorter axons, we categorized axon lengths. Already at 24 hpf almost all axons had grown ventrally beyond the horizontal myoseptum. At 24 hpf (4.3%) and 33 hpf (1.7%), few axons had not reached the horizontal myoseptum in morphants. Strikingly, 34.6% of the axons had extended only to the position of the horizontal myoseptum, significantly more than in control morpholino injected embryos (0.2%) at 24 hpf. At 33 hpf, 31.3% of the segments still showed axons at the level of the horizontal myoseptum. This was not significantly different from the proportion at 24 hpf, suggesting that almost a third of the CaP axons were completely arrested at the horizontal myoseptum over the observation period. At 24 hpf, 54% of the axons had grown beyond the horizontal myoseptum but were not of wild-type length and only 8% appeared to be of normal length. At 33 hpf, 39% of the axons - almost five times more than at 24 hpf - were of normal length, suggesting that axons grew relatively quickly once they passed the horizontal myoseptum. Combined, this distribution of axon lengths indicates that axons reach the horizontal myoseptum similar to controls and then spend a disproportionally long time at the horizontal myoseptum to either continue growth or stop at the horizontal myoseptum (Fig. 3.12).

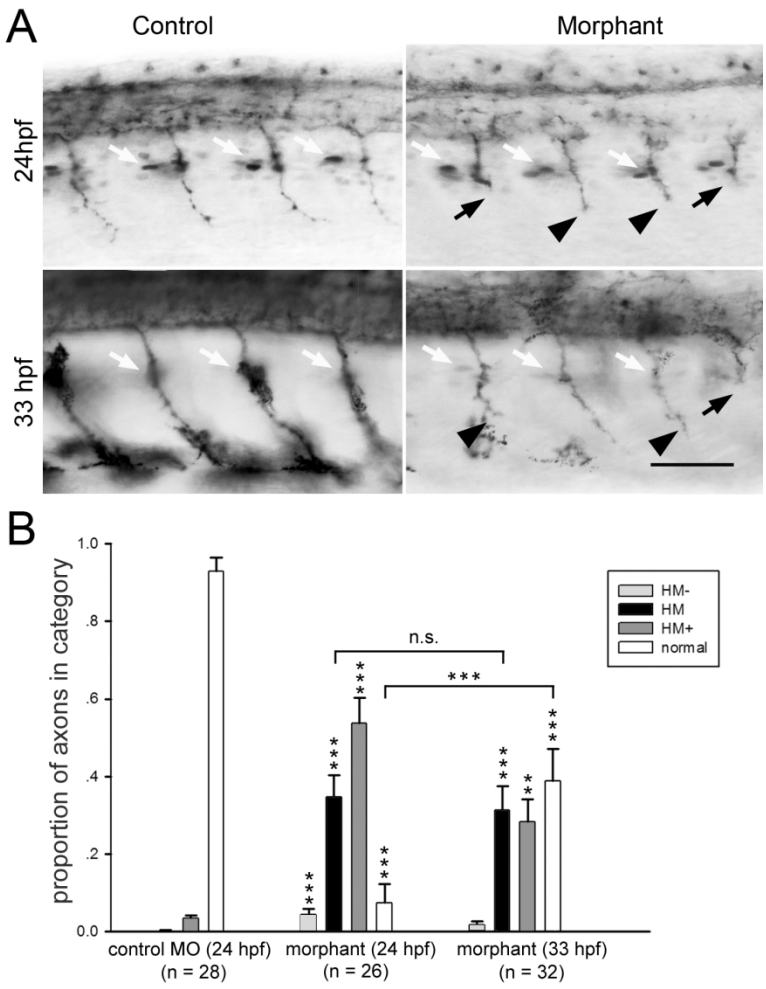

Fig. 3.12 Classification of axon defects by Chodl MO knockdown in 24hpf and 33hpf zebrafish. Axons stall preferentially at the horizontal myoseptum in *chodl* morphants. (control: 1mM control morpholino; morphant: 1 mM MO3, for all panels) 1mM control morpholino; morphant: 1 mM MO3) **A:** Lateral trunk views at 24 and 33 hpf are shown (orientation as in Fig. 1A). The position of the horizontal myoseptum is revealed by engrailed immuno-labeled muscle pioneer cells and axons are labeled by znp-1. The position of the horizontal myoseptum is indicated by white arrows. At 33 hpf, muscle pioneer cells are not always visible because they are located in a different focal plane. Axons that are stalled at the horizontal myoseptum are indicated by black arrows. Axons that have grown beyond it, but are still shorter than in controls, are indicated by arrowheads. Scale bar= 50μm.

Confocal time-lapse imaging was used to analyse axon outgrowth from 18h pf to 27 hpf, when only the CaP axons projects into the ventral myotome (Beattie, 2000). CaP axon growth velocity was determined based on the axon length quantification in

time-lapse still images. To analyse the spatial and temporal detail of CaP axon projection, I divided CaP axon outgrowth into three phases according to the axon growth velocity: CaP axons grew at a similar velocity between control and morphant (Morphant1) before they arrived at HM (control: 7.1±0.7μm/h, n=4 axons; morphant: 8.3±1.2 μm/h, n=8 axons ;p=0.54). Axon growth slowed down in control (5.4±1.3μm/h, n=4) and morphant embryos (4.1±0.8um/h, n=6) during navigation in HM area. After they exited the HM, CaP axons started with higher speed to project towards the ventral edge of the myoseptum (control=9.6±1.2 um/h, n=4; morphant: 10.5±2.6 um/h, n=3; P = 0.7). This is in agreement with the first report of CaP axon average growth speed (7.1±1.3μm/h)(Myers et al., 1986). We observed significant differences in axon length between two the groups from 24.5hpf (Two Way Analysis of Variance, $p < 0.05$) as morphant axons remain in HM significantly longer (4.5hours from 21 to 25.5hpf) than control axons (3 hours from 21 to 24hpf). Live-imaging demonstrates that Chodl is an important guidance receptor which can lead CaP axons past the horizontal myoseptum (Fig. 3.13 *stalling*).

There is another phenotype of morphant axons which cannot pass the HM choice point, in contrast, their growth cones expanded then dissolved, and finally disappeared in the ventral myotome after 24 hpf (n=4). (Fig. 3.13 *stopping*)

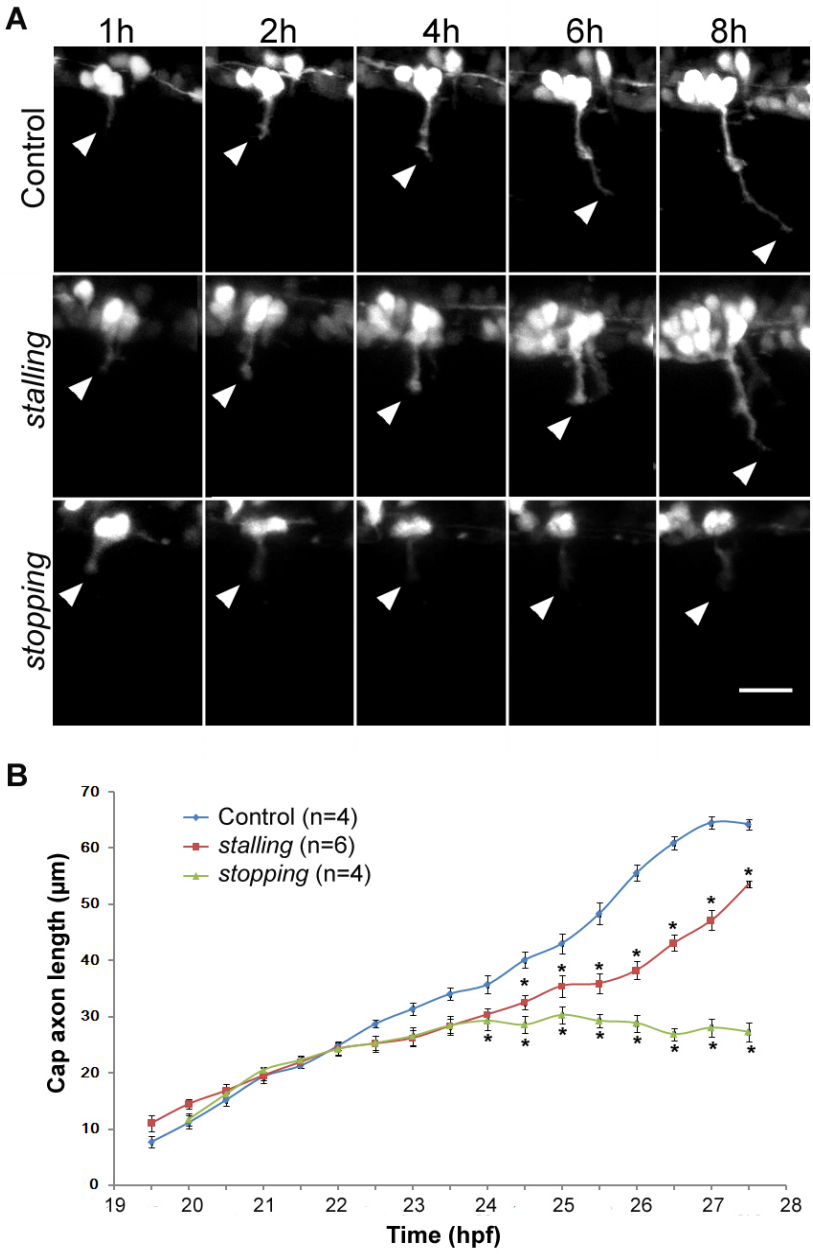

Fig. 3.13 A) Still images from time-lapse movies show the growth of single CaP axons from the spinal cord into the myotome. Morphant axons delayed while passing the horizontal myoseptum (case 1 and case 2) compared with the control. Case1 sped up after passing HM while case 2 axons stalled in HM and dissolved after 24hpf, representing a serious knock-down. n=axons number. (Two CaP axons were analysized in each embryo) B) Cap axon growth speeds (axon length quantification) were analysed based on time-lapse with ZEN2009. All the axons grew at a similar speed from the start and morphants slowed down during HM. The growth speed starts showing significant difference at 390min between morphant and control as morphant still stay in the HM for a while after the controls have passed it. (Two Way Analysis of Variance, $p < 0.1$) scale bar=20µm

3.2.4.3 Chodl is also required for MiP axon dorsal projection

As CaP axon projection to the ventral myotome was delayed by knocking down Chodl with morpholinos, this suggested that Chodl functions as a ventral motor axon guidance molecule. As Chodl is expressed in all the primary motor neurons before axon extension (Fig. 3. 5 and 3.6), we investigated if it is required for MiP axon extension as well. Motor axons were labeled with the znp1 antibody and scanned by confocal microscope. In morphant embryos, some MiP axons were shorter, some curved and some were missing within the strong fluorescence background of the spinal cord. 46% of MiP axons were affected following 1mM Chodl MO3 injection (Fig. 3.14). So Chodl might guide both ventral axon and dorsal axon pathfinding at HM, the pivotal choice point.

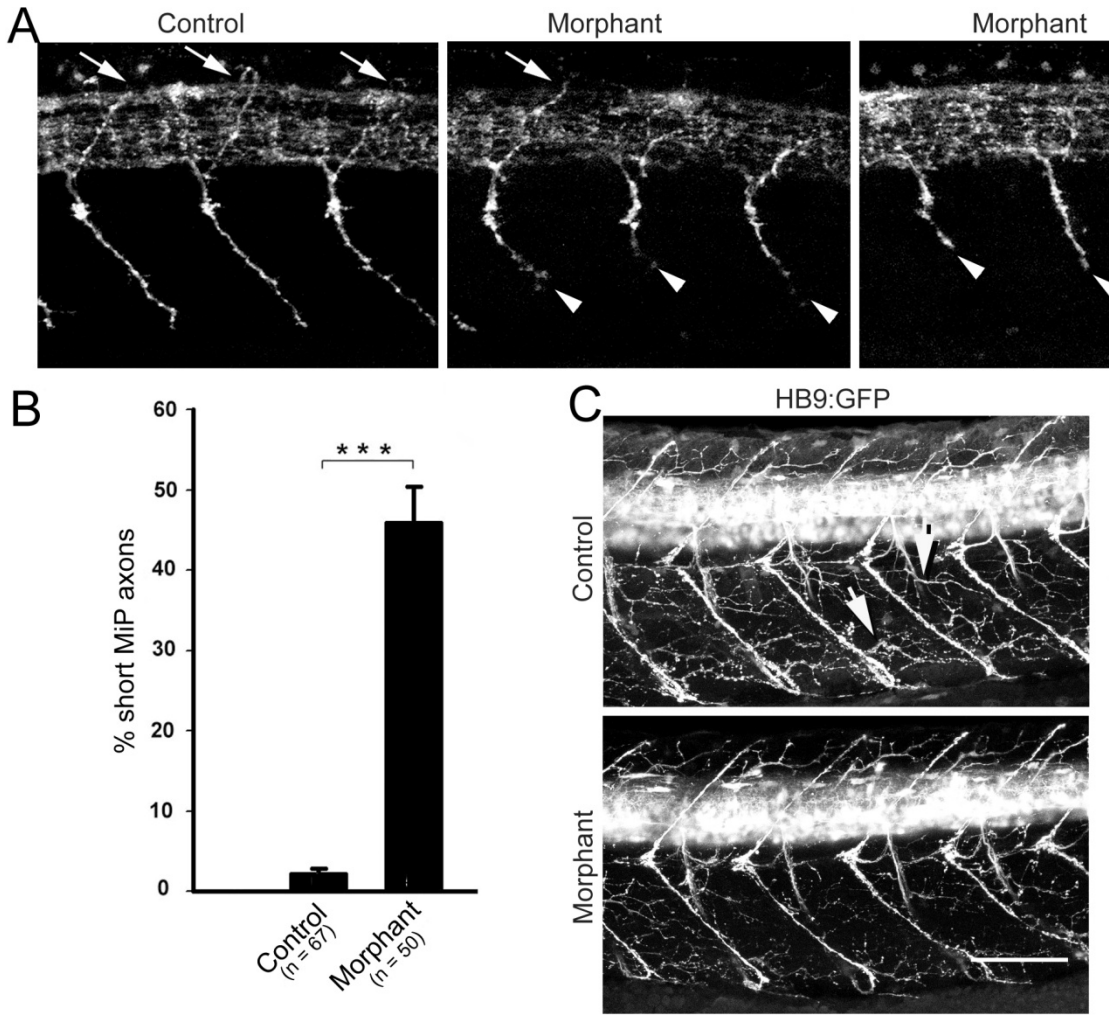

Fig. 3.14 Chodl Morpholino knock-down affects Mip axons growth and reducing the branching of motor axons on myotoms at the later developmental stage. A) Lateral views at mid-trunk level of 33hpf HB9:GFP transgenic zebrafish. Motor axons are stained with znp1 antibody. CaP motor axons grow ventrally and MiP axons grow dorsally out of the spinal cord in control morpholino injected embryos. Most of the CaP axons are shorter in morphants (arrowhead) compared with control. MO also affects MiP axon growth (arrow indicates the normal axon growth which arrives at the top level of the spinal cord border). Some of the MIP axons are shorter, and some of them are either missing or so short that they cannot be discerned against the underlying strong fluorescence of the spinal cord. Scale bar= 50μm. B) Quantification of shorter or missed Mip axons in morphants is around 45%. MiP axons were analyzed over 50 embryos in each group, and 16 hemi-segments were examined per embryo. C) Lateral view of 72hpf embryos shows reduced motor axon branching in myotoms in morpant. Two examples of axon branching was picked by arrows in control. Scale bar= 80μm.

3.2.4.4 Chodl affected secondary motor axon pathfinding

I examined the effect of *chodl* MO on secondary motor axon pathfinding by zn-5 monoclonal antibody, which recognizes the DM-GRASP (Fashena and Westerfield, 1999; Ott et al., 2001). In control embryos, zn-5 antibody stained the secondary motor neurons and axons at 33hpf, which arrived at the ventral edge of myotome with branching. While in *chodl* morphants, some of the ventral secondary motor axons did not reach HM or stalled at HM, some of them passed the HM but did not reach the the ventral edge of myotome (Fig.3.15). Although the secondary motor axons can navigate correctly when the primary motor neurons are ablated (Eisen et al., 1989), they do follow the paths of the primary axons (Myers et al., 1986), and perturbations that affect the primary axons can also affect the secondary axons (Beattie et al., 2000; Zhang et al., 2001). Chodl prevents axon pathfinding of both primary and secondary motor axons.

To assess later effects of *chodl* knock down I observed branching of motor axons onto the myotomes in HB9:GFP transgenic animals at 72 hpf. Indeed, the density of motor axons at this time point was still reduced compared to control morpholino

injected animals (Fig. 3.14 C). Thus, *chodl* knock impairs growth of motor axons for at least 72 hpf.

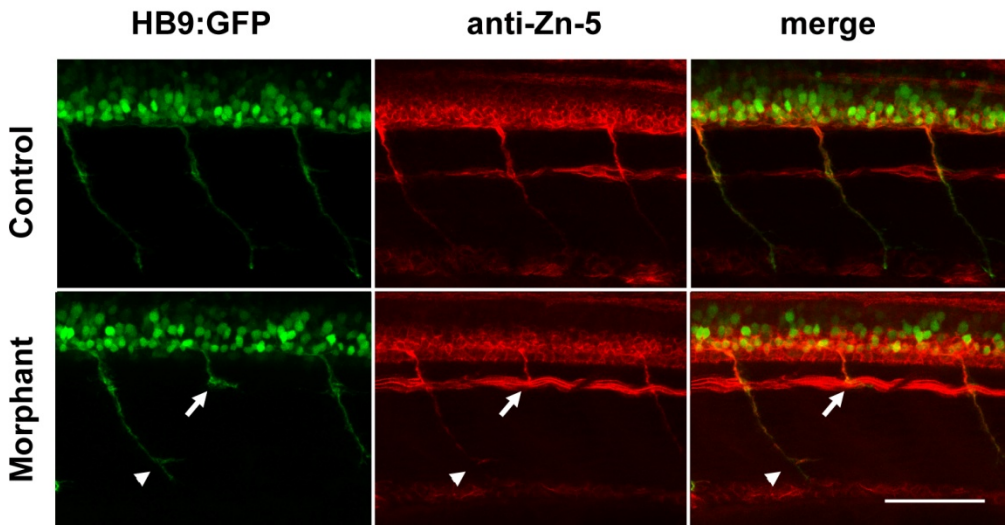

Fig.3.15 Chodl prevents the secondary motor axon pathfinding. In control, zn-5 antibody stained the secondary motor neurons and axons at 33hpf in HB9:GFP transgenic zebrafish embryos, which arrived at the ventral edge of myoseptum with branching. While in *chodl* morphants, some of the ventral secondary motor axons were shorter than HM (arrow), some of them passed the HM but cannot reach the edge of the ventral edge of myoseptum (arrowhead). Scale bar= 50μm.

3.2.4.5 Chodl guides motor axon pathfinding without affecting synaptogenesis

It has been found that in vertebrates, including zebrafish, acetylcholine receptors (AChR) are arranged in prepatterned clusters along the prospective path of the motor axons before the axons reach these points. Pre-existing AChR clusters are integrated into mature neuro-muscular synapses upon arrival of the axon (Kummer et al., 2006). Time-lapse analysis has shown that when filopodia contact a pre-existing AChR cluster，these contacts are selectively stabilized and newly formed filopodia are extended into the central band of AChR clusters, followed by the advance of the growth cone (Fumio Nakamura, 2000; Flanagan-Steet et al., 2005). This implies a guidance function of prepatterned synaptic sites (Vock et al., 2008).To test if Chodl

affects synaptogenesis which could result in aberrant axon guidance, acetylcholine receptors (AChR) were labelled by bungarotoxin. We can see synapses are formed along the CaP and MiP axon pathway in 33hpf embryos and no difference in the synapses morphology was observed between control and morphant, suggesting that Chodl guides motor axon pathfinding not by affecting synapse formation (Fig3.16).

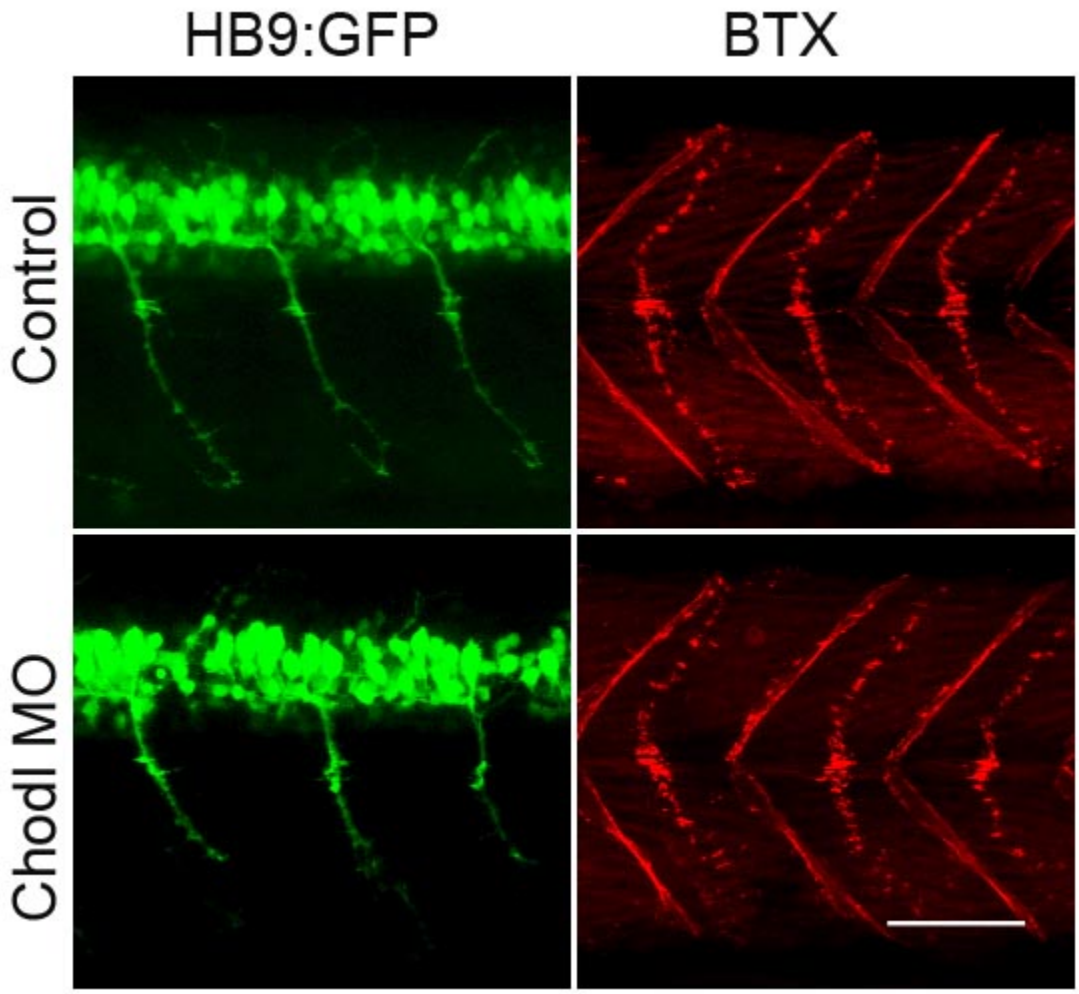

Fig. 3.16 Lateral views at mid-trunk level of 33 hpf HB9:GFP transgenic zebrafish. Chondrolectin morphants with truncated CaP motor axons show no difference in synapse development by BTX (fluorescently labelled bungarotoxin) labeling. Scale bar=50μm

3.2.4.6 RNA over expression and rescue experiment

Full-length *chodl* gene was cloned and ligated with pcDNA3-IRES-EGFP bicistronic vector (Fig.2.2 gifted by Dr. Lee Tan, Fudan University). RNA in vitro transcription was performed with mMessage mMachine (Ambion, Huntingdon, England), and RNA was injected to 1-2 cell stage HB9:GFP transgenic embryos. To find out if RNA can rescue the effect by gene knock-down, chodl RNA injected with start-codon MO together was compared with injection by control RNA and MO. Injected embryos were fixed at 24hpf and motor axons were quantified according to the GFP transgene fluorescence.

In chodl RNA over-expression embryos, we can see ubiquitous GFP expression in whole embryos, and only 31% axons were of wild-type length which is significant difference ($p<0.001$) compared with 75% of wild-type length axons in control RNA injected embryos. This suggests the ubiquitous chodl RNA over-expression perturbs the growth of motor axons in proportion (Fig3.17A,B).

In RNA rescue experiment, when MO (0.5mM) co-injected with control RNA, only 16.5% axons were of wild-type length. In contrast, co-injection with chodl RNA results in ~3 times more axons of wild-type length (57%), which was significant highly difference ($p<0.001$). So chodl RNA can partially rescue the morphant by MO knock-down. Combined results indicate that the level of Chodl is critical for motor axon correct growth (Fig3.17 C,D).

3.2.4.7 Chodl genetically interacts with Col Ⅸ in intermediate target

Chodl morphant is strongly resemble Stumpy/ Col Ⅸ mutant and this ECM component localized in horizontal myoseptum, which suggests that Chodl could be involved in Col Ⅸ interactions of growth cone at the horizontal myoseptum. To test this hyperthesis, I co-injected the Chodl MO with Col Ⅸ MO and find out there is a synergistic effect. 0.25mM Chodl MO3 caused 9.7% axons stall at horizontal

myoseptum and 0.5mM Col Ⅸ MO caused 1.6% axons stall, while combined Chodl MO3(0.25mM) and Col Ⅸ(0.5mM) MO results in 39% axons stalling at horizontal myoseptum. This was a significant difference from single MO injection and almost 3.5 fold more than the theoretical additive effect of 11.3% ($p<0.0001$) (Fig.3.17 E,F).

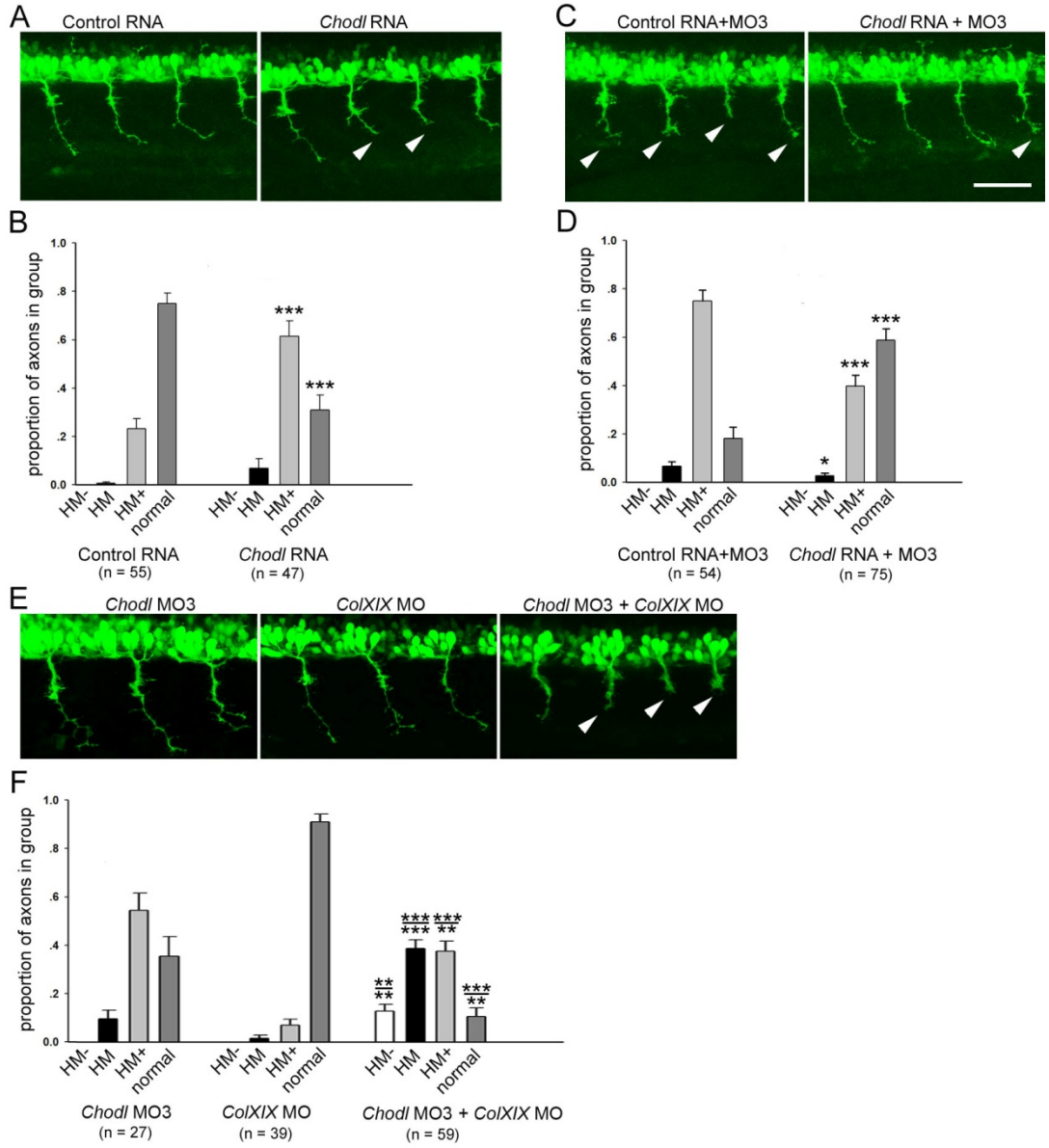

Fig.3.17 C*hodl* morpholino effects are rescued by mRNA over-expression and show synergistic effects with *colXIX* morpholino. Lateral trunk views of HB9:GFP transgenic embryos are shown. Categories in B, D and F are the same as in Fig. 3.12. **A,B:** Injection of *chodl* mRNA alone induces shorter CaP axons (arrowheads in A). **C,D:** Shorter axons induced by *chodl* MO3 (arrowheads in C) are rescued by *chodl*

RNA. **E,F:** Combining low concentrations of *chodl* MO3 (0.25 mM) and *colXIX* morpholino (0.5 mM) synergistically stalls axons at the horizontal myoseptum. All categories in double-morpholino treatment are significantly different from both single morpholinos, indicated by two rows of asterisks (top row: significance against *chodl* MO3, bottom row: significance against *colXIX* morpholino) *P < 0.05; **P< 0.01; ***P < 0.001. Scale bar in C= 50 μm for A,C,E.

3.3 Discussion

3.3.1 DN-CLIM blocks motor axon pathfinding but does not change the motor neuron fate

Primary motor neurons cannot grow their axons out of the spinal cord and extend their axons within the spinal cord after DN-CLIM injection, which is the consequence that DNCLIM competes with endogenous CLIM to bind with LIM domains of LIM-HDs and blocks the downstream gene transicription of LIM-HDs. Immunofluorescence showed that motor neurons without axon outgrowth from the spinal cord still expressed Hb9 and Islet1/2 motor neuron markers but not Pax2a and GABA interneuron markers, suggesting that these cells kept their motor neuron identity. In our approach we reasoned that HB9:GFP+ neurons may retain expression of genes needed to maintain motor neuron identity to a certain degree and general axon growth after DN-CLIM treatment. Thus, genes involved in motor axon navigation should be enriched in the list of down-regulated genes after DN-CLIM treatment. Lower numbers of $HB9^{+}$ and GFP^{+} motor neurons after DN-CLIM injection suggests that fewer Hb9 expressing cells were born or that cell death occurred under the influence of DN-CLIM over-expression. We observed significant down-regulation of ChAT expression, which is a marker for mature motor neurons. Given that combinatorial expression of LIM-HD factors controls motor neuron fate in vertebrates (Tsuchida et al., 1994; Pfaff et al., 1996), including zebrafish (Inoue et al., 1994; Appel et al., 1995; Tokumoto et al., 1995; Hutchinson and Eisen, 2006; Hutchinson et al., 2007), it is likely that HB9:GFP^{+} neurons lose some aspects of their

motor neuron identity under DN-CLIM treatment. LIM-HDs act in a combinatorial fashion in motor neuron specification and axon guidance at different choice points (Hutchinson and Eisen, 2006). As DN-CLIM overexpression blocks the function of all combinations of LIM-HDs (including *islet1* and *islet2*) it may affect a number of axon pathway decision and recognition molecules involved in these decision. Thus it is not surprising to find that *plexinA3* (Julia Feldner, 2005; Feldner et al., 2007), regulating exit of axons from the spinal cord, as well as *chodl*, regulating pathfinding at the horizontal myoseptum, are both dysregulated by DN-CLIM overexpression.

3.3.2 We performed a successful pilot screen for potential new axon pathfinding related genes in motor neurons.

We recovered 28 genes by cross-correlating a list of genes that are underepresented in HB9:GFP cells after DN-CLIM treatment with a list of genes that are over-represented in wild type HB9:GFP^{+} motor neurons vs. GFP- cells. We narrowed down the list of interesting genes by verifying motor neuron-specific expression using online expression data (zfin.org) and in situ hybridisation. *Chodl, calca* and *tac1* were co-localized with GFP^{+} motor neurons in HB9:GFP transgenic zebrafish and down-regulated after DN-CLIM over-expression. The Chodl morphant, in which motor neurons lost their ability to direct axon growth, verified that this is a successful array approach to reveal the gene expression programme specific for motor axon pathfinding. Comparing the DN-CLIM phenotype with that of the Chodl morphant at 24hpf, the latter shows a less severe phenotype as most of the motor axons still grew out of the spinal cord, even though they were shorter than wildtype axons. This may be explained by the finding that *chodl* is only one of the downstream genes of the LIM-HD signaling pathway. More guidance molecules down-stream of LIM-HDs could cooperate with Chodl to direct motor axon pathfinding. PlexinA3 and Nrp1a are well-known axon guidance receptors downstream of LIM-HDs. Nrp1a (Feldner et al., 2005) and PlexinA3 (Feldner et al., 2007; Palaisa and Granato, 2007;

Tanaka et al., 2007) are necessary for motor axons to exit the spinal cord and grow in a midsegmental pathway onto the myotome, whereas Chodl is important for interactions with the HM choice point.

We did not retrieve *plexinA3* and *nrp1a*, which can be considered an internal control, from any of our microarray screens and some genes (like *nkx2.1lb*) from the motor neuron expression profile were found not to be expressed in motor neurons by *in situ* hybridisation. This shows that the noise level of our expression profiling was relatively high. Due to funding restraints we were unable to run three biological replicates, which are necessary to reduce the noise level of the method and to facilitate statistical analysis of the results. A repeat screen is likely to discovery more genes involved in pathfinding and synaptogenesis of motor axons. Nevertheless, our approach already yielded some interesting candidate genes.

3.3.3 Chodl is required for motor axon pathfinding

The zebrafish *chodl* gene belongs to the C-type lectin family, which is distinguished from other lectins by the presence of a $Ca2^{+}$-dependent carbohydrate recognition domain (CRD) in their protein sequence. CLEC-38, another transmembrane protein with C-Type lectin-like domains, has been demonstrated to regulate UNC-40-mediated axon outgrowth as well as the organization of presynaptic terminals in *Caenorhabditis elegans.* CLEC-38 can inhibit the ventral and dorsal axon outgrowth signal activated by UNC-40. A mutation also suggests that C-lectin domain is required for CLEC-38 function (Kulkarni et al., 2008). Spinal Muscular Atrophy (SMA) is a severe motor neuron disease by inactivating mutations in survivor motor neuron protein (SMN) which lead to reduced full-length functional SMN protein. Its already known that knock-down of SMN in zebrafish results in defects in motor axon outgrowth and pathfinding (McWhorter et al., 2003b). Gene array analysis in a mouse model shows that *chodl* is also significantly down-regulated as a late feature of the disease, implicating *chodl* involved in motor neuron disease (Bäumer et al., 2009).

Interestingly, the promoter region of chodl contains multiple recognition motifs (AT rich sequences containing ATTA/TAAT motifs) for the LIM-HDs *islet1* and *lhx3*, which are essential for motor neuron differentiation (Bridwell et al., 2001; Yaden et al., 2005). This indicates that the gene could even be a direct target of LIM-HDs. The Chodl protein sequence is highly conserved in vertebrates (94% identity with chicken and *Xenopus*, and 92% with mouse and human Chodl) and *chodl* of all species encode a type I membrane-associated polypeptide which contains an N-terminal signal sequence, C-type lectin domain, transmembrane region and an intracellular terminus. This suggests that Chodl is a transmembrane protein interacting with extracellular guidance cues. The zebrafish mutants *topped* (Rodino-Klapac and Beattie, 2004) and *stumpy* (Beattie et al., 2000) show similar phenotypes as chodl morphants. The *topped* gene has not been cloned yet, however, the chromosome position (chodl: Chromosome 24: 24,622,828-24,636,183. while *topped* is on Chromosom 24 close to the centromere) as well as the slightly different phenotypes suggests they are not the same gene. Expression of Chodl mRNA in *topped* mutants shows no difference from wildtype zebrafish (data not shown), indicating that *chodl* expression is not regulated by *topped*. A FACIT collagen collagenXIXa1 (colXIX) has been cloned from *stumpy* mutant and shown to function in guiding ventral motor axons through intermediate targets (Hilario et al., 2010). The indentical phenotypes as well as the evidence of synergistic knock-down effection of colXIX MO with Chodl MO in Cap axon guidance suggest that there is some genetic interachtion between these two genes in guiding Cap axon through horizontal myoseptum. To explore the mechanism of Chodl and ColXIX interaction with each other, futher functional experiments should be added.

In situ hybridization shows that the chodl mRNA signal is localized to RoP, MiP and CaP cell bodies, which fits in with the finding that in mice *chodl* is expressed selectively in motor neurons innervating the fast musculature (Enjin et al., 2010), and PMNs also innervate the fast musculature in zebrafish (Devoto et al., 1996). Chodl is

expressed in PMNs in a temporally regulated manner, as shown by its dynamic expression pattern between 12hpf and 24hpf (Fig. 3.8), 2-3 hours after PMNs are born and before they extend their axons. This is consistent with the *chodl* expression pattern in all the segments with and without Cap axons at 22 hpf, when the youngest segments are continuously added to the tail (Fig. 3.6). Thus we conclude that Chodl expression starts before there is contact of axons with the muscle periphery.

Histological preparations of morphant embryos show that 53% of the CaP axons are stalled at the horizontal myoseptum at 24 hpf. At this time point, CaP axons have already extended to the ventral edge of spinal cord in control embryos. There were still 25.6% of CaP axons remaining at the HM until 33hpf, which suggests that the axons stall at the HM in Chodl morphant. Similar growth speeds between wild-type and morphant CaP axons before and after the HM was reached during ventral motor axon growth was verified by time-lapes image analysis, which also shows that morphant axons took a longer time to pass this intermediate target (5 hours) than wild-type (3 hours). So Chodl, cooperated with ColXIX, is an important guidance receptor that can lead motor axons past the horizontal myoseptum, while it does not affect growth in other parts of the ventral pathway. We also show that Chodl is necessary for MiP axon growth. Moreover, Chodl is an important molecule for secondary motor axons as well, as their growth was also stalled in morphant embryos.

3.3.4 The morphant is a specific gene knock-down phenotype

There are three commonly-used strategies for confirming specificity of a morpholino oligonucleotide. Chodl morphant phenotype controlled by the following experiments indicates specificity of the gene knock-down. 1) Control MO. A standard control can be a MO targeting an exogenous gene or a 5-mismatch MO. For example, a “standard control” supplied by gene-tool is used in this project and it directs against human β-globin pre-mRNA. All effects are compared to control morpholino. 2) A second non-overlapping MO experiment. Two different morpholinos (one

translation-blocking MO and one splice-inhibiting MO in my project) show identical phenotypes when injected alone. This is a strong control making sequence-dependent off target effects of single morpholinos unlikely. A third morpholino, which is too weak to cause phenotypes on its own, synergistically enhanced effects of single MO when combined with another splice-inhibiting MOs. Again, synergistic action of unrelated MOs is a criterion for specificity (Eisen and Smith, 2008). For the two splice-inhibiting MOs, we show directly by PCR that splicing of the target gene is perturbed. Effects of the translation-blocking MO are concentration dependent. 3) mRNA rescue experiment The last but the most important point is that the lateral line nerve, generally used to stage embryos, grows unaltered in morpholino-injected embryos, indicating that morpholino injections do not simply retard development of embryos.

3.3.5 What are the ligands of Chodl?

The *chodl* structure carries the hallmarks of an ECM receptor, with a signal peptide, a transmembrane domain and a C-type lectin domain, shown to interact with ECM molecules (Lundell et al., 2004). Here we show genetic interactions for *chodl* and the ECM component *colXIX* by double morpholino treatment resulting in synergistic effects. Moreover, the phenotypes of *chodl* morphants and *colXIX* mutants are similar (Beattie et al., 2000; Hilario et al., 2010). Both show normal growth of axons along the common pathway. *Chodl* morphants and *colXIX* mutants and morphants show stalling of almost all axons at the horizontal myseptum. For many axons, stalling in the horizontal myoseptum is only transient for perturbations of both genes. In both conditions, MiP axons are also affected. Finally, *chodl* morphants and *colXIX* mutants show defects of myotomal axon branching at later stages of development. However, to determine whether Chodl and ColXIX physically interact, future biochemical studies will be necessary.

There are also other ECM factors accumulated at the horizontal myoseptum

that could interact with Chodl. For example, Tenascin-C (Schweitzer et al., 2005) and chondroitin sulfates (Bernhardt and Schachner, 2000) are accumulated at the horizontal myoseptum and play a role in motor axon growth. In the muscle specific tyrosine kinase mutant *unplugged*, in which deposition of Tenascin-C and chondroitin sulfates is defective, motor axons make inappropriate pathway decisions at the horizontal myoseptum (Zhang et al., 2004; Schweitzer et al., 2005). Interestingly, C-type lectin domains, such as that in Chodl, have been shown to interact with Tenascin-C (Lundell et al., 2004). Moreover, the myotome derived type XVIII collagen is also involved in motor axon guidance (Schneider and Granato, 2006). Finally, the *topped* mutation represents an unknown muscle-derived activity (Rodino-Klapac and Beattie, 2004), which also leads to stalling of CaP axons at the horizontal myoseptum.

3.3.6 Two neuropeptide coding-genes in spinal motor neurons were recovered from the gene array

These two neuropeptides from the gene list not only validate the gene array, but also supply additional promising candidate genes for specific action during motor axon pathfinding.

One gene is *calcitonin/calcitonin-related polypeptide, alpha (calca)*, which codes for the calcitonin-related polypeptide, alpha (CGRP). Its promoter region contains multiple binding sites for *lhx3* and *islet1*, suggesting LIM-HDs specifically regulate *calca* function during neuron development. *In situ* hybridization shows that *calca* is specifically expressed in motor neurons from 19hpf to 24hpf (zfin.org), when PMNs undergo axon growth and synaptogenesis (Birely et al., 2005). The narrow time window of expression indicates potential specific functions in motor axon outgrowth and synapse formation. *calca* is only expressed in one or two PMNs in each hemi-segment, indicating that *calca* may be important for only specific types of

motor axon pathfinding. Calcitonin gene related peptide (CGRP) drives expression of the neuromuscular junction associated collagen ColQ in cultured myotubes and may thus be involved in maturation of the neuromuscular junction (Choi et al., 2007), which could in turn influence growth of the motor axons as collagens play an important role in motor axon growth in zebrafish (Schneider and Granato, 2006; Hilario et al., 2010). No phenotype at the neuromuscular junction has been found in a CGRP knock out mouse (Lu et al., 1999). However, timing and accuracy of initial motor axon outgrowth could not be assessed in mice, because of the internal development of the embryos, but this could be done with comparative ease in zebrafish embryos. Further functional tests of *calca* during zebrafish development could reveal its role in axon pathfinding.

The other gene is *tachykinin1* (*tac1*), which codes for three different protein precursors by differential splicing. These proteins are further processed to produce neuropeptides, of which substance P and neurokinin A are the best studied (Maggi et al., 1997). We found that expression of *tac1* (from 16 hpf to 24 hpf) is highly specific in PMNs and exactly overlaps with growth of their axons between 18 and 24 hpf. In spinal cord, substance P, secreted from neurons, has been implicated in axon guidance as a signal for floor plate cells to increase expression of guidance molecules (De Felipe et al., 1995). At the neuromuscular junction of the enteric nervous system, these neuropeptides mediate non-cholinergic neurotransmission via neurokinin receptors (Maggi et al., 1997). Substance P positive nerve terminals have been found on subtypes of skeletal muscles in fish (Funakoshi et al., 2000). So *tac1* is a potential candidate gene to be involved in initial motor axon growth and synaptogenesis.

3.3.7 Cap axons survival may depend on contact with appropriate muscle

Survival of vertebrate motoneurons has been linked to receiving proper trophic support from target muscles (Oppenheim, 1996). *stumpy* CaP axons died by 72hpf because they cannot extend to ventral muscle target which supply trophic support

(Beattie et al., 2000). Interestingly, we observed that part of the axons, which cannot extend beyond the horizontal myoseptum die and degenerate. In time-lapse videos, we firstly observe the growth cone expanding, and then disappeared in the ventral myotome after 24 hpf (n=4 axons). While in morphology histology sample at 33hpf, these degenerating axons still can be stained with znp-1 antibody, representing HM- or HM axon group. In contrast, other morphant axons can still extend past HM, even though they stay longer at the HM than control axons. My results support that motor axons need trophic support from muscle to survive.

Taken together our data support the following model: Chodl is a guidance receptor which is localized in motor axons and interacts with guidance cues in the HM which enables the motor axons to pass the HM. Revealing the exact mechanism of this interaction will have to wait discovery of the ligand.

In summary, DN-CLIM over expression in zebrafish abrogates primary motor axon outgrowth from the spinal cord, which provide us with an excellent research model to elucidate a specific gene expression programme for axon pathfinding down-stream of the LIM-HD signaling pathway. We retrieved three genes (*chodl, tac1* and *calca*) from a gene array. *Chodl*, is an important guidance receptor in motor axon pathfinding as the morphant shows us specific aberrant motor axon growth, which can be phenocopied by different non-overlapping morpholino. Taken together, we successfully retrieved an important motor axon guidance receptor from gene profiling in zebrafish.

Table 8 28 genes down-regulated by DN-CLIM overexpression are also enriched in HB9:GFP+ motor neurons in zebrafish spinal cord.

Chip1: DN-CLIM chip; numbers represent down regulated fold change in GFP+ cells sorted from 26hpf HB9:GFP embryos after DN-CLIM injection

Chip2: GFP^+ Vs. GFP^-; numbers represent gene expression fold change in GFP^+ cells compared with GFP^- cells sorted from 26 hpf tails only.

fold in DN-CLIM downregulation (Chip1)	fold in GFP^+vs.GFP^- (Chip2)	sequence name	gene name
-4.0901	3.0531	vsx2	vsx2
-3.3734	18.8099	nkx1.2lb	nkx1.2lb
-3.2371	8.68663	TC285423	chodl
-3.127	2.79665	flj13639	36k
-2.9492	7.22032	tal2	tal2
-2.8507	8.51966	zgc:92886	calca
-2.8159	3.47611	wu:fk57g06	--
-2.7056	7.35989	hlxb9	mnx1
-2.6079	34.3453	BC083533	tac1
-2.5928	12.2849	slc6a5	glyt2
-2.5894	7.01896	BI864161	syt6
-2.5822	2.78151	TC282185	lmo1
-2.5659	2.06127	try	try
-2.4778	2.22156	TC299721	zgc:165474
-2.4615	7.0457	BI476673	--
-2.3383	2.90834	ENSDART00000013302	slc6a17
-2.3125	2.26726	CK397088	--
-2.2928	10.3374	CK705301	st18
-2.2926	2.30332	tpbgl	tpbgl
-2.2236	7.93957	ENSDART00000022233	--
-2.1145	13.2798	zgc:101108	nxph1
-2.1115	2.11138	zgc:92208	mllt10
-2.0953	2.05984	BC055562	tada2
-2.0502	26.233	gad1	gad1
-2.0441	3.32192	tlx1	tlx1
-2.0315	3.02975	BI840491	--
-2.0157	2.3796	AL725137	eif3ha
-2.0045	2.13384	TC273590	cbx1b

Table 9 Genes down-regulated after DN-CLIM injection. Numbers represent fold down regulation in GFP^+ cells sorted from 26hpf HB9:GFP embryos after DN-CLIM injection.

Fold Change	Sequence Name(s)	name
9.66112	rx1	rx1
9.06309	rx2	rx2
7.83446	TC269649	mrps31
7.23551	TC279001	VIP36-like
7.21402	ARAF	araf
6.33038	six3b	six3b
5.26502	TC270544	six6b
4.59562	prl	prl
4.43617	cdh17	cdh17
4.39909	hsp70	hsp70
4.39423	TC293988	bmp2b
4.14532	TC280214	hspa4
4.09009	vsx2	vsx2
3.97757	fezl	fezf2
3.89935	TC273326	--
3.85816	he1	he1
3.85094	TC269112	dnajb1b
3.65649	TC283566	--
3.62376	pth1	pth1
3.44155	zgc:56557	map2k1
3.42359	zgc:100991	nr2e1
3.40901	TC289968	ctsl
3.37336	nkx1.2lb	nkx1.2lb
3.36994	cx43	cx43
3.23708	TC285423	chodl
3.18308	atoh7	atoh7
3.13792	wu:fj30d06	pvalb5
3.12696	flj13639	36k
3.11601	wu:fj01a12	s100a10a
3.09609	B-H2	barhl2
3.09607	zgc:91875	syt9b
3.07275	f10	f10
3.05495	hsp90b	hsp90b
3.00219	CN507295	GrpE-like 1
2.99645	hsp90b	hsp90b
2.99389	wu:fb09b10	cpeb4

2.9849	BI476322	--
2.94922	tal2	tal2
2.945	Dlm	rgma
2.91811	TC293948	--
2.91348	zgc:76875	foxd11
2.90379	TC282339	loxl2
2.87348	six3a	six3a
2.85073	zgc:92886	calca
2.83999	ctsla	ctsla
2.81588	wu:fk57g06	--
2.81	zgc:100963	zgc:100963
2.79452	otx1	otx1
2.78011	pou1f1	pou1f1
2.77839	ENSDART00000014116	dnaja11
2.7184	foxd3	foxd3
2.70559	hlxb9	mnx1
2.69769	TC299705	wls
2.695	wu:fc44h01	--
2.68254	zgc:65831	tsc22d3
2.66697	zgc:73262	zgc:73262
2.65218	ctslb	ctslb
2.61911	eng2a	eng2a
2.60793	BC083533	tac1
2.59801	zgc:77251	nbl1
2.59356	vax1	vax1
2.59275	slc6a5	slc6a5
2.58938	BI864161	synaptotagmin-6-like
2.58621	wu:fb67h01	PARP14
2.58224	TC282185	lmo1
2.57508	otx1	otx1
2.56585	try	try
2.56058	BC083533	tac1
2.55092	im:7141428	ctdsp1
2.53679	otx2	otx2
2.53575	A_15_P112643	--
2.52083	sb:cb367	--
2.50031	TC299047	zgc:110045
2.49979	wu:fc56b06	--
2.48691	CO350175	rcp9
2.48433	wu:fa01b10	snapc3
2.47776	TC299721	dcps

2.47199	hsp90a	hsp90a
2.47053	hsp47	hsp47
2.46698	TC281868	GFMLCK1
2.46352	ENSDART00000013604	lemd3
2.46189	BI845250	--
2.46147	BI476673	--
2.41834	hrmt1l2	prmt1
2.40146	TC281745	slc25a16
2.39801	ENSDART00000037807	usp53
2.39042	foxd3	foxd3
2.36882	CA470646	slc4a2
2.36651	zgc:92346	ing2
2.33826	ENSDART00000013302	slc6a17
2.33745	A_15_P112370	--
2.31979	wu:fb73a09	--
2.31249	CK397088	--
2.30193	zgc:86630	mrpl23
2.29956	zgc:77592	tpm3
2.29867	CN013497	--
2.29279	CK705301	--
2.29256	tpbgl	tpbgl
2.28708	tbx4	tbx4
2.25494	trpv6	trpv6
2.25381	otx1l	otx1l
2.25	CK236800	rcan1
2.24734	eng2b	eng2b
2.24053	sb:cb252	sb:cb252
2.23291	zgc:101784	fgf13
2.22681	CD604713	--
2.22355	ENSDART00000022233	zgc:112161
2.22338	zgc:100956	ifrd2
2.22292	ENSDART00000034133	--
2.2221	LOC402802	zgc:162119
2.22018	zgc:92411	zgc:92411
2.20445	zgc:86909	msrb3
2.19736	TC272638	arl4ca
2.19048	sb:cb379	--
2.17938	TC294661	--
2.17929	TC301566	prp19
2.17335	zgc:103628	stam2
2.16496	zgc:66469	phf23b

2.16133	ENSDART00000013379	--
2.15628	BI865621	KIAA1867 protein-like
2.1519	ENSDART00000027366	ifrd1
2.14798	aldoa	aldoa
2.13382	ahsa1l	ahsa1l
2.13336	zgc:103587	fabp11a
2.12451	ccnl1	ccnl1
2.11637	zgc:56197	rad9a
2.11447	zgc:101108	nxph1
2.11147	zgc:92208	mllt10
2.11024	dlx2b	dlx2b
2.10722	ndrg1	ndrg1
2.09534	BC055562	tada2b
2.09331	ENSDART00000045449	whsc1
2.08943	lect1	lect1
2.08789	TC300982	alx4
2.08172	id:ibd2923	crygm4
2.07437	mitfa	mitfa
2.0741	TC293954	slc35e3
2.06854	TC294122	zgc:92723
2.06261	ENSDART00000040665	bmp7
2.05836	heg	heg
2.05813	im:7138745	pcf11
2.05017	gad1	gad1
2.04412	tlx1	tlx1
2.04193	tbx15	tbx15
2.0391	wu:fc75c02	wu:fc75c02
2.03863	zgc:55954	rorab
2.03517	ENSDART00000017641	zgc:153332
2.03444	CK030112	flii
2.03434	sepx1	sepx1
2.03355	zgc:92217	zgc:92217
2.03151	nkx2.7	nkx2.7
2.03146	BI840491	--
2.0261	ENSDART00000038058	adnp
2.01876	c10orf119	mcmbp
2.01566	AL725137	--
2.01388	TC290305	rpl4
2.00449	TC273590	cbx1b
2.0007	klf2a	klf2a

4. Chapter two: SSDP cofactors regulate neural patterning and differentiation of specific axonal projections

4.1 Introduction

LIM homeodomain transcription factors regulate the development of a variety of different cell types and structures in the nervous system (Bach, 2000) (Hobert and Westphal, 2000; Lee and Pfaff, 2001). The association of the LIM domains with the LIM interaction domain (LID) of CLIM cofactors (also known as NLI, Ldb or Chip) is required to exert the *in vivo* activity of LIM-HD proteins (Matthews and Visvader, 2003). Indeed, disturbing the interaction between CLIM and LIM domains via overexpression of the LID causes phenotypes that are similar/comparable to inhibitions of specific LIM-HD genes (Becker et al., 2002; Mukhopadhyay et al., 2003; Thaler et al., 2002).

Single stranded DNA Binding protein 1 (SSDP1) was originally identified by its ability to bind to single-stranded poly-pyrimidine sequences (Bayarsaihan et al., 1998). Later it was found to participate in protein complexes recruited by CLIM cofactors. SSDP1 synergizes with Xlim1/Lhx1 and Ldb1/CLIM2 during gastrulation in *Xenopus*, and with Apterous and Chip/CLIM during wing development in *Drosophila* (Chen et al., 2002; van Meyel et al., 2003). Intronic disruption of the SSDP1 gene in mice revealed important roles in the development of late head organizer tissues by activating the Lim1/Lhx1-Ldb1/CLIM complex (Nishioka et al., 2005). SSDP1 exerts parts of its positive activity by preventing the binding of the ubiquitin ligase RLIM to CLIM thereby protecting the LIM-HD/CLIM complex from proteasomal degradation in cells in culture (Xu et al., 2007) (Gungor et al., 2007; . This is mediated by the N-terminal 94 amino acids that harbor the CLIM interaction domain.

Protein complexes assembled by LIM-HDs are dynamic and vary in different

cell types. The formation of tetrameric complexes consisting of two LIM-HD/CLIM dimers appear widespread (van Meyel et al., 1999; Milan and Cohen, 1999). Indeed, the development of specific interneurons requires the formation of a tetrameric complex consisting of Lhx3 bound to CLIM. However, for the differentiation of motor neurons which originate from a common precursor cell, additional expression of the LIM-HD Islet1 and the transient formation of a hexamer complex consisting of each of two Lhx3/ Islet1/CLIM molecules is indispensable (Thaler et al., 2002). This illustrates that the composition of LIM-HD multiprotein complexes dictates the developmental read-out. Thus, the correct formation of LIM-HD complexes is critical and cellular stoichiometries of proteins that participate in LIM-HD complexes are crucial for the correct formation of LIM-HD complexes (Fernandez-Funez et al., 1998; Matthews and Visvader, 2003; Hiratani et al., 2003; Song et al., 2009).

To better understand how SSDP1 proteins control these varied and specific functions of LIM-HD complexes *in vivo*, an analysis of specific SSDP1 phenotypes in relation to CLIM phenotypes is necessary. Although the genes encoding CLIM and SSDP1 cofactors have been mutated/disrupted in several organisms, their functions in conjunction with LIM-HDs and mechanisms of regulation are poorly understood due to the complexity of the knockout/mutant phenotypes and the widespread developmental effects caused by mutation/deletion of SSDP1 and CLIM genes (Mukhopadhyay et al., 2003; van Meyel et al., 2003; (Nishioka et al., 2005).

We have used embryonic zebrafish to elucidate the expression and developmental functions of SSDP1 cofactors during neural development *in vivo*. Inhibiting SSDP cofactors results in specific defects of axon growth of trigeminal as well as Rohon-Beard sensory neurons, and perturbs patterning of the eye and the mid-hindbrain boundary. Morpholino knock down indicate a specific function for SSDP1b in sensory axon growth. The observed phenotypes overlap with those resulting from CLIM perturbation. A truncated form of SSDP1 stabilizes CLIM in zebrafish and rescues motor axon pathfinding errors induced by CLIM perturbation.

Thus, our results reveal functions of SSDP1 in instructing axon outgrowth from specific neuronal populations and in neural patterning, exerted at least in part via stabilization of CLIM cofactors.

4.2 Results

4.2.1 Cloning of SSDP1s in zebrafish

We cloned two SSDP1 genes from the zebrafish genome, SSDP1a (bankit1264174 GQ903695) and SSDP1b (bankit1264294 GQ903696), encoding proteins of 373 and 364 amino acids (aa), respectively (Fig. 4.1). Sequence comparisons reveal that SSDP1a and SSDP1b share 70% aa identity. The predicted overall aa identities with human and mouse SSDP1 are 78% and 77% for SSDP1a, respectively, and 76% and 81% for SSDP1b, respectively (Fig. 4.2). These high sequence conservations suggest important functions of both zebrafish SSDP1s.

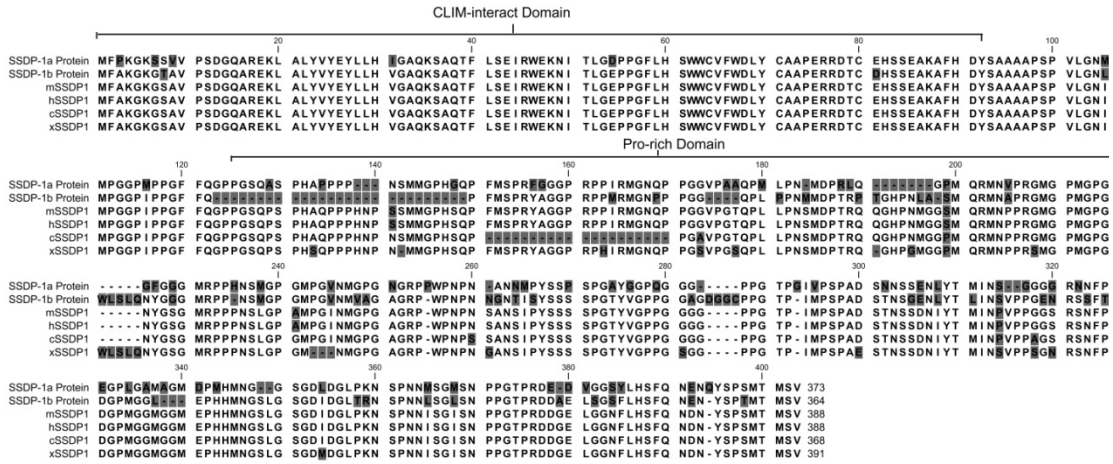

Fig. 4.1 Zebrafish SSDP1s shares sequence homologies with SSDP1 of other vertebrate species. The deduced amino acid sequence of zebrafish SSDP1s is aligned with mouse, human, chicken and Xenopus SSDP1. Gray shading represents different amino acids among them. m, mouse; h, human; c; chicken; x, Xenopus.
CLIM-interact Domain means this domain can bind with CLIM (cofactor of LIM).
Pro-rich domain means this domain is rich of proline amino acids.

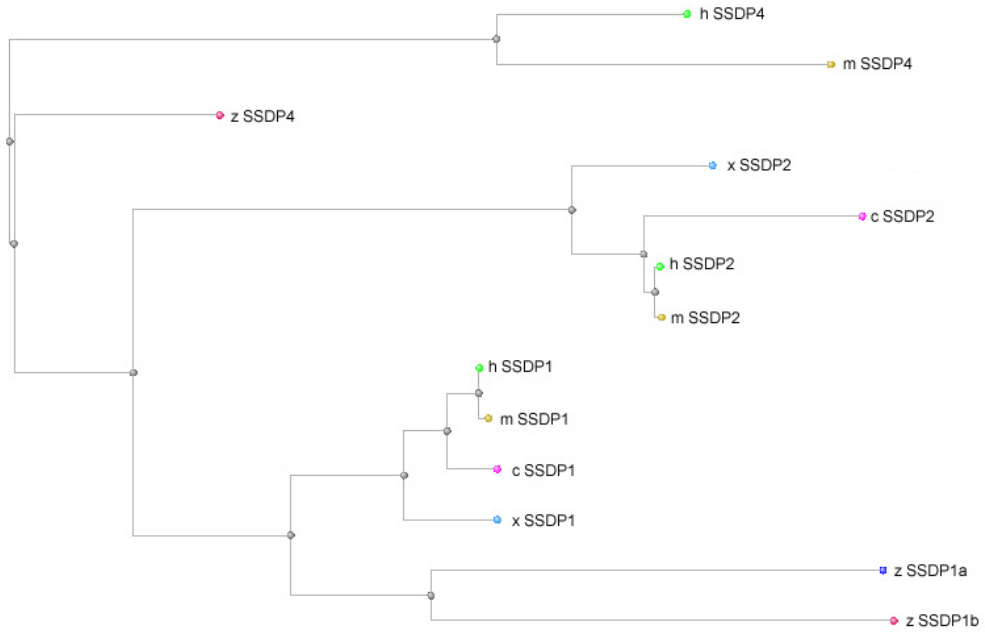

Fig. 4.2 Multiple comparisons in a phylogenetic tree group zebrafish SSDP1s with SSDP1s homologs in other vertebrates. z, Zebrafish; m, mouse; h, human; c; chicken; x, Xenopus; The phylogenetic tree is constructed by the fast minimum evolution method (Desper R and Gascuel O, Mol Biol Evol 21:587-98, 2004 PMID: 14694080) based on Grishin tree distance (Grishin NV, J Mol Evol, 41:675-79, 1995 PMID: 18345592).

4.2.2 SSDP1s co-localized with CLIM in specific neuronal cell types during zebrafish development

To investigate developmental functions of SSDP1 genes we first localized gene expression by in situ hybridization. This showed that SSDP1a mRNA was ubiquitously detectable in the developing embryo from 2 to 12 hours post-fertilization (hpf) (Fig. 4.3A). At 18-24 hpf the expression of SSDP1a was still widespread but concentrated more towards anterior embryonic regions including brain and eye (Fig. 4.3A, B). Similar to SSDP1a, mRNA encoding SSDP1b was also highly and ubiquitously transcribed from 2hpf to 4hpf (Fig. 4.3C). However, in contrast to SSDP1a, at 8hpf we detected only very low SSDP1b mRNAs levels. SSDP1b mRNA expression reappeared from 12hpf in Rohon Beard neurons and in trigeminal neurons from 20hpf onwards (Fig. 4.3 C, D). These results suggest that the mRNA detectable at 2-4 hpf is maternally derived and zygotic expression of SSDP1b only starts at 12 hpf in sensory neurons. In zebrafish, zygotic mRNA synthesis starts at approximately 3 hpf (Kane and Kimmel, 1993). Our data show a highly dynamic expression pattern of SSDP1 mRNAs and suggest functions of SSDP1b for the development of trigeminal and Rohon-Beard neurons.

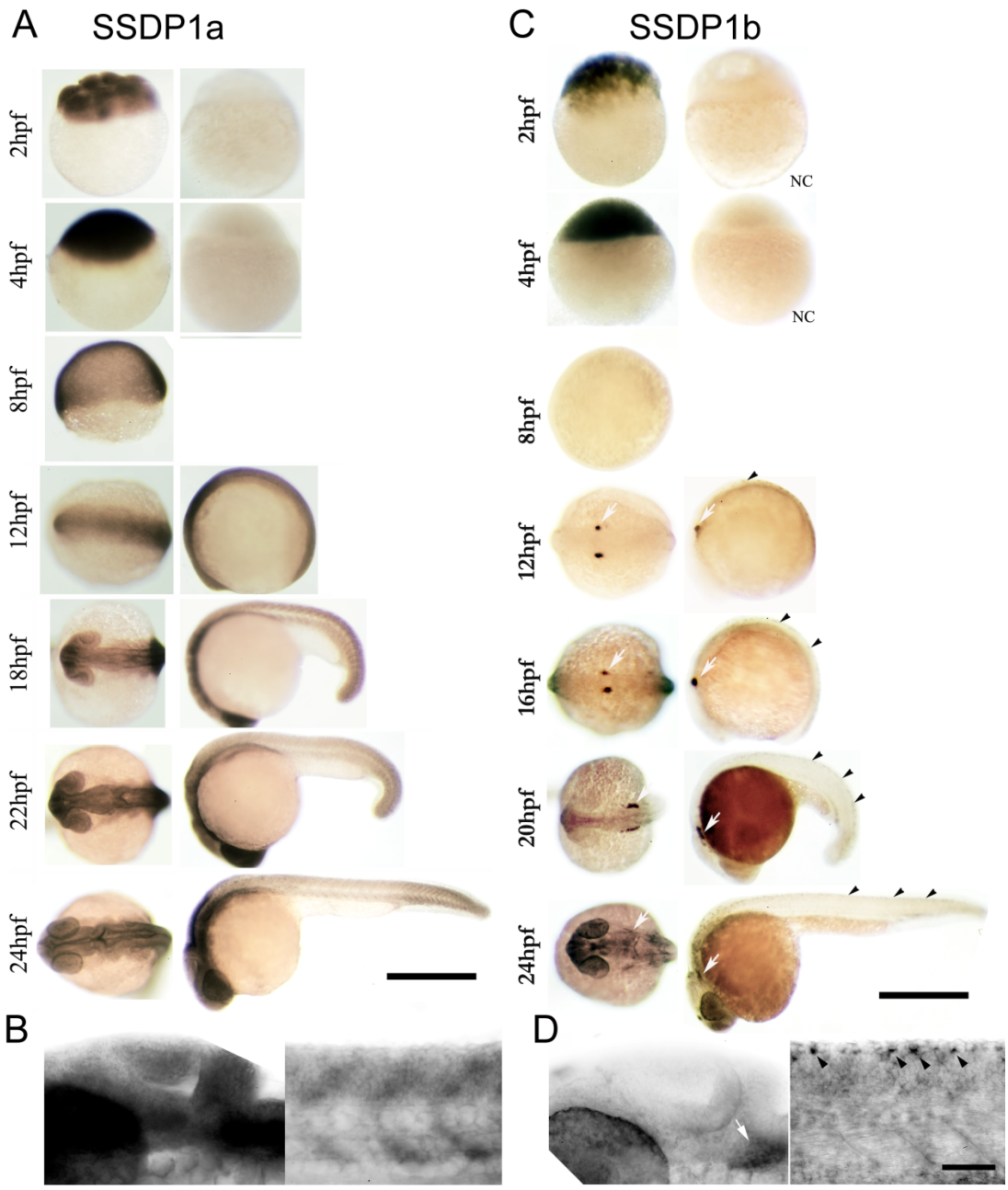

Fig. 4.3 In situ hybridization analysis of SSDP1s in embryonic zebrafish developmental stages. Whole-mount in situ hybridization between 2 and 24 hpf indicates that SSDP1a is ubiquitously expressed with stronger expression in the head, whereas SSDP1b mRNA is most strongly expressed in trigeminal (white arrows) and Rohon-Beard (black arrowheads) neurons. Dorsal view, anterior is to the left. Lateral view, anterior is to the left and dorsal is to the top except where noted. Higher magnification pictures in lower row show lateral views of the head (left) and trunk (right). Upper scale bar in C = 500 μm for low magnification pictures; lower scale bar = 50 μm for high magnification pictures. NC: negative control.

To further elucidate expression of SSDP1 in conjunction with the LIM-HD/CLIM complex we compared the expression profile of SSDP1 and CLIM cofactors early during zebrafish development at the protein level, as LIM-HD recruited protein complexes are regulated by the proteasome (Gungor et al., 2007). We used a specific SSDP1 antibody that recognizes predominantly zebrafish SSDP1b. This was indicated by recognition of a protein band in zebrafish tissue that was identical in size to that found in mouse cells in Western blot analysis and by reduced immunohistochemical labeling after selective morpholino knock down of SSDP1a and SSDP1b in embryos (Fig. 4.5 F, G). We found widespread expression in embryos at 24 hours post-fertilization (hpf) in various neuronal structures including telencephalon and midhindbrain boundary (MHB) (Fig. 4.4A). Double-labeling experiments with antibodies directed against the HNK-1 epitope, recognizing neuronal cell membranes and Golgi apparatus (Becker et al., 2001), identified Rohon-Beard and trigeminal neurons as cells with particularly high expression of SSDP1 protein (Fig 4.4B). This was expected because of the strong expression of SSDP1b mRNA in these cell types and the preferential labeling of SSDP1b by the antibody. CLIM was also strongly expressed in Rohon-Beard and trigeminal neurons. Antibody labeling of SSDP1 and CLIM in transgenic fish, in which motor neurons express green fluorescent protein under the motor neuron specific promoter *Hb9* (Flanagan-Steet et al., 2005), revealed lower expression of SSDP1 and CLIM in primary motor neurons (Fig. 4.4B). All trigeminal and Rohon-Beard cells, defined by HNK-1 immunohistochemistry, and all motor neurons, defined by HB9:GFP transgene, were immuno-positive for SSDP1 and CLIM in their nuclei, indicating co-localization of the antigens. These results are consistent with the expression profile of SSDP1 mRNAs and show that cofactors SSDP1 and CLIM co-localize in specific neuronal cell types including trigeminal neurons, Rohon-Beard neurons and primary motor neurons.

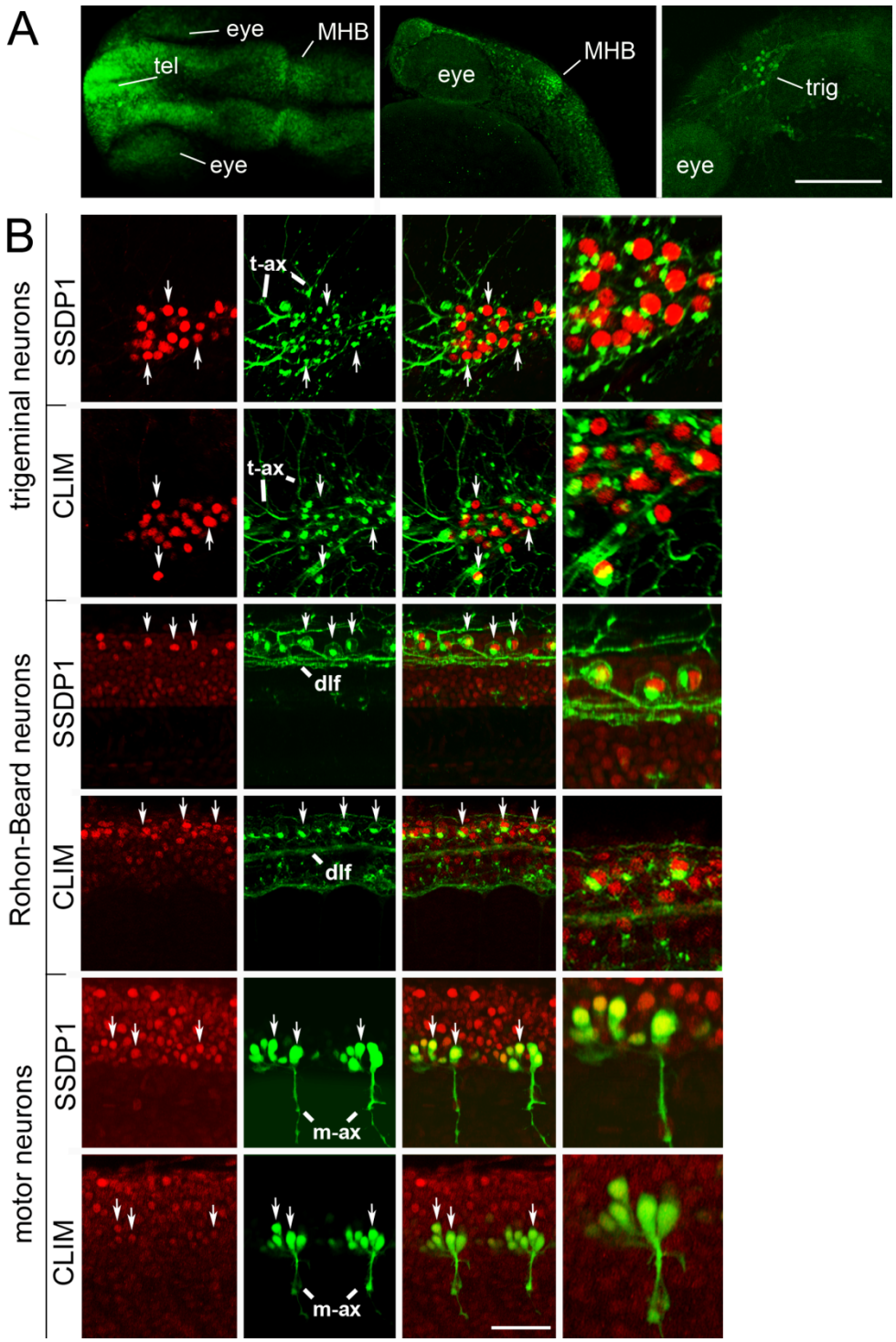

Fig. 4.4 SSDP1 protein expression corresponds to in situ hybridization patterns and SSDP1 is co-expressed with CLIM protein in neuronal cell types. **A:** Dorsal (left) and lateral (middle, right) views of the head labeled with SSDP1 antibodies at 24 hpf are shown. Strong immuno-reactivity is detectable in the telencephalon (tel), in the MHB and in the trigeminal ganglion (trig). The right panel is a selective z-stack of the epidermal region. Scale bar: 200 µm. **B:** Neuronal localization of SSDP1 and CLIM

immunoreactivity (red) is revealed by co-labeling with an HNK-1 antibody (trigeminal and Rohon-Beard neurons in green) or by transgenic GFP expression in HB9:GFP transgenic embryos (motor neurons in green) at 24 hpf. The right outer column gives a higher magnification of double-labeled neurons. HNK-1 is strongly labeled on axonal membranes and Golgi-apparatus next to nuclear labeling of SSDP1 and CLIM in trigeminal and Rohon-Beard neuron. In GFP expressing motor neurons, nuclear labeling is found inside the somata. Some double-labeled neurons are indicated by arrows. Trigeminal (t-ax) and motor axons (m-ax) as well as the dorsal longitudinal fascicle (dlf) are indicated for orientation. Scale bar: 50 μm for low and 100 μm for high magnification.

4.2.3 An N-terminal fragment of SSDP1 does not transactivate LIM-HDs, but protects CLIM in vivo

SSDP1 forms complexes with CLIM and LIM-HDs on DNA (Fig. 4.5A). We have previously generated a dominant-negative CLIM (DN-CLIM) molecule that contains the LIM interaction domain (LID) of CLIM, able to compete with endogenous CLIM for binding to LIM domains (Bach et al., 1999). When ectopically over-expressed early during zebrafish development, DN-CLIM induces specific phenotypes that resemble phenotypes of targeted LIM-HD gene deletions in mice (Becker et al., 2002). To evaluate whether such an approach is also feasible for the elucidation of functions of SSDP1 we examined the potential of the N-terminal 92 amino acids of SSDP1 (N-SSDP1), which contains the CLIM-interaction domain (van Meyel et al., 2003), but lacks a proline-rich domain (Enkhmandakh et al., 2006) as well as a C-terminal transactivation domain (Wu, 2006) (Fig. 4.5B). We used the pituitary T3 cell line (Windle et al., 1990) to test effects of N-SSDP1 on the transcriptional activations mediated by LIM-HD proteins. This cell line endogenously expresses the LIM network proteins Lhx3, CLIM and SSDP1 and the Lhx3 target gene GSU (Bach et al., 1995). Indeed, cofactors CLIM and SSDP1 associate with the GSU promoter critically regulating GSU transcription in these cells (Bach et al., 1997; Gungor et al., 2007). Over-expression of SSDP1 in full length fused to GFP via

lentiviral infection led to increased endogenous GSU mRNA levels in T3 cells. In contrast, over-expression of GFP-N-SSDP1 resulted in significantly decreased GSU mRNA levels when compared to control (Fig. 5C).

Another activity of SSDP1 is its ability to stabilize CLIM cofactors in cells in culture (Gungor et al., 2007; Xu et al., 2007). To test the ability of N-SSDP1 to stabilize CLIM cofactors in vivo we injected mRNA encoding Myc-N-SSDP1 into zebrafish embryos at the one-to-two cell stage and tested endogenous CLIM levels. The over-expression of N-SSDP1 resulted in 3.2x increased CLIM levels in Western blots of extracts prepared from 24 hpf embryos when compared with NLS-myc control mRNA injected animals (Fig.4.5D). In addition, although non-quantitative, the immunoreactivity of CLIM antibodies in immunohistochemical experiments was stronger in embryos injected with N-SSDP1 when compared to control (Fig. 4.5E). These results show that while N-SSDP1 has lost its ability for enhancing the transcriptional activity of LIM-HD complexes *in vitro*, it still protects CLIM co-factors from proteasomal turn-over in zebrafish embryos. Thus, the overexpression of N-SSDP1 in cells is predicted to inhibit functions mediated by C-terminal sequences of SSDP1 and SSDP2 including their transactivation potentials, but not their CLIM-stabilizing functions mediated by N-terminal sequences.

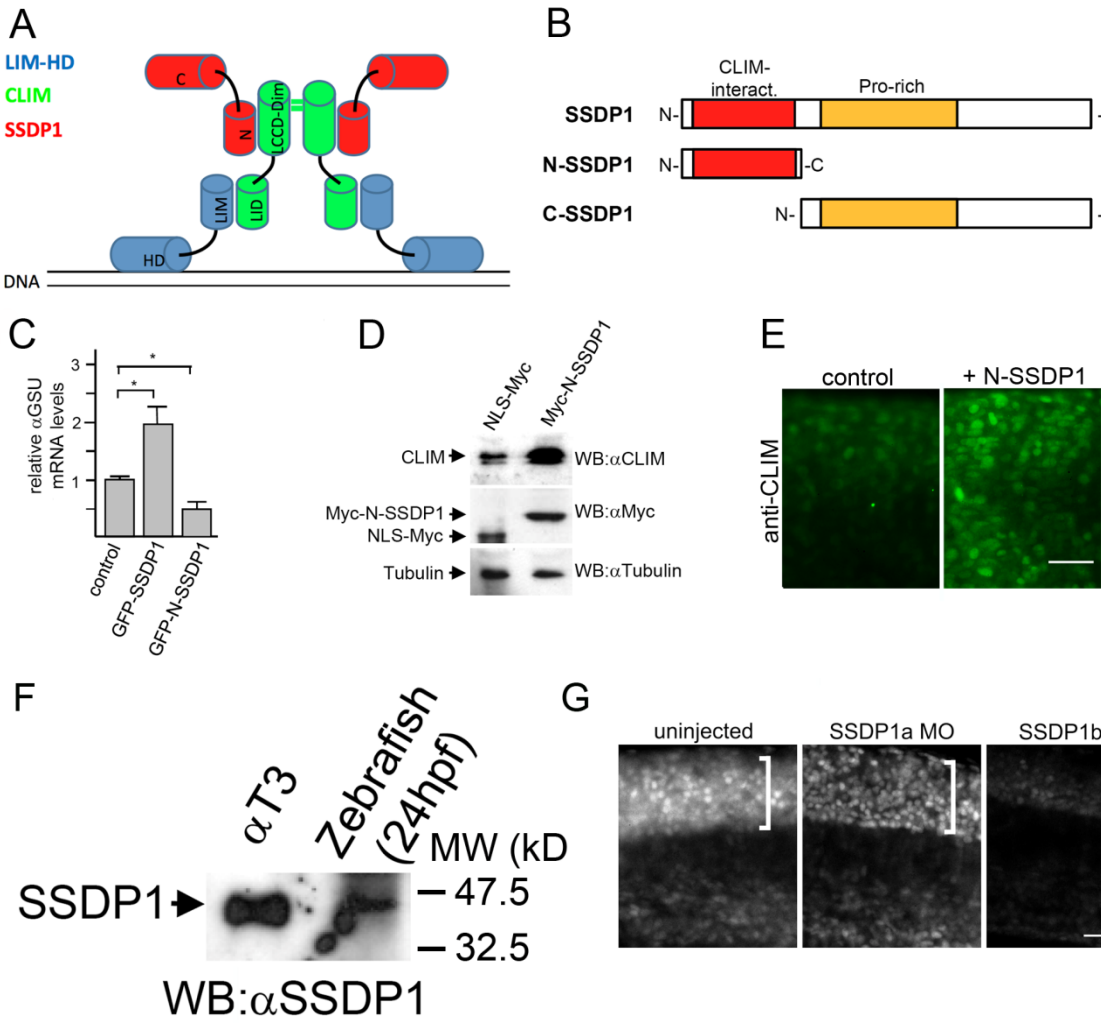

Fig. 4.5 N-SSDP1 inhibits LIM-HD transcriptional complex *in vitro* and stabilizes CLIM *in vivo*. **A:** Model of transcriptional complexes consisting of LIM-HDs (blue), CLIM (green) and SSDP1 (red) on DNA. LIM domain (LIM); homeodomain (HD); LIM interaction domain (LID); Ldb/Chip conserved domain (LCCD); dimerization domain (dim); N- and C-terminal portions of SSDP1 (N and C, respectively) are indicated. **B:** N-SSDP1 contains the CLIM interacting domain, but not the proline-rich domain. C-SSDP1 lacks the CLIM interacting domain of SSDP1. **C:** Overexpression of full-length SSDP1 in alphaT3 cells significantly increases transcriptional activity of LIM-HD factors in these cells whereas GFP-N-SSDP1 decreases it, as indicated by relative levels of the target alphaGSU mRNA measured by RT-qPCR. **D:** Western Blot analysis of embryos (24 hpf) after over-expression of myc-tagged N-SSDP1 shows increased CLIM protein levels as compared to embryos injected with control mRNA for myc-tagged NLS. **E:** N-SSDP1 mRNA injection increases CLIM immunofluorescence in embryos, confirming Western Blot results. Lateral views of the trunk region of whole-mounted embryos (24 hpf) are shown.

Scale bar = 25 μm. **F**. Western blot analysis indicates that the SSDP1 antibody detects a band of the same molecular weight in protein extracts of alphaT3 cells and zebrafish embryos, suggesting specific reactivity of the antibody in zebrafish embryos. **G:** Immunodetectability of SSDP1 is slightly reduced by SSDP1a and strongly reduced by SSDP1b morpholino injection, indicating that the antibody predominantly recognizes SSDP1b. Lateral trunk views of whole-mounted embryos are shown. The strongly immunoreactive spinal cord level is indicated by brackets.

4.2.4 N-SSDP1 over-expression inhibits eye development and midbrain-hindbrain boundary development as well

To elucidate functions of SSDP1 in conjunction with LIM-HDs, we compared phenotypes induced by ectopic over-expression of N-SSDP1 and DN-CLIM in developing zebrafish. We have previously shown that DN-CLIM over-expression inhibited the development of eyes, the MHB, and peripheral axonal projections of Rohon-Beard neurons, trigeminal neurons and primary motor neurons (Becker et al., 2002). Indeed, differential interference contrast (DIC) on live (Fig. 4.6A) and fixed embryos (Fig. 4.6B) revealed that the eye size of DN-CLIM and N-SSDP1 over-expressing animals was significantly reduced (Fig. 4.6C). Over-expression of full length zebrafish SSDP1b also significantly reduced eye size (Fig. 4.8A). However, N-SSDP1 and SSDP1b over-expression only reduced eye size, whereas upon DN-CLIM overexpression eyes were usually lost completely.

In situ hybridization for Pax2a revealed that the development of the MHB was also affected by N-SSDP1 over-expression at 24 hpf (Figs. 4.6D). However, Wnt-1 and engrailed transcript levels in the MHB were reduced but still detectable (Fig. 4.6D), indicating that this phenotype was milder when compared to DN-CLIM over-expression, which completely abolishes expression of both mRNAs at this stage (Becker et al., 2002).

To determine the influence of N-SSDP1 and DN-CLIM on hindbrain

differentiation, we analyzed differentiation of the Mauthner neurons, a pair of early differentiating neurons with descending axons to the spinal cord, which are situated in the hindbrain caudal to the MHB. Immunohistochemistry with the 3A10 antibody indicated that in DN-CLIM mRNA injected embryos these neurons did not form, whereas N-SSDP1 over-expression had no influence on their differentiation (Fig. 4.6G). This again indicates a greater influence of DN-CLIM than N-SSDP1 on MHB differentiation.

In situ hybridization for Otx2, Pax6a, NeuroD and Six3a showed that the overall brain patterning, except for eyes and MHB, appeared grossly normal in N-SSDP1 mRNA injected embryos. However, N-SSDP1 over-expression resulted in generally smaller structures (Fig. 4.6E). This is very similar to DN-CLIM overexpression (Becker et al., 2002). Because embryos over-expressing NLS-Myc protein were indistinguishable from wild-type animals, phenotypes induced by N-SSDP1 were specific. Furthermore, we did not detect an effect on zebrafish development upon overexpression of the C-terminal of SSDP1 (Fig. 4.6F). Strong resemblance of N-SSDP1 and DN-CLIM (Becker et al., 2002) patterning phenotypes in eye and MHB, but not hindbrain, suggests overlapping functions for SSDP1 and CLIM in brain patterning.

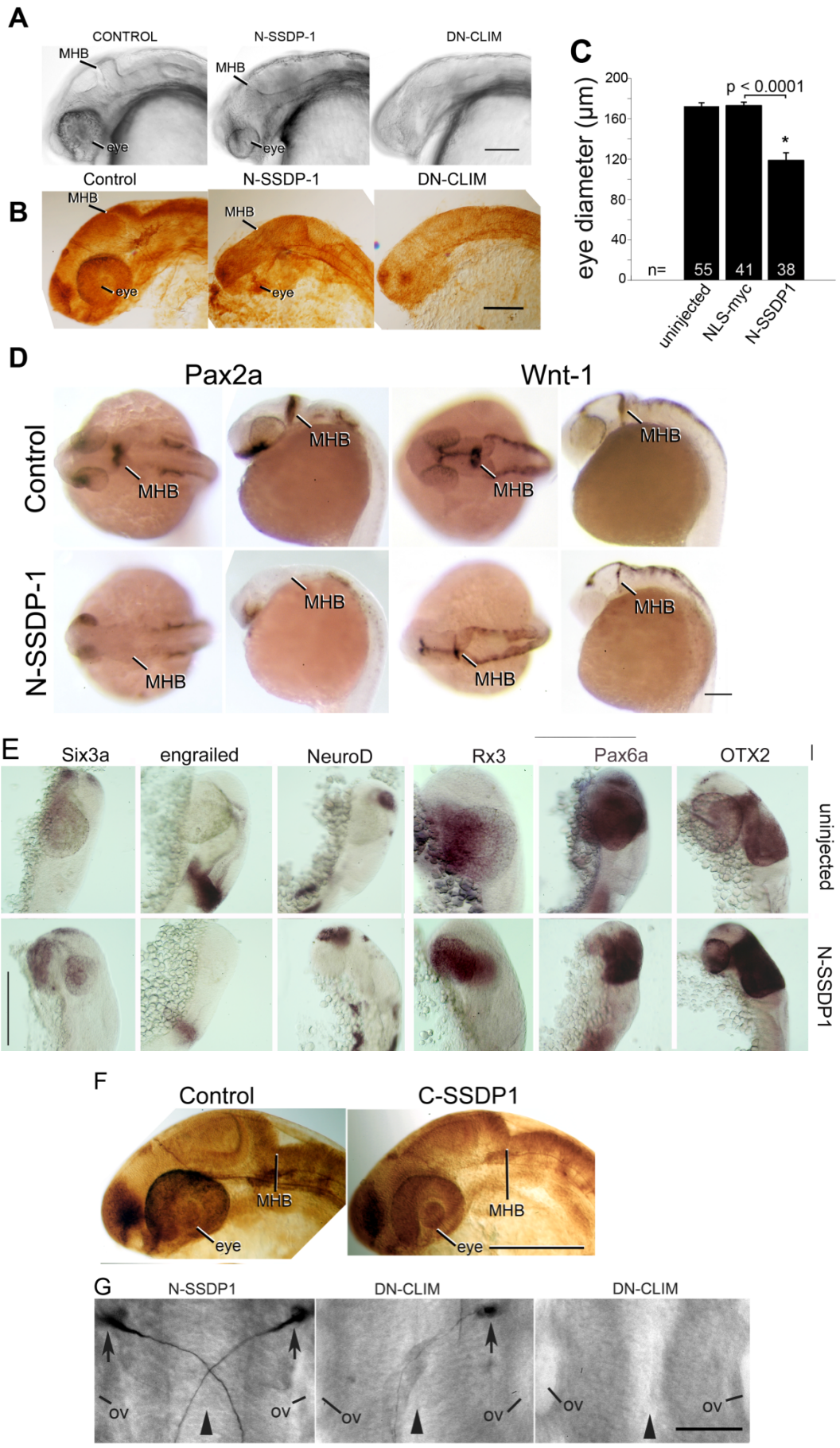
A
CONTROL
N-SSDP-1
DN-CLIM
MHB
eye
B
Control
N-SSDP-1
DN-CLIM
C
eye diameter (µm)
p < 0.0001
n=
55
41
38
uninjected
NLS-myc
N-SSDP1
D
Pax2a
Wnt-1
Control
N-SSDP-1
E
Six3a
engrailed
NeuroD
Rx3
Pax6a
OTX2
uninjected
N-SSDP1
F
Control
C-SSDP1
G
N-SSDP1
DN-CLIM
ov

Fig. 4.6 N-SSDP impairs eye and MHB development. A,B: Lateral views of the heads of living (A) or fixed, anti-tubulin immuno-labeled (B) 24 hpf embryos are shown. N-SSDP1 mRNA injection leads to reduced eye and MHB size compared to control embryos. DN-CLIM mRNA completely inhibits eye development and more strongly affects the MHB. C: Eye size is significantly reduced after N-SSDP1 mRNA over-expression compared to NLS-myc control mRNA over-expression. D: Dorsal (left columns) and lateral views (right columns) of whole-mounted 24 hpf embryos reveal loss of Pax2a and reduction of Wnt-1 mRNA expression in the MHB after N-SSDP1 mRNA over-expression. E. Lateral views of the heads of 24 hpf embryos after in situ hybridization are shown. All the indicated markers except for *eng2* retain their general expression patterns when N-SSDP1 is over-expressed. F. Lateral views of anti-tubulin labeled embryos at 24 hpf are shown. Over-expression of C-SSDP1, which lacks the CLIM-interacting domain, does not induce phenotypes in eye or MHB. G. Dorsal views of the hindbrain (rostral is up) of 24 hpf embryos immuno-labelled with the 3A10 antibody are shown. Development of Mauthner neurons (arrows) and crossing of their axons at the brain midline (arrowhead) is not affected by N-SSDP1 over-expression. In contrast, DN-CLIM over-expression leads to complete or partial loss of Mauthner neurons. Note that in those cases in which only one Mauthner neuron is present its axonal trajectory is not altered (ov = otic vesicle). Scale bars = 200 μm (A, B, D,E, F). Scale bars = 50 μm (G)

4.2.5 SSDP1 regulates axon outgrowth of trigeminal and Rohon-Beard neurons but not motor neurons

Next, we examined the effects of N-SSDP1 over-expression on the development of peripheral axons of trigeminal neurons, Rohon-Beard neurons and primary motor neurons, as we have shown previously that DN-CLIM inhibits the development of these projections (Becker et al., 2002). Indeed, over-expression of N-SSDP1 resulted in significantly decreased numbers of peripheral trigeminal as well as Rohon-Beard axons, but not primary motor axons in anti-tubulin immunohistochemistry (Fig. 4.7 A, B). These effects were specific as axons in NLS-Myc or C-SSDP1 over-expressing animals appeared normal (Fig. 4.8B). The reduction in the number of peripheral Rohon-Beard axons was not due to cell loss, as we observed 40.3 ± 0.71 Rohon-Beard

neurons in NLS-myc injected embryos (n = 30) and 41.9 ± 0.99 RHB neurons in N-SSDP1 injected embryos, which was not statistically different (P = 0.24). Trigeminal neurons were also present but could not be quantified due to their dense packing. This is very similar to DN-CLIM injected embryos, in which somata of sensory neurons are also retained (Becker et al., 2002). Moreover, we did not find any effect of N-SSDP1 or DN-CLIM over-expression on the differentiation of a spinal intrinsic neuron, the commissural primary ascending interneuron (CoPA). CoPAs differentiate in the dorsal spinal cord. Their axons course ventrally, cross the midline at the floorplate and ascend in the contra-lateral side of the spinal cord in the dorsal longitudinal fascicle. Immunohistochemistry with the 3A10 antibody selectively labeled these neurons in N-SSDP1 and DN-CLIM mRNA injected embryos in a pattern that was indistinguishable from uninjected embryos (Fig. 4.8C). This suggests the absence of general effects of N-SSDP1 and DN-CLIM on spinal floorplate differentiation and axon growth inside the spinal cord.

The absence of an effect of N-SSDP1 overexpression on the development of PMN axons in anti-tubulin immunohistochemistry was surprising because over-expression of DN-CLIM strongly inhibited PMN axon development (Becker et al., 2002) and it is well established that LIM-HD proteins play crucial roles for the development of motor axons in many vertebrates including zebrafish (Lee and Pfaff, 2001; Hutchinson and Eisen, 2006). Therefore, we decided to examine the effects of N-SSDP1 and DN-CLIM over-expression on PMN axon development in greater detail. We used HB9:GFP transgenic animals, in which PMNs and their axons can be readily visualized. At 31 hpf, ventrally projecting CaP axons and dorsally projecting MiP axons are detectable in these embryos. Both types of projections require the activity of LIM-HDs of the Isl class (Hutchinson and Eisen, 2006). The use of HB9:GFP embryos revealed that DN-CLIM inhibited both the ventral projection by CaP and the dorsal projection by MiP, whereas N-SSDP1 had no effect on either projection (Fig. 4.7C). In contrast to unperturbed PMN axons GFP-positive axons in DN-CLIM

over-expressing embryos extended inside the spinal cord along the rostral-caudal axis at the ventral border of the spinal cord (Fig. 4.7D), indicating that CLIM cofactors are required for PMN axons to exit the spinal cord.

To elucidate possible mechanisms of SSDP1 action, we also injected mRNAs encoding zebrafish SSDP1b in full length (zf SSDP1b). Indeed, similar to phenotypes observed for N-SSDP1, embryos overexpressing zf SSDP1b developed smaller eyes and the development of trigeminal and Rohon-Beard axons was inhibited (Fig. 4.8A). These phenotypes were weaker when compared to the ones induced by N-SSDP1 (compare Figs. 4.7 and Fig. 4.6), probably due to lower protein stability in cells.

Fig. 4.7 Phenotypes induced by N-SSDP over-expression partially overlap with those induced by DN-CLIM over-expression. **A:** Lateral views of anti-tubulin immuno-labeled whole-mounted 24 hpf embryos are shown. Injection of N-SSDP1 mRNA leads to loss of peripheral axons of trigeminal (trig) and Rohon-Beard neurons, but not of ventral motor axons (NLS-myc = control mRNA). DN-CLIM mRNA injections affect all three types of axons. Arrows indicate axons. **B:** Quantification confirms significant loss of peripheral sensory but not motor axons upon N-SSDP1 over-expression, whereas DN-CLIM over-expression affects also motor axons. **C:** DN-CLIM, but not N-SSDP1 over-expression inhibits growth of dorsal MiP axons (arrows), as shown in lateral trunk views of HB9:GFP transgenic embryos at 28 hpf. **D:** Higher magnification of the ventral border of the caudal spinal cord (arrows) at 24 hpf shows that HB9:GFP^{+} motor neurons grow axons (arrowheads) ventrally out of the spinal cord in controls. In DN-CLIM mRNA injected embryos axons grow along the ventral border of the spinal cord. Scale bars = 50 μm.

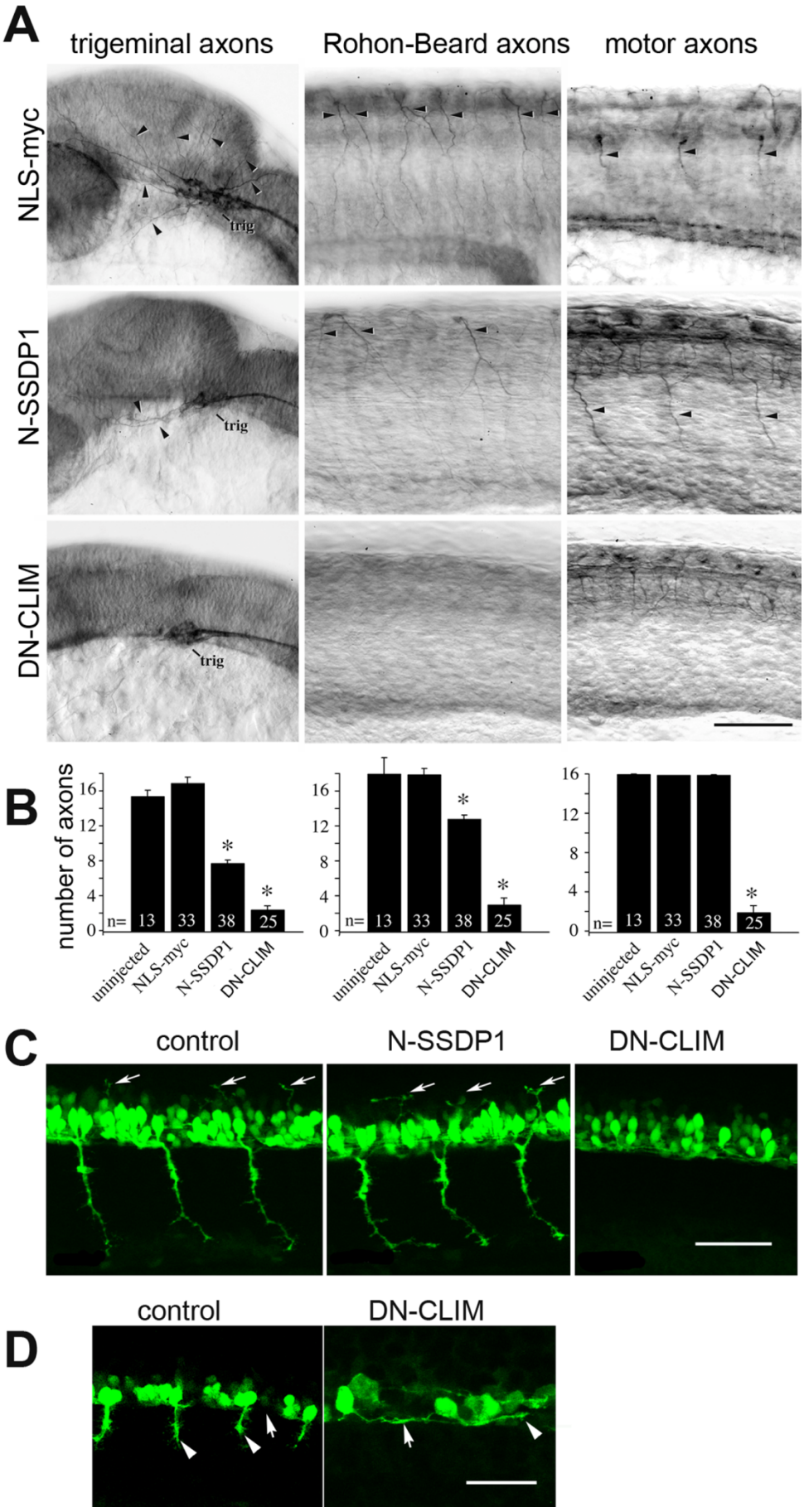
A
trigeminal axons
Rohon-Beard axons
motor axons
NLS-myc
N-SSDP1
DN-CLIM
trig
B
number of axons
n=
13
33
38
25
uninjected
NLS-myc
N-SSDP1
DN-CLIM
C
control
N-SSDP1
DN-CLIM
D
control
DN-CLIM

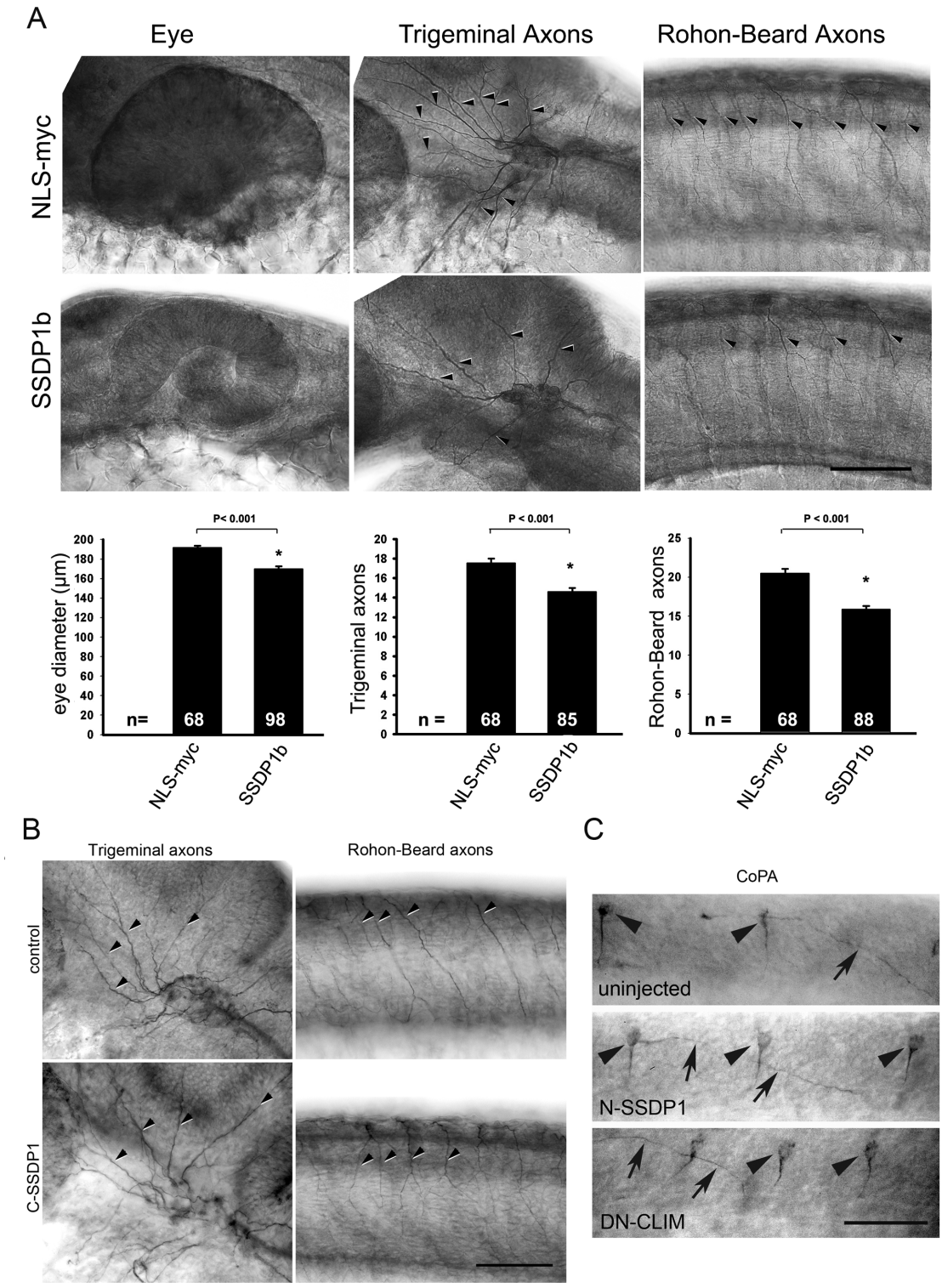

Fig. 4.8 **A**. Full length zebrafish SSDP1b over-expression has similar effects to N-SSDP1. Lateral views of anti-tubulin labeled whole-mounted 24 hpf embryos are shown. Arrowheads indicate axons. Eye size as well as axon numbers of trigeminal and Rohon-Beard neurons are significantly reduced by SSDP1b over-expression compared to NLS-myc control. Scale bar = 50 µm. **B**. C-SSDP1 overexpression does not affect peripheral trigeminal or Rohon-Beard axons. Lateral views of head (for

trigeminal axons) and trunk (for Rohon-Beard axons) are shown. Some of the axons are indicated by arrows. Scale bar = 100 µm. **C:** Lateral views of the spinal cord show that 3A10 immuno-labelled CoPA neurons (arrowheads) and their commissural axons (arrows) are not affected by N-SSDP1 or DN-CLIM over-expression. Scale bars = 50 µm.

To confirm the roles of SSDP1a and SSDP1b for zebrafish development we generated specific SSDP1 morpholino oligonucleotides to knock down levels of SSDP1 early during zebrafish development (Fig. 4.9). RT-PCR experiments confirmed the functionality of our morpholinos. Whereas the injection of SSDP1a morpholino (MO SSDP1a) resulted in undetectable mRNA levels, probably due to non-sense mediated decay (Bill et al., 2009), the morpholino against SSDP1b (MO SSDP1b) induced a shift in the size of the amplicon from 327 bp to 254bp in the morphant. This led to a frame shift thereby introducing an early stop codon at the beginning of exon 3, such that it is highly unlikely that functional protein was transcribed (Fig. 4.9 &Fig. 4.10A).

Next, we examined the developmental effects caused by individually or simultaneously knocking down SSDP1a and SSDP1b. These experiments revealed that the knockdown of SSDP1b, but not SSDP1a, significantly inhibited the development of peripheral axons of trigeminal and Rohon-Beard neurons (Figs. 4.10 C-E). This is consistent with conspicuous expression of SSDP1b, but not SSDP1a mRNA in these neuronal cell types (see Fig. 4.3). To exclude that effects of morpholinos were a consequence of retarded overall development we determined the segmental position of the lateral line primordium, an indicator of embryonic developmental stage (Kimmel et al., 1995), and found no differences between any of the morpholino injected groups and uninjected embryos (data not shown). This suggests specificity of the axonal phenotypes in morphants.

However, we did not detect significant effects on eye and MHB development nor on PMN axons by knocking down SSDP1a, b or both (data not shown). These

results indicate specific functions of SSDP1b for developing peripheral axons of trigeminal and Rohon-Beard neurons. The fact that eye and MHB development was inhibited upon overexpression of N-SSDP1 (Fig. 4.6) but not in our SSDP1 knockdown experiments (data not shown) suggests that members of the SSDP family other than SSDP1 may participate in LIM-HD/CLIM complexes in these structures and act redundantly with SSDP1a,b.

The eye phenotype caused by N-SSDP1 over-expression was partially rescued by simultaneously knocking down endogenous SSDP1a and b (Fig. 4.10B). Because there is only a 6 out of 25 morpholino bases overlap with N-SSDP1, and morpholinos lose all activity when more than 4 bases are mis-matched it is highly likely that neither of the morpholino oligonucleotides recognize mouse-derived N-SSDP1. This may be explained by opposing actions of N-SSDP1 and SSDP1 morpholinos on CLIM stability. This rescue experiment also suggests specific action of the morpholinos.

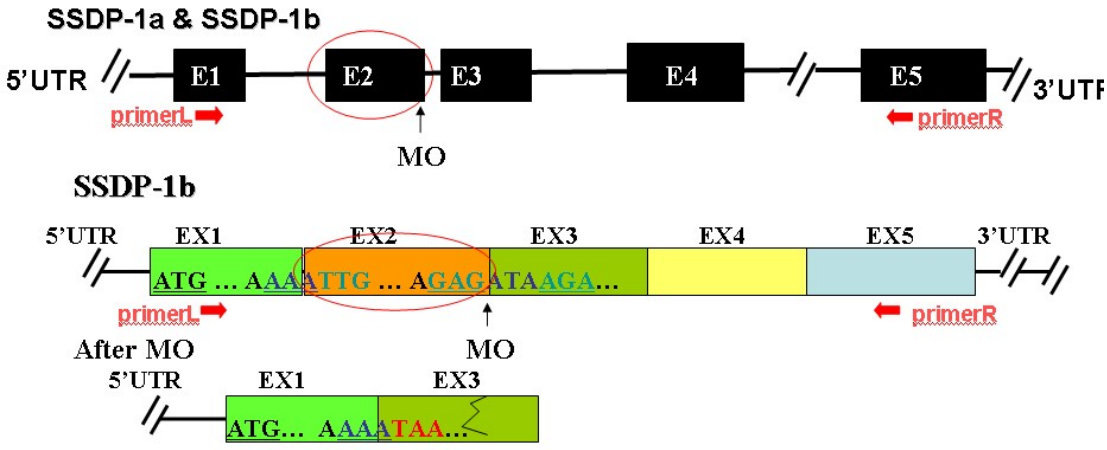

Fig. 4.9 Morpholinos designed to knockdown SSDP1a & SSDP1b. Two splice site directed morpholino were designed to target exon2_intron2 splice junction and should result in the complete or partial deletion of exon2. SSDP-1b MO induces skipping of exon2 of SSDP-1b mRNA, producing an aberrant RNA transcript that fuses exon3 directly to exon1 showed by sequencing.

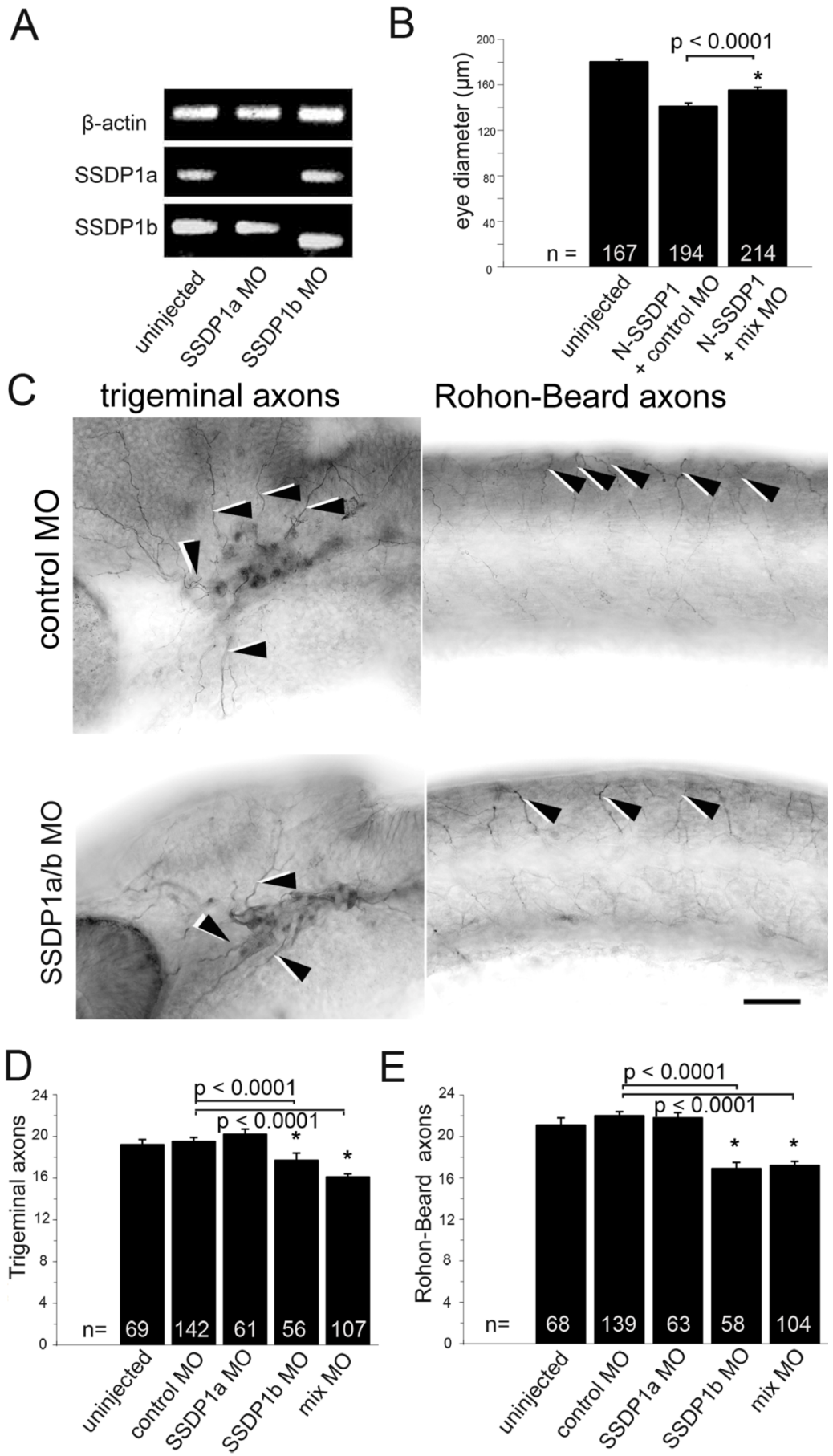
A
β-actin
SSDP1a
SSDP1b
uninjected
SSDP1a MO
SSDP1b MO
B
eye diameter (μm)
p < 0.0001
*
n =
167
194
214
uninjected
N-SSDP1 + control MO
N-SSDP1 + mix MO
C
trigeminal axons
Rohon-Beard axons
control MO
SSDP1a/b MO
D
Trigeminal axons
p < 0.0001
p ≤ 0.0001
n=
69
142
61
56
107
uninjected
control MO
SSDP1a MO
SSDP1b MO
mix MO
E
Rohon-Beard axons
p < 0.0001
p ≤ 0.0001
n=
68
139
63
58
104
uninjected
control MO
SSDP1a MO
SSDP1b MO
mix MO

Fig. 4.10 Knock-down of SSDP1b, but not SSDP1a partially inhibits growth of peripheral axons of trigeminal and Rohon-Beard neurons. **A:** Morpholino knock-down reduces levels of correctly spliced SSDP1a and SSDP1b to levels that are undetectable by PCR. An ectopic band is amplified after SSDP1b knock-down, which contains premature stop codons and, therefore, cannot lead to functional protein. Beta-actin was used to equalize cDNA concentrations. **B:** Morpholinos to SSDP1 partially rescue reduced eye size induced by N-SSDP1 over-expression, suggesting specificity of the morpholinos. **C:** Lateral views of anti-tubulin immuno-labeled whole-mounted 24 hpf embryos injected with Morpholinos against SSDP1a/b are shown. Arrowheads point to trigeminal and Rohon-Beard axons, respectively. Scale bar = 50 μm. **D,E:** Quantifications indicate significant loss of peripheral axons of trigeminal and Rohon-Beard neurons after Morpholino knock-down of SSDP1b.

4.2.6 SSDPs stabilize CLIM during PMN development

The finding that in contrast to DN-CLIM, overexpression of N-SSDP1 or zebrafish SSDP1b did not affect peripheral axons of primary motor neurons (Fig. 4.7 &Fig. 4.8) showed that either SSDPs are dispensable for primary motor neuron development or that only N-terminal sequences of SSDPs are important for a correct formation and functioning of LIM-HD complexes. To examine if SSDP1 exerts functions via CLIM stabilization we co-injected DN-CLIM together with N-SSDP1. In these co-injection experiments we titrated the amount of DN-CLIM mRNA (75%) to only moderately affect axon growth. Indeed, co-injection of N-SSDP1 (25%) partially rescued the effect of DN-CLIM on PMN axons as well as trigeminal axons in a significant manner, whereas no effect was detected on DN-CLIM-mediated inhibition of RB peripheral axon formation (Fig. 4.11). Although the average eye size was 45% larger in N-SSDP1/DN-CLIM co-injected embryos when compared to DN-CLIM injected embryos, this difference was not significant. The MHB could not be quantitatively assessed. Because N-SSDP1 is able to stabilize CLIM (Fig. 4.5) and overexpression of N-SSDP1 or knockdown of SSDP1 does not affect PMN axons (Fig. 4.7), the rescue in this cell type is likely due to a stabilization of endogenous

CLIM cofactors by N-SSDP1. Thus, these results reveal a function for SSDPs for the stabilization of LIM-HD multiprotein complexes in primary motor neurons.

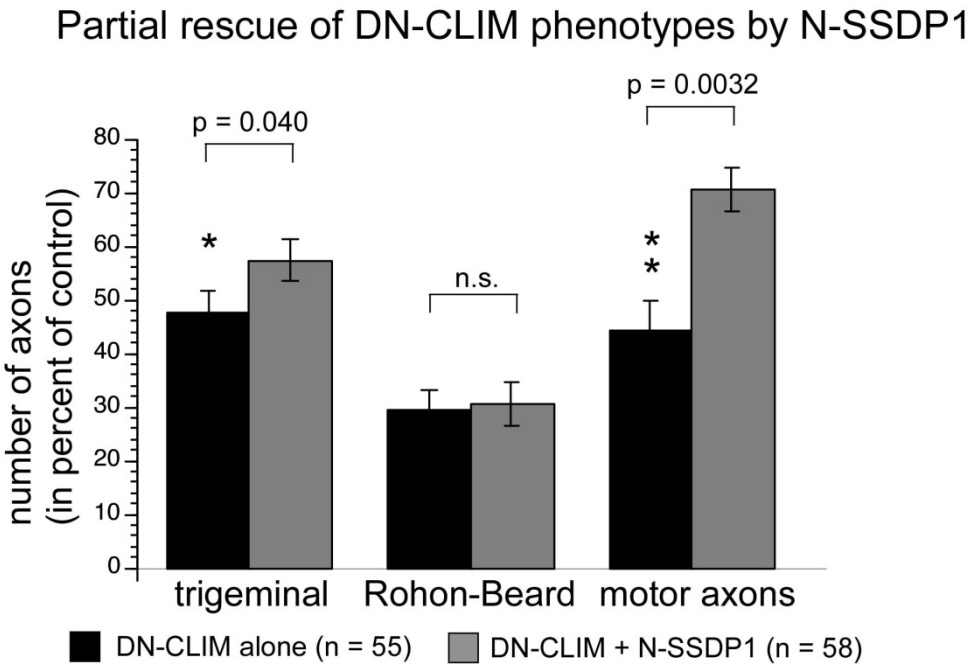

Fig. 4.11 N-SSDP1 over-expression partially rescues phenotypes induced by DN-CLIM. Significantly fewer axons of trigeminal neurons and motor neurons, but not of Rohon-Beard neurons, are lost when N-SSDP1 mRNA is co-injected with DN-CLIM mRNA, compared to DN-CLIM mRNA injection alone.

4.3 Discussion

We show previously unknown and highly specific functions of SSDP1 co-factors in the development of peripheral sensory axons and in patterning of the anterior CNS. Our results provide evidence that these functions are mediated at least in part by stabilization of CLIM cofactors.

4.3.1 Specific functions of SSDP1b in sensory axon growth

Expression analysis of SSDP1a and SSDP1b mRNAs indicated widespread

expression throughout embryonic development for both genes, in agreement with multiple functions of these co-factors. However, SSDP1b showed specific accumulation in sensory trigeminal and Rohon-Beard neurons. This is reminiscent of the expression of CLIM cofactors with wide expression of CLIM2 and a more restricted expression pattern of CLIM1 (Bach et al., 1997) Bach et al., 1999; Ostendorff et al., 2006). Because co-factor levels are under tight proteasomal regulation (Gungor et al., 2007; Xu et al., 2007) we also analyzed the protein distribution of SSDP1 and CLIM. This confirmed specific accumulation of both SSDP1 and CLIM in trigeminal and Rohon-Beard neurons, suggesting specific roles of these co-factors here. Interfering with SSDP1 function, either by over-expression of N-SSDP1, SSDP1b in full length or by morpholino knockdown of SSDP1b, impaired outgrowth of peripheral trigeminal and Rohon-Beard axons. This phenotype strongly resembles that of over-expression of a dominant-negative form of the CLIM co-factor, DN-CLIM. The effects of SSDP1 manipulations and DN-CLIM were highly cell type-specific, because another spinal cell type, the CoPA neuron, showed an unaffected axonal trajectory inside the spinal cord. Interestingly, the LIM-HD *islet1/2* is strongly expressed in trigeminal and Rohon-Beard neurons (Becker et al., 2002), suggesting that SSDP1 and CLIM could participate in *islet1/2* transcriptional complexes in these sensory neurons. Taken together, these observations are consistent with functions of SSDP1b/CLIM interactions in the formation of sensory axons during early development.

4.3.2 SSDP1/CLIM interactions may be involved in motor axon pathfinding

Extending on previous findings we show here that DN-CLIM overexpression affects ventral and dorsal motor axon growth. Instead of inhibiting axon formation altogether, as for sensory axons, axons of HB9:GFP positive cells still grow, but are unable to exit the spinal cord. Axons grow along the ventral edge of the spinal cord, close to the floor plate. This phenotype is similar to that observed after knock down of

the LIM-HDs *islet1* and *islet2* (Hutchinsen and Eisen, 2006). The fact that CoPA neurons showed correct growth inside the spinal cord, including commissural growth at the floor plate, indicated that patterning of the spinal cord was largely unaffected by DN-CLIM overexpression. This suggests that LIM-HD complexes could be involved in the expression of specific guidance receptors or proteins in only motor neurons that lead their axons to their specific targets (Lee et al., 2008). For example we have shown for another cell type, trigeminal neurons, that expression of the axonal recognition molecule Contactin1 is dramatically reduced when DN-CLIM is overexpressed (Gimnopoulos et al., 2002). The lack of a motor axon phenotype by manipulations of SSDP1 was the only non-overlapping finding with those of DN-CLIM overexpression. However, N-SSDP1 overexpression partially rescued the axon pathfinding defect elicited by DN-CLIM. This suggests that SSDP1/CLIM interactions may also play roles in motor axon pathfinding.

4.3.3 SSDP1 is involved in patterning of the anterior CNS

Patterning defects induced by N-SSDP1 over-expression in the eye and MHB were also similar to those observed after DN-CLIM over-expression. We show that SSDP1 and CLIM proteins are co-expressed in these structures. However, DN-CLIM generally had stronger effects. The reduction of eye size and loss of MHB marker expression was more severe in DN-CLIM overexpressing embryos compared to N-SSDP1 or SSDP1b overexpressing embryos. N-SSDP1 over-expressions lead to complete loss of pax2 and a reduction of engrailed and wnt-1 labeling in the MHB, whereas after DN-CLIM injection all three markers are lost (Becker et al., 2002). Here we show that DN-CLIM inhibits differentiation of the Mauthner neurons in the hindbrain, whereas N-SSDP1 over-expression was not sufficient to inhibit differentiation of this cell type.

The fact that knock down of SSDP1a and b had no apparent effect on eyes and MHB could be explained by the fact that at least five different SSDP and four CLIM

proteins are present in zebrafish (zfin.org), which may act redundantly. Indeed, SSDP2 has been shown to participate in LIM-HD complexes (Cai et al., 2008) and to be necessary to maintain levels of CLIM protein (Wang et al., 2010). Overall, patterning effects of manipulations of SSDP1 and CLIM cofactors on CNS patterning resemble those observed in mouse mutants for SSDP1 and CLIM, in which genetically linked smaller or absent head structures have been reported (Mukhopadhyay et al., 2003; van Meyel et al., 2003; Nishioka et al., 2005; Enkhmandakh et al., 2006). Axonal phenotypes have not been demonstrated in mice. We show here highly specific functions of SSDPs in axon formation and pathfinding.

4.3.4 Evidence that effects of SSDP1 manipulation are mediated by CLIM in vivo.

Too low or too high CLIM levels inhibit LIM-HDs (Fernandez-Funez et al., 1998; Matthews and Visvader, 2003). The inhibition of LIM-HD/CLIM transcriptional complexes via overexpression of DN-CLIM in zebrafish (Becker et al., 2002) is reminiscent of the phenotypes obtained by disturbing SSDP1 via overexpression or knockdown. Thus, because our overexpression of SSDP1 leads to an increase and the knockdown of SSDP1 via morpholino leads to a decrease in endogenous CLIM levels (Fig. 4.5; Gungor et al., 2007), most of the phenotypes observed by disturbing SSDP1 might be explained by induced changes in cellular CLIM/LIM-HD stoichiometries leading to a functional inhibition of these complexes.

Further support for the significance of the CLIM stabilization of SSDP1 stems from our observation that both N-SSDP1 and SSDP1 full length forms lead to increased cellular CLIM levels when overexpressed (Gungor et al., 2007) and that the induced phenotypes are very similar (Fig. 4.7,4.8 and 4.10). These results argue against dominant-negative effects of N-SSDP1. In addition, overexpression of N-SSDP1 that contains the CLIM interaction domain rescues phenotypes induced by DN-CLIM in motor axon pathfinding and formation of trigeminal axons. This is

consistent with a scenario in which N-SSDP1 stabilizes endogenous CLIM, such that it can compete with DN-CLIM to form functional LIM-HD complexes. In Rohon-Beard neurons, for which no rescue of peripheral axon growth was observed, N-SSDP1 overexpression might not have stabilized CLIM proteins to functional levels.

Taken together, stabilization of CLIM by SSDP1 in vivo, rescue of DN-CLIM induced motor axon phenotypes by DN-CLIM and overlapping phenotypes of DN-CLIM overexpression and SSDP1 manipulations are consistent with in a role of SSDP1 in the control of the transcriptional activity of LIM-HD complexes by stabilizing and protecting CLIM cofactors from proteasomal degradation (Gungor et al., 2007; Xu et al., 2007). However, as overexpression of N-SSDP1 inhibits endogenous alphaGSU expression in pituitary cells *in vitro* (Fig. 4.5) and a proline-rich region that is deleted in N-SSDP1 appears important for at least some of its functions in LIM-HD complexes (Enkhmandakh et al., 2006), we cannot exclude the possibility that dominant-negative actions contribute to the phenotype observed in embryos overexpressing N-SSDP1. Finally, it has to be noted that SSDP1/CLIM interactions may have functions independent of LIM-HDs, as CLIM co-factors have been shown to interact with several non-LIM domain-containing transcription factors (Torigoi et al., 2000; Heitzler et al., 2003; Gungor et al., 2007; Johnsen et al., 2009).

In summary, overlapping expression patterns and perturbation phenotypes of SSDP1 and CLIM, as well as *in vivo* stabilization of CLIM and rescue of DN-CLIM phenotypes by N-SSDP1 indicate important regulatory functions of SSDP1/CLIM interactions for CNS patterning, as well as growth and pathfinding of specific axon types.

5. Summary

The zebrafish is a powerful model to study vertebrate developmental biology, because processes can be studied that are impossible or difficult to analyze in other vertebrates. For example, we can trace the differentiation of individual neurons during embryonic development with different molecular and histological methods in zebrafish. So the zebrafish provides us with an excellent research tool to study neuronal development as well as axon pathfinding. The aim of this thesis was to find out the function of co-factors of LIM-homeodomain transcription factors (LIM-HDs) in neuronal development as well as axon pathfinding in zebrafish.

LIM-HDs constitute an important class of transcription factors in neuronal development. Specific LIM-HD transcription factor combinations determine neuronal fate specification as well as axon pathfinding. It is known that SSDP/CLIM/LIM-HD transcription complexes function as a cascade to protect LIM-HDs from proteosomal degradation (Gungor et al., 2007; Xu et al., 2007). Dominant negative CLIM (DN-CLIM) competes with endogenous CLIM to bind the LIM domain of LIM-HD and blocks the downstream gene transcription of LIM-HDs. In DN-CLIM injected zebrafish, motor axons cannot project out of the spinal cord (Segawa et al., 2001; Becker et al., 2002). Analysis of cell identity after DN-CLIM injection shows that most motor neurons maintain expression of HB9 and Islet1/2 even though part of them lost expression of the mature MN marker ChAT. Further evidence suggests that motor neurons in the ventral spinal cord of embryos overexpressing DN-CLIM can still grow axons, but only inside the spinal cord. This provides a model in which to determine the down-stream genes of LIM-HDs that control motor axon pathfinding, while leaving genes that determine motor neuron identity largely unaffected. Gene array analysis was performed on FAC sorted HB9:GFP^{+} motor neurons after DN-CLIM treatment. Twenty-eight genes were found to be both downregulated by DN-CLIM and enriched in motor neurons.

Chodl, calca and *tac-1*, three genes retrieved from gene array list, are specifically expressed in motor neurons and obviously down-regulated after DN-CLIM injection, as confirmed by in situ hybridization. This validates the gene array paradigm as a method to discover new genes associated with motor neuron differentiation. Knock down of *chodl* using morpholinos shows that motor axons stall at the horizontal myoseptum for a longer time than in control MO injected group, which suggests that *chodl* is an important axon guidance molecular downstream of LIM-HDs.

Single stranded DNA binding protein 1 (SSDP1, also known as SSBP3) works as the activator of LIM-HD transcriptional complexes in head development of mouse embryos (Nishioka et al., 2005). To further study how SSDP/CLIM/LIM-HD transcription factor complexes work in neuronal development, zebrafish Ensemble database sequences ENSDARG00000030155 and ENSDARG00000058237 (we named them as SSDP1a and SSDP1b separately), which are most closely related to mouse and human SSDP1, were cloned. SSDP1a is widely expressed in whole embryo during development while SSDP1b is specifically expressed in trigeminal and Rohon-Beard (RB) neurons. SSDP1 and CLIM are co-expressed in trigeminal, RB as well as motor neurons. The N-terminus of SSDP1 (N-SSDP1) or full-length SSDP1b over-expression prevents outgrowth of sensory trigeminal & RB axons and inhibits the development of eyes and midbrain-hindbrain-boundary (MHB). SSDP1b knock-down by MO significantly inhibited the peripheral axonal projection of trigeminal and RB neurons but did not affect eye and MHB development. The overlapping phenotypes of SSDP1 and DN-CLIM in anterior central nervous system (CNS) pattering and peripheral sensory axon outgrowth, as well as in vivo stabilization of CLIM and the rescue of DN-CLIM effects by N-SSDP1 indicate that specific SSDP1 functions in neural development by stabilizing the CLIM/LIM-HD complex.

This study focused on the role of co-factors of LIM-HDs transcription factors in

regulating neuron development and axon pathfinding (Fig. 5.1). We found new down-stream genes of LIM-HDs, which are involved in motor axon pathfinding. We demonstrated that SSDP1 functions in sensory axon development as well as neuronal patterning, which is partly due to interaction with CLIM. Finding more motor axon guidance molecules, especially down-stream genes of LIM-HDs, will help us to further understand the mechanism of SSDP/CLIM/LIM-HDs transcriptional complexes in motor neuron development as well as in axon guidance. A better understanding of the basic differentiation processes in motor neurons may ultimately inform therapeutic strategies for motor neuron disease.

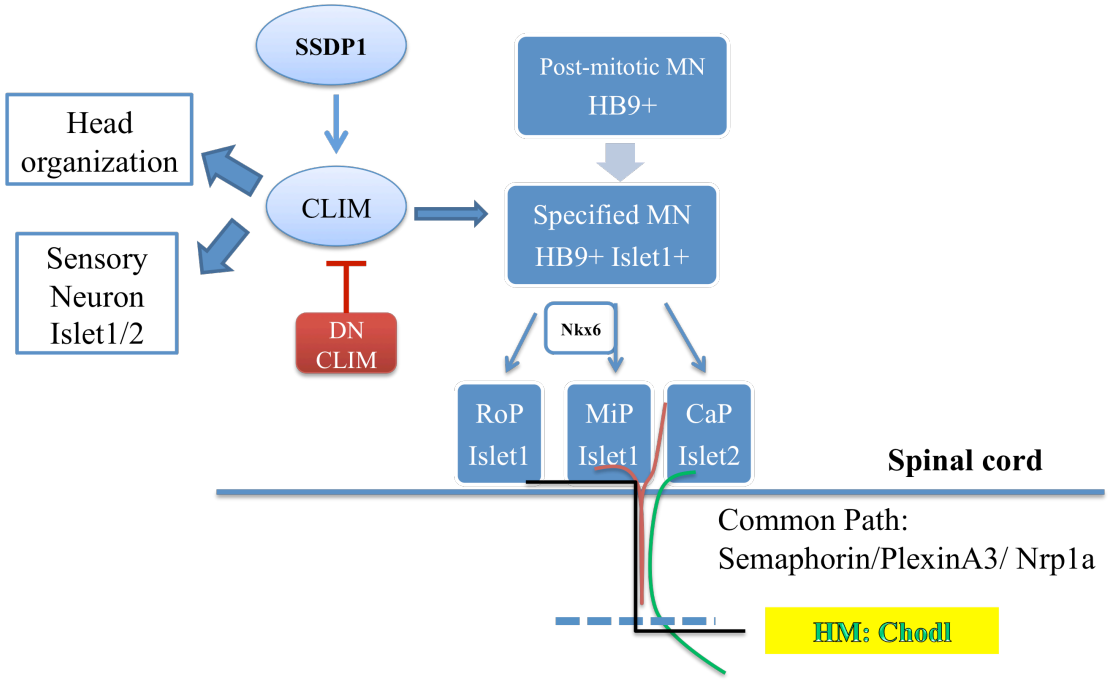

Fig. 5.1 Schematic of co-factors of LIM-HDs in neuronal development with special reference to motor neuorn differentiation. Stabilization of CLIM by SSDP1 is involved in CNS patterning and sensory neuron as well as motor neuron development. DN-CLIM out-competes endogenous CLIM to bind to LIM domains of LIM-HDs and thus blocks the downstream gene transcription of LIM-HDs. Gene profiling of DN-CLIM injected embryos identified chodl, an important axon pathfidning gene that acts at the horizontal myoseptum. PlexinA3 and Nrp1a have also been found to be down-stream of LIM-HDs.

6. Discussion

6.1 Motor neuron formation, specification and axon pathfinding is dynamically regulated by different molecules during development.

Motor neurons develop from the motor neuron progenitor domain (pMN) in the ventral spinal cord. A number of transcription factors are involved in this process. Hh signaling induces the development of $Olig2^+$ progenitor cells, which give rise to motor neurons as well as oligodendrocytes. Specification of motor neurons and oligodendrocytes requires not only Olig2 but also Hh signaling, as overexpression of Olig2 cannot rescue the the lack of motor neurons or oligodendrocytes in a mutant with disrupted Hh signaling (Park et al., 2002). Motor neuron progenitors down-regulate Olig2 and up-regulate Ngn2 during differentiating into post-mitotic $HB9^+$ motor neuron (Lee et al., 2005). Under the regulation of sequential expression of NeuroM in post-mitotic motor neurons and NeuroD in more mature motor neurons, motor neurons acquire their $HB9^+$ identity and start to project their axons into specific muscles (Sommer et al., 1996; Roztocil et al., 1997). After motor neurons have formed, different patterns of LIM-HDs transcription factors are induced, for example by Nkx6 transcription factors, to further specify the subtype identity of motor neurons (Sander, 2000; Vallstedt, 2001; Hutchinson et al., 2007). There are two phases of LIM-HD expression during primary motor neuron development. All primary motor neurons start to express *islet1* after exiting the cell cycle. CaP, one of the primary motor neurons, initiates *islet2* expression when still expressing *islet1* at around 14hpf, after that, it down-regulates *islet1* expression. So CaPs have an early *islet1* expression phase and a later *islet2* expression phase. In contrast, MiPs reinitiate *islet1* expression after transient down-regulation at around 16hpf, thus MiPs express *islet1* in both the early and the late phase of differentiation. The early expression phase of *islet1* is required for the formation of all primary motor neurons, while the late unique expression phase decides their specific axon pathfinding, respectively (Hutchinson et

al., 2007; Hutchinson & Eisen, 2006). Thus, precise temporal regulation of transcription factors, including LIM-HDs, is essential for all aspects of motor neuron differentiation.

The phenotype of DN-CLIM overexpression and *islet1* knock-down are similar. In both manipulations PMNs still form, but their axons fail to exit the spinal cord, suggesting CLIM/Islet1 interactions (first expression phase) regulate axon pathfinding. At the same time, Islet1 is partly required to inhibit interneuron formation. This might explain why we observed increased GABA expression in some PMNs as well as decreased numbers of HB9:GFP^{+} motor neurons after DN-CLIM over-expression (data not shown). *Islet2* MO only partly blocked the Cap axon pathfinding but did not inhibit the CaP specification as axons still grew ventrally out of the spinal cord (Segawa et al., 2001).

The second phase of *islet1* and *islet2* regulates the MiP and CaP axon guidance, respectively (Hutchinson and Eisen, 2006; Hutchinson et al., 2007). The primary motor neuron also lost their specifications as they did not project their axons to the specific muscle and axons only extended within the spinal cord after DN-CLIM injection (Zhong et al., 2011), which is a more complete inhibition of axon pathfinding compared with *islet2* MO effects. This was expected, as DN-CLIM should disrupt the first and second expression phase of *islet* genes.

Gene array analysis of DN-CLIM injected fish further clarified CLIM/LIM-HD down-stream genes, which are involved in axon pathfinding. *Chodl* is one of the genes from the list of genes down-regulated after DN-CLIM injection and it regulates the interaction of motor growth cones with the horizontal myoseptum during axon pathfinding. Thus two layers of gene regulation control motor neuron targeting: An upper layer is for motor neuron specification, which instructs rostral-caudal identitity of CaP/ MiP; a lower layer of regulation is involved in specific sequential pathway decisions of motor axons. We conclude that CLIM is presumably involved in both processes. RT-PCR shows that the expression of *chodl* was decreased also after

SSDP1 overexpression in zebrafish (data not shown), which suggests that *chodl* is regulated by SSDP1/CLIM/LIM-HD transcription factor complexes. Also in amniotes, LIM-HDs and Hox genes function in a combinatorial manner to regulate the motor neuron subtype identities at the level of pools and columns. Subsequently, LIM-HD transcription factor expression changes to coincide with different choice points reached by motor axons. At the same time, other "local" guidance factors, for example, EphA/ephrinA in MMC, EphA/ephrinA in LMCl and EphB/ephrinB in LMCm are involved in regulating successive motor axon pathway choices. These are the upper and lower layer of motor neuron regulation in amniotes.

It is still not clear how the interaction of Chodl with the horizontal myoseptum guides motor axons. The *stumpy* mutant, which shows a similar phenotype as the *chodl* morphant (Beattie et al., 2000), may help to find the corresponding guidance cues for the Chodl receptor. The synergistic effect of double knock-down of *Chodl and ColXIX* supports the interaction between these two genes, while physical interaction must be demonstrated by further biochemical experiments. Investigating the function of *calca* and *tac-1*, the two other motor neuron expressed genes identified in expression profiling, may further uncover the mechanism of LIM-HDs signaling pathway in motor axon guidance.

6.2 SSDPs function in sensory neuron development and head organization

As previous work already showed the strong expression of *islet1/2* in sensory neurons (Becker et al., 2002) overlaps with that of CLIM and Single Stranded DNA binding Protein 1 (SSDP1). The fact that SSDP1b functions in periphery sensory axons outgrowth is also consistent with the phenotype that overexpression of dominant negative CLIM (DN-CLIM) can block sensory axon growth in zebrafish (Becker et al., 2002). Combined with recent publications showing that LIM-HD

transcription factors Islet1 and Islet2 are involved in trigeminal sensory ganglion neuron axon branching (Yeo et al., 2004) and RB axon outgrowth (Tanaka et al., 2011) respectively, we can draw the conclusion that SSDP1/CLIM/LIMHD transcription factors are involved in sensory peripheral axon growth and Islet1/2 may be controlled by SSDP1/CLIM indirectly or directly.

SSDP1 is involved in the head organization during mouse embryo development. The Midbrain-Hindbrain-Boundary (MHB) acts as an organizing center for tectum formation and the subsequent establishment of the retinotectal projection. One of the LIM-HD molecules, *islet3*, is expressed in the central neuron system, especially in eyes and tectum (Tokumoto et al., 1995). Over-expressing the LIM domain of Islet3 severely impaired eye and MHB formation suggesting that this LIM-HD plays an important role in central nerve system development (Kikuchi et al., 1997). DN-CLIM also impaired eye and MHB development in zebrafish. The expression of marker genes for MHB (wnt1, eng2, pax2a, fgf8, ephrinA5b) and eyes (RxC, Six3.1) were almost lost after DN-CLIM injection (Becker et al., 2002). Investigation of SSDP1 function in eye and MHB development in this study showed that the SSDP1 overexpression reduced eye and MHB size. Obvious down-regulation of pax2a, eng2 and wnt1 gene expression was observed with N-SSDP1 overexpression, while expression of other marker genes (RxC, Six3.1, otx2, pax6a and neuroD) was retained. So the effects of overexpression of N-SSDP1 on MHB are weaker than after DN-CLIM overexpression. Another evidence of the greater effects of DN-CLIM on MHB is that DN-CLIM completely inhibited Mauthner neuron development in the hindbrain, while N-SSDP1 did not have any effects on the differentiation of this neuron. These data further confirmed that SSDP/DNCLIM/LIMHD complexs are involved in MHB and eye development. The absence of effects of SSDP1 knock-down in eye and MHB development could be explained by other homologous SSDP genes interacting with CLIM to regulate anterior CNS patterning. Further study of the individual function of other SSDP homologs will help to clarify the mechanism

of SSDP/CLIM/LIM-HD action in neuronal development as well as its function in other organisms.

6.3 Conserved protein interactions control neuronal development from invertebrate to vertebrate

In the past decades CLIM/LIM-HD transcription factors have been indentified in fly, zebrafish, chick, mouse and human, and their function in neuronal development as well as specification has also been clarified. The "LIM code" in different subclasses of neurons can be correlated with distinct characteristics of neurons such as specific axon pathfinding, which is strikingly conserved from invertebrates to vertebrates (Jurata et al., 2000). For example, The combinatorial expression of LIM code *islet1, slet2, Lim1* and *Lim3* in chick defines the subclass of motor neurons which occupy the different column in spinal cord and project to specific axonal pathway in periphery (Tsuchida, 1994). Similar combinatorial code of LIM-HD genes were also identified in zebrafish primary motor neurons (Appel et al., 1995) and mouse spinal motor neurons (Pfaff et al., 1996). These work were the first providing functional evidence for a LIM code to be involved in determining motor neuron subtype identity.

We discovered that the LIM-HD down-stream gene *chodl* plays an important role in motor axon pathfinding. Chodl, belonging to C-lectin family, shows a highly conserved sequence compared with other vertebrates. Chodl was found expressed in a subclass of motor neurons in mice which specifically innervate to fast musculature, which indicates that Chodl may be involved in the function of this particular subclass of neurons (Enjin et al., 2010). CLEC-38, another C-type lectin protein functions in axon pathfinding in *Caenorhabditis elegans* (Kulkarni et al., 2008).

Phylogenetic comparison of Ldb1 (CLIM) protein shows that their three important modules (LID, LCCD and DD) are remarkably conserved from *C. elegans* to mammanian. All vertebrate SSDP proteins also show high levels of sequence identity with mouse and human SSDP in N-terminal CLIM-interaction domain and

C-terminal proline-rich domain. In this study, we cloned the SSDP1 gene in zebrafish, which contains the CLIM interaction domain and a proline-rich domain, which is highly homologous to those found in other species. SSDP1 in *C. elegans* is short and only contains a CLIM-interaction domain, while the proline-rich domain of significant similarity to mammalian sequences was found in *C. elegans* Ldb1 (Enkhmandakh et al., 2006), which suggests the important function of proline-rich domain during development. The "LIM Code" as well as SSDP/CLIM/LIM-HD complexes, recruiting all the domains in position, regulates neuronal differentiation and specification throughout evolution. These new findings in axon guidance as well as neuronal development will accelerate the process to further understand the mechanism of motor neuron disease in human, and more and more treatment targets will be identified as a consequence.

7. Perspective

Motor neuron development and axon guidance are relevant to motor neuron diseases in humans. Many axon guidance molecules are involved in the pathogenesis of neurodegenerative disease and have become novel treatment targets (Schmidt et al., 2009). A variety of evidence has suggested that the pathogenesis mechanisms are phylogenetically conserved, supporting that observations and insights gained in the zebrafish model can be applied to human conditions (Sager et al., 2010).

The preliminary data support that the genetic interaction between *Chodl* and *ColXIX* may be involved in PMN pathfinding in the horizontal myoseptum. To demonstrate physical interaction between these genes, more biochemical experiments are necessary. Apart from these two factors, other ECM factors (Tenascin-C (Schweitzer et al., 2005) and chondroitin sulfates (Bernhardt and Schachner, 2000), as well as other guidance cues, such as Netrin, in horizontal myoseptum may also be involved in the interaction with the Chodl receptor. The futher discovery of the mechanism of guidance factor interactions in the horizontal myseptum will further our understanding of motor axon pathfinding.

Even though specific neurodegenerative disease models in zebrafish have been constructed successfully (Ramesh et al., 2010; Hao et al., 2011), their pathogenesis mechanisms are still not very clear. Using exon profiling in mouse models of spinal muscular atrophy (SMA), specific isoform changes for *chodl* have been found already at early symptomatic stages, whereas most genes were dysregulated only at late symptomatic stages (Zhang et al., 2008; Baumer et al., 2009). Reduced expression of *SMN*, causally linked to SMA, leads to shorter motor axons of mice in vitro (Rossoll et al., 2003), and one of the phenotypes in developing zebrafish (McWhorter et al., 2003a) and mice (Liu et al., 2010) is also shorter axons. Thus, part of the phenotypes could be mediated through altered *chodl* expression. Such a defect could eventually

lead to degeneration of these motor neurons, possibly due to a lack of trophic support from the muscle targets (Gould and Oppenheim, 2011). To determine if and how *chodl* is involved in the maintenance of motor neurons and/or their axons and how altered expression of *chodl* could contribute to the disease at a later stage will help us to further study SMA pathogenesis mechanisms. These new findings in axon guidance as well as neuron development will accelerate the process to further understand the mechanism of motor neuron disease in humans. More and more treatment targets will be clarified as a consequence of discovering more guidance factors.

Bibliography

Agulnick AD, Taira M, Breen JJ, Tanaka T, Dawid IB and Westphal H (1996). "Interactions of the LIM-domain-binding factor Ldb1 with LIM homeodomain proteins." Nature **384**(6606): 270-2.

Alestrom P, Holter JL and Nourizadeh-Lillabadi R (2006). "Zebrafish in functional genomics and aquatic biomedicine." Trends in Biotechnology **24**(1): 15-21.

Appel B, Korzh V, Glasgow E, Thor S, Edlund T, Dawid IB and Eisen JS (1995). "Motoneuron fate specification revealed by patterned LIM homeobox gene expression in embryonic zebrafish." Development **121**(12): 4117-25.

Arber S (1999). "Requirement for the homeobox gene Hb9 in the consolidation of motor neuron identity." Neuron **23**: 659-674.

Arvidsson U, Riedl M, Elde R and Meister B (1997). "Vesicular acetylcholine transporter (VAChT) protein: a novel and unique marker for cholinergic neurons in the central and peripheral nervous systems." J Comp Neurol **378**(4): 454-67.

Avraham O, Hadas Y, Vald L, Zisman S, Schejter A, Visel A and Klar A (2009). "Transcriptional control of axonal guidance and sorting in dorsal interneurons by the Lim-HD proteins Lhx9 and Lhx1." Neural Development **4**(1): 21.

Bäumer D, Lee S, Nicholson G, Davies JL, Parkinson NJ, Murray LM, Gillingwater TH, Ansorge O, Davies KE and Talbot K (2009). "Alternative Splicing Events Are a Late Feature of Pathology in a Mouse Model of Spinal Muscular Atrophy." PLoS Genet **5**(12): e1000773.

Bach I (2000). "The LIM domain: regulation by association." Mech Dev **91**(1-2): 5-17.

Bach I, Carriere C, Ostendorff HP, Andersen B and Rosenfeld MG (1997). "A family of LIM domain-associated cofactors confer transcriptional synergism between LIM and Otx homeodomain proteins." Genes Dev **11**(11): 1370-80.

Bach I, Rhodes SJ, Pearse RV, 2nd, Heinzel T, Gloss B, Scully KM, Sawchenko PE and Rosenfeld MG (1995). "P-Lim, a LIM homeodomain factor, is expressed during pituitary organ and cell commitment and synergizes with Pit-1." Proc Natl Acad Sci U S A **92**(7): 2720-4.

Baumer D, Lee S, Nicholson G, Davies JL, Parkinson NJ, Murray LM, Gillingwater TH, Ansorge O, Davies KE and Talbot K (2009). "Alternative splicing events are a late feature of pathology in a mouse model of spinal muscular atrophy." PLoS Genet **5**(12): e1000773.

Beattie CE (2000). "Control of motor axon guidance in the zebrafish embryo." Brain Research Bulletin **53**(5): 489-500.

Beattie CE, Melancon E and Eisen JS (2000). "Mutations in the stumpy gene reveal intermediate targets for zebrafish motor axons." Development **127**(12): 2653-62.

Becker CG, Lieberoth BC, Morellini F, Feldner J, Becker T and Schachner M (2004). "L1.1 Is Involved in Spinal Cord Regeneration in Adult Zebrafish." The Journal of Neuroscience **24**(36): 7837-7842.

Becker CG, Schweitzer J, Feldner J, Becker T and Schachner M (2003). "Tenascin-R as a repellent guidance molecule for developing optic axons in zebrafish." J Neurosci **23**(15): 6232-7.

Becker T, Ostendorff HP, Bossenz M, Schluter A, Becker CG, Peirano RI and Bach I (2002). "Multiple functions of LIM domain-binding CLIM/NLI/Ldb cofactors during zebrafish development." Mechanisms of Development **117**(1-2): 75-85.

Bernhardt RR (1999). "Cellular and Molecular Bases of Axonal Regeneration in the Fish Central Nervous System." Experimental Neurology **157**(2): 223-240.

Bernhardt RR, Chitnis AB, Lindamer L and Kuwada JY (1990). "Identification of spinal neurons in the embryonic and larval zebrafish." J Comp Neurol **302**(3): 603-16.

Bernhardt RR and Schachner M (2000). "Chondroitin sulfates affect the formation of the segmental motor nerves in zebrafish embryos." Dev Biol **221**(1): 206-19.

Bill BR, Petzold AM, Clark KJ, Schimmenti LA and Ekker SC (2009). "A primer for morpholino use in zebrafish." Zebrafish **6**(1): 69-77.

Birely J, Schneider VA, Santana E, Dosch R, Wagner DS, Mullins MC and Granato M (2005). "Genetic screens for genes controlling motor nerve-muscle development and interactions." Dev Biol **280**(1): 162-76.

Bridwell JL, Price JR, Parker GE, McCutchan Schiller A, Sloop KW and Rhodes SJ (2001). "Role of the LIM domains in DNA recognition by the Lhx3 neuroendocrine transcription factor." Gene **277**(1-2): 239-250.

Bronstein R, Levkovitz L, Yosef N, Yanku M, Ruppin E, Sharan R, Westphal H, Oliver B and Segal D (2010). "Transcriptional Regulation by CHIP/LDB Complexes." PLoS Genet **6**(8): e1001063.

Brose K, Bland KS, Wang KH, Arnott D, Henzel W, Goodman CS, Tessier-Lavigne M and Kidd T (1999). "Slit Proteins Bind Robo Receptors and Have an Evolutionarily Conserved Role in Repulsive Axon Guidance." Cell **96**(6): 795-806.

Cai Y, Xu Z, Nagarajan L and Brandt SJ (2008). "Single-stranded DNA-binding proteins regulate the abundance and function of the LIM-homeodomain transcription factor LHX2 in pituitary cells." Biochem Biophys Res Commun **373**(2): 303-8.

Cerda GA, Hargrave M and Lewis KE (2009). "RNA profiling of FAC-sorted neurons from the developing zebrafish spinal cord." Dev Dyn **238**(1): 150-61.

Chen L, Segal D, Hukriede NA, Podtelejnikov AV, Bayarsaihan D, Kennison JA, Ogryzko VV, Dawid IB and Westphal H (2002). "Ssdp proteins interact with the LIM-domain-binding protein Ldb1 to regulate development." Proceedings of the National Academy of Sciences of the United States of America **99**(22): 14320-14325.

Choi RCY, Ting AKL, Lau FTC, Xie HQ, Leung KW, Chen VP, Siow NL and Tsim KWK (2007). "Calcitonin gene-related peptide induces the expression of acetylcholinesterase-associated collagen ColQ in muscle: a distinction in driving two different promoters between fast- and slow-twitch muscle fibers." Journal Of Neurochemistry **102**(4): 1316-1328.

Colamarino SA and Tessier-Lavigne M (1995). "The axonal chemoattractant netrin-1 is also a chemorepellent for trochlear motor axons." Cell **81**(4): 621-629.

Coonrod SA, Bolling LC, Wright PW, Visconti PE and Herr JC (2001). "A morpholino phenocopy of the mouse MOS mutation." Genesis **30**(3): 198-200.

Covassin L, Amigo JD, Suzuki K, Teplyuk V, Straubhaar J and Lawson ND (2006). "Global analysis of hematopoietic and vascular endothelial gene expression by tissue specific microarray profiling in zebrafish." Dev Biol **299**(2): 551-62.

Dasen JS, Liu JP and Jessell TM (2003). "Motor neuron columnar fate imposed by sequential phases of Hox-c activity." Nature **425**: 926 - 933.

Dasen JS, Tice BC, Brenner-Morton S and Jessell TM (2005). "A Hox regulatory network establishes motor neuron pool identity and target-muscle connectivity." Cell **123**: 477 - 491.

Dawid IB, Breen JJ and Toyama R (1998). "LIM domains: multiple roles as adapters and functional modifiers in protein interactions." Trends Genet **14**(4): 156-62.

De Felipe C, Pinnock RD and Hunt SP (1995). "Modulation of chemotropism in the developing spinal cord by substance P." Science **267**(5199): 899-902.

Devoto SH, Melancon E, Eisen JS and Westerfield M (1996). "Identification of separate slow and fast muscle precursor cells in vivo, prior to somite formation." Development **122**(11): 3371-80.

Draper BW, Morcos PA and Kimmel CB (2001). "Inhibition of zebrafish fgf8 pre-mRNA splicing with morpholino oligos: a quantifiable method for gene knockdown." Genesis **30**(3): 154-6.

Eberhart J, Swartz ME, Koblar SA, Pasquale EB and Krull CE (2002). "EphA4 constitutes a population-specific guidance cue for motor neurons." Dev Biol **247**(1): 89-101.

Eisen JS (1999). "Patterning motoneurons in the vertebrate nervous system." Trends in Neurosciences **22**(7): 321-326.

Eisen JS and Melancon E (2001). "Interactions with identified muscle cells break motoneuron equivalence in embryonic zebrafish." Nat Neurosci **4**(11): 1065-1070.

Eisen JS, Myers PZ and Westerfield M (1986). "Pathway selection by growth cones of identified motoneurones in live zebra fish embryos." Nature **320**(6059): 269-71.

Eisen JS, Pike SH and Debu B (1989). "The growth cones of identified motoneurons in embryonic zebrafish select appropriate pathways in the absence of specific cellular interactions." Neuron **2**(1): 1097-1104.

Eisen JS, Pike SH and Romancier B (1990). "An identified motoneuron with variable

fates in embryonic zebrafish." J. Neurosci. **10**(1): 34-43.

Eisen JS and Smith JC (2008). "Controlling morpholino experiments: don't stop making antisense." Development **135**(10): 1735-1743.

Ekker SC (2008). "Zinc Finger-Based Knockout Punches for Zebrafish Genes." Zebrafish **5**(2): 121-123.

Enjin A, Rabe N, Nakanishi ST, Vallstedt A, Gezelius H, Memic F, Lind M, Hjalt T, Tourtellotte WG, Bruder C, Eichele G, Whelan PJ and Kullander K (2010). "Identification of novel spinal cholinergic genetic subtypes disclose Chodl and Pitx2 as markers for fast motor neurons and partition cells." The Journal of Comparative Neurology **518**(12): 2284-2304.

Enkhmandakh B, Makeyev AV and Bayarsaihan D (2006). "The role of the proline-rich domain of Ssdp1 in the modular architecture of the vertebrate head organizer." Proceedings of the National Academy of Sciences **103**(31): 11631-11636.

Fan L, Moon J, Wong TT, Crodian J and Collodi P (2008). "Zebrafish primordial germ cell cultures derived from vasa::RFP transgenic embryos." Stem Cells Dev **17**(3): 585-97.

Fashena D and Westerfield M (1999). "Secondary motoneuron axons localize DM-GRASP on their fasciculated segments." The Journal of Comparative Neurology **406**(3): 415-424.

Feldner J, Becker T, Goishi K, Schweitzer J, Lee P, Schachner M, Klagsbrun M and Becker CG (2005). "Neuropilin-1a is involved in trunk motor axon outgrowth in embryonic zebrafish." Dev Dyn **234**(3): 535-49.

Feldner J, Reimer MM, Schweitzer J, Wendik B, Meyer D, Becker T and Becker CG (2007). "PlexinA3 restricts spinal exit points and branching of trunk motor nerves in embryonic zebrafish." J Neurosci **27**(18): 4978-83.

Fetcho JR (2007). "The utility of zebrafish for studies of the comparative biology of motor systems." Journal of Experimental Zoology Part B: Molecular and Developmental Evolution **308B**(5): 550-562.

Fishman MC (2001). "Zebrafish--the Canonical Vertebrate." Science **294**(5545): 1290-1291.

Flanagan-Steet H, Fox MA, Meyer D and Sanes JR (2005). "Neuromuscular synapses can form in vivo by incorporation of initially aneural postsynaptic specializations." Development **132**(20): 4471-4481.

Fricke C, Lee JS, Geiger-Rudolph S, Bonhoeffer F and Chien CB (2001). "astray, a zebrafish roundabout homolog required for retinal axon guidance." Science **292**(5516): 507-10.

Fumio Nakamura RGKSMS (2000). "Molecular basis of semaphorin-mediated axon guidance." Journal of Neurobiology **44**(2): 219-229.

Funakoshi K, Kadota T, Atobe Y, Nakano M, Tsukagoshi M, Goris RC and Kishida R (2000). "Differential innervation of the goldfish tonic red muscles and twitch white muscles by neuropeptide-immunoreactive motoneurons." Brain Res Bull

52(6): 547-52.

Gimnopoulos D, Becker CG, Ostendorff HP, Bach I, Schachner M and Becker T (2002). "Expression of the zebrafish recognition molecule F3/F11/contactin in a subset of differentiating neurons is regulated by cofactors associated with LIM domains." Mech Dev **119 Suppl 1**: S135-41.

Gould TW and Oppenheim RW (2011). "Motor neuron trophic factors: Therapeutic use in ALS?" Brain Res Rev **67**(1-2): 1-39.

Gungor C, Taniguchi-Ishigaki N, Ma H, Drung A, Tursun B, Ostendorff HP, Bossenz M, Becker CG, Becker T and Bach I (2007). "Proteasomal selection of multiprotein complexes recruited by LIM homeodomain transcription factors." Proceedings of the National Academy of Sciences **104**(38): 15000-15005.

Guthrie S (2004). "Neuronal Development: Putting Motor Neurons in Their Place." Current Biology **14**(4): R166-R168.

Halloran MC, Sato-Maeda M, Warren JT, Su F, Lele Z, Krone PH, Kuwada JY and Shoji W (2000). "Laser-induced gene expression in specific cells of transgenic zebrafish." Development **127**(9): 1953-60.

Halpern ME, Rhee J, Goll MG, Akitake CM, Parsons M and Leach SD (2008). "Gal4/UAS Transgenic Tools and Their Application to Zebrafish." Zebrafish **5**(2): 97-110.

Hammond R, Vivancos V, Naeem A, Chilton J, Mambitisaeva E, Andrews W, Sundaresan V and Guthrie S (2005). "Slit-mediated repulsion is a key regulator of motor axon pathfinding in the hindbrain." Development **132**(20): 4483-4495.

Hao L, Burghes A and Beattie C (2011). "Generation and Characterization of a zebrafish model of SMA carrying the human SMN2 gene." Molecular Neurodegeneration **6**(1): 24.

Heitzler P, Vanolst L, Biryukova I and Ramain P (2003). "Enhancer-promoter communication mediated by Chip during Pannier-driven proneural patterning is regulated by Osa." Genes Dev **17**(5): 591-6.

Hilario JD, Wang C and Beattie CE (2010). "Collagen XIXa1 is crucial for motor axon navigation at intermediate targets." Development **137**(24): 4261-9.

Hiratani I, Yamamoto N, Mochizuki T, Ohmori S-y and Taira M (2003). "Selective degradation of excess Ldb1 by Rnf12/RLIM confers proper Ldb1 expression levels and Xlim-1/Ldb1 stoichiometry in Xenopus organizer functions." Development **130**(17): 4161-4175.

Hobert O and Westphal H (2000). "Functions of LIM-homeobox genes." Trends in Genetics **16**(2): 75-83.

Huber AB, Kania A, Tran TS, Gu C, De Marco Garcia N, Lieberam I, Johnson D, Jessell TM, Ginty DD and Kolodkin AL (2005). "Distinct Roles for Secreted Semaphorin Signaling in Spinal Motor Axon Guidance." Neuron **48**(6): 949-964.

Hutchinson SA, Cheesman SE, Hale LA, Boone JQ and Eisen JS (2007). "Nkx6

proteins specify one zebrafish primary motoneuron subtype by regulating late islet1 expression." Development **134**(9): 1671-7.

Hutchinson SA and Eisen JS (2006). "Islet1 and Islet2 have equivalent abilities to promote motoneuron formation and to specify motoneuron subtype identity." Development **133**(11): 2137-47.

Inoue A, Takahashi M, Hatta K, Hotta Y and Okamoto H (1994). "Developmental regulation of islet-1 mRNA expression during neuronal differentiation in embryonic zebrafish." Dev Dyn **199**: 1-11.

Jing L, Gordon LR, Shtibin E and Granato M (2010). "Temporal and Spatial Requirements of unplugged/MuSK Function during Zebrafish Neuromuscular Development." PLoS ONE **5**(1): e8843.

Johnsen SA, Gungor C, Prenzel T, Riethdorf S, Riethdorf L, Taniguchi-Ishigaki N, Rau T, Tursun B, Furlow JD, Sauter G, Scheffner M, Pantel K, Gannon F and Bach I (2009). "Regulation of estrogen-dependent transcription by the LIM cofactors CLIM and RLIM in breast cancer." Cancer Res **69**(1): 128-36.

Julia Feldner TBKGJSPLMSMKCGB (2005). "Neuropilin-1a is involved in trunk motor axon outgrowth in embryonic zebrafish." Developmental Dynamics **234**(3): 535-549.

Jurata LW and Gill GN (1997). "Functional analysis of the nuclear LIM domain interactor NLI." Mol. Cell. Biol. **17**: 5688-5698.

Jurata LW, Kenny DA and Gill GN (1996). "Nuclear LIM interactor, a rhombotin and LIM homeodomain interacting protein, is expressed early in neuronal development." Proc Natl Acad Sci U S A **93**(21): 11693-8.

Jurata LW, Thomas JB and Pfaff SL (2000). "Transcriptional mechanisms in the development of motor control." Current Opinion in Neurobiology **10**(1): 72-79.

Kane DA and Kimmel CB (1993). "The zebrafish midblastula transition." Development **119**(2): 447-456.

Kania A and Jessell TM (2003). "Topographic motor projections in the limb imposed by LIM homeodomain protein regulation of ephrin-A:EphA interactions." Neuron **38**: 581-596.

Kania A, Johnson RL and Jessell TM (2000). "Coordinate roles for LIM homeobox genes in directing the dorsoventral trajectory of motor axons in the vertebrate limb." Cell **102**: 161-173.

Key B and Devine CA (2003). "Zebrafish as an experimental model: strategies for developmental and molecular neurobiology studies." Methods Cell Sci **25**(1-2): 1-6.

Kikuchi Y, Segawa H, Tokumoto M, Tsubokawa T, Hotta Y, Uyemura K and Okamoto H (1997). "Ocular and Cerebellar Defects in Zebrafish Induced by Overexpression of the LIM Domains of the Islet-3 LIM/Homeodomain Protein." Neuron **18**(3): 369-382.

Kimmel CB, Ballard WW, Kimmel SR, Ullmann B and Schilling TF (1995). "Stages

of embryonic development of the zebrafish." Dev Dyn **203**(3): 253-310.

Kimmel CB, Warga RM and Kane DA (1994). "Cell cycles and clonal strings during formation of the zebrafish central nervous system." Development **120**(2): 265-276.

Kimmel CB and Westerfield M (1990). "Primary neurons of the zebrafish. ." In Signal and Sense, G.M. Edelman, W.E. Gall, and M.W. Cowan, eds. **New York: Wiley-Liss** 561-588.

Korn H and Faber DS (2005). "The Mauthner Cell Half a Century Later: A Neurobiological Model for Decision-Making?" Neuron **47**(1): 13-28.

Kos R, Reedy MV, Johnson RL and Erickson CA (2001). "The winged-helix transcription factor FoxD3 is important for establishing the neural crest lineage and repressing melanogenesis in avian embryos." Development **128**(8): 1467-1479.

Kudoh T, Wilson SW and Dawid IB (2002). "Distinct roles for Fgf, Wnt and retinoic acid in posteriorizing the neural ectoderm." Development **129**(18): 4335-46.

Kulkarni G, Li H and Wadsworth WG (2008). "CLEC-38, a transmembrane protein with C-type lectin-like domains, negatively regulates UNC-40-mediated axon outgrowth and promotes presynaptic development in Caenorhabditis elegans." J Neurosci **28**(17): 4541-50.

Kummer TT, Misgeld T and Sanes JR (2006). "Assembly of the postsynaptic membrane at the neuromuscular junction: paradigm lost." Curr Opin Neurobiol **16**(1): 74-82.

Lee KJ and Jessell TM (1999). "The specification of dorsal cell fates in the vertebrate central nervous system." Annu Rev Neurosci **22**: 261-94.

Lee S-K, Jurata LW, Funahashi J, Ruiz EC and Pfaff SL (2004). "Analysis of embryonic motoneuron gene regulation: derepression of general activators function in concert with enhancer factors." Development **131**(14): 3295-3306.

Lee S-K, Lee B, Ruiz EC and Pfaff SL (2005). "Olig2 and Ngn2 function in opposition to modulate gene expression in motor neuron progenitor cells." Genes & Development **19**(2): 282-294.

Lee S-K and Pfaff SL (2001). "Transcriptional networks regulating neuronal identity in the developing spinal cord." Nat Neurosci(4): 1183-1191.

Lee S-K and Pfaff SL (2003). "Synchronization of Neurogenesis and Motor Neuron Specification by Direct Coupling of bHLH and Homeodomain Transcription Factors." Neuron **38**(5): 731-745.

Lee S, Lee B, Joshi K, Pfaff SL, Lee JW and Lee SK (2008). "A regulatory network to segregate the identity of neuronal subtypes." Dev Cell. 2008 Jun;14(6):877-89.

Lewis K.E. EJS (2003). "From cells to circuits: development of the zebrafish spinal cord." Progress in Neurobiology **69**: 419-449.

Liang X, Song MR, Xu Z, Lanuza GM, Liu Y, Zhuang T, Chen Y, Pfaff SL, Evans SM and Sun Y (2011). "Isl1 is required for multiple aspects of motor neuron

development." Mol Cell Neurosci **47**(3): 215-22.

Lim AH, Suli A, Yaniv K, Weinstein B, Li DY and Chien CB (2011). "Motoneurons are essential for vascular pathfinding." Development **138**(17): 3847-57.

Litingtung Y and Chiang C (2000). "Specification of ventral neuron types is mediated by an antagonistic interaction between Shh and Gli3." Nat. Neurosci. **3**: 979-985.

Liu DW and Westerfield M (1988). "Function of identified motoneurones and co-ordination of primary and secondary motor systems during zebra fish swimming." The Journal of Physiology **403**(1): 73-89.

Liu H, Shafey D, Moores JN and Kothary R (2010). "Neurodevelopmental consequences of Smn depletion in a mouse model of spinal muscular atrophy." J Neurosci Res **88**(1): 111-22.

Lu JT, Son YJ, Lee J, Jetton TL, Shiota M, Moscoso L, Niswender KD, Loewy AD, Magnuson MA, Sanes JR and Emeson RB (1999). "Mice lacking alpha-calcitonin gene-related peptide exhibit normal cardiovascular regulation and neuromuscular development." Mol Cell Neurosci **14**(2): 99-120.

Lundell A, Olin AI, Morgelin M, al-Karadaghi S, Aspberg A and Logan DT (2004). "Structural basis for interactions between tenascins and lectican C-type lectin domains: evidence for a crosslinking role for tenascins." Structure **12**(8): 1495-506.

Luria V, Krawchuk D, Jessell TM, Laufer E and Kania A (2008). "Specification of Motor Axon Trajectory by Ephrin-B:EphB Signaling: Symmetrical Control of Axonal Patterning in the Developing Limb." Neuron **60**(6): 1039-1053.

Maggi CA, Catalioto RM, Criscuoli M, Cucchi P, Giuliani S, Lecci A, Lippi A, Meini S, Patacchini R, Renzetti AR, Santicioli P, Tramontana M, Zagorodnyuk V and Giachetti A (1997). "Tachykinin receptors and intestinal motility." Can J Physiol Pharmacol **75**(6): 696-703.

Mason I (2007). "Initiation to end point: the multiple roles of fibroblast growth factors in neural development." Nat Rev Neurosci **8**(8): 583-96.

McCallum CM, Comai L, Greene EA and Henikoff S (2000). "Targeting Induced LocalLesions IN Genomes (TILLING) for Plant Functional Genomics." Plant Physiology **123**(2): 439-442.

McWhorter ML, Monani UR, Burghes AH and Beattie CE (2003a). "Knockdown of the survival motor neuron (Smn) protein in zebrafish causes defects in motor axon outgrowth and pathfinding." J Cell Biol **162**(5): 919-31.

McWhorter ML, Monani UR, Burghes AHM and Beattie CE (2003b). "Knockdown of the survival motor neuron (Smn) protein in zebrafish causes defects in motor axon outgrowth and pathfinding." Journal of Cell Biology **162**(5): 919-31.

Melancon E, Liu DWC, Westerfield M and Eisen JS (1997). "Pathfinding by Identified Zebrafish Motoneurons in the Absence of Muscle Pioneers." Journal of Neuroscience **17**(20): 7796-7804.

Melton KR, Iulianella A and Trainor PA (2004). "Gene expression and regulation of hindbrain and spinal cord development." Front Biosci **9**: 117-38.

Metcalfe WK, Myers PZ, Trevarrow B, Bass MB and Kimmel CB (1990). "Primary neurons that express the L2/HNK-1 carbohydrate during early development in the zebrafish." Development **110**(2): 491-504.

Milan M, Diaz-Benjumea FJ and Cohen SM (1998). "Beadex encodes an LMO protein that regulates Apterous LIM-homeodomain activity in Drosophila wing development: a model for LMO oncogene function." Genes & Development **12**(18): 2912-2920.

Mizuguchi R (2001). "Combinatorial roles of olig2 and neurogenin2 in the coordinated induction of pan-neuronal and subtype-specific properties of motoneurons." Neuron **31**: 757-771.

Mukhopadhyay M, Teufel A, Yamashita T, Agulnick AD, Chen L, Downs KM, Schindler A, Grinberg A, Huang SP, Dorward D and Westphal H (2003). "Functional ablation of the mouse Ldb1 gene results in severe patterning defects during gastrulation." Development **130**(3): 495-505.

Murray A, Naeem A, Barnes S, Drescher U and Guthrie S (2010). "Slit and Netrin-1 guide cranial motor axon pathfinding via Rho-kinase, myosin light chain kinase and myosin II." Neural Development **5**(1): 16.

Myers PZ, Eisen JS and Westerfield M (1986). "Development and axonal outgrowth of identified motoneurons in the zebrafish." J. Neurosci. **6**(8): 2278-2289.

Nakano T, Windrem M, Zappavigna V and Goldman SA (2005). "Identification of a conserved 125 base-pair Hb9 enhancer that specifies gene expression to spinal motor neurons." Developmental Biology **283**(2): 474-485.

Nishioka N, Nagano S, Nakayama R, Kiyonari H, Ijiri T, Taniguchi K, Shawlot W, Hayashizaki Y, Westphal H, Behringer RR, Matsuda Y, Sakoda S, Kondoh H and Sasaki H (2005). "Ssdp1 regulates head morphogenesis of mouse embryos by activating the Lim1-Ldb1 complex." Development **132**(11): 2535-2546.

Novitch BG, Chen AI and Jessell TM (2001). "Coordinate regulation of motor neuron subtype identity and pan-neuronal properties by the bHLH repressor Olig2." Neuron **31**: 773-789.

Nutt SL, Bronchain OJ, Hartley KO and Amaya E (2001). "Comparison of morpholino based translational inhibition during the development of Xenopus laevis and Xenopus tropicalis." Genesis **30**(3): 110-113.

Oates AC, Bruce AEE and Ho RK (2000). "Too Much Interference: Injection of Double-Stranded RNA Has Nonspecific Effects in the Zebrafish Embryo." Developmental Biology **224**(1): 20-28.

Ott H, Diekmann H, Stuermer CAO and Bastmeyer M (2001). "Function of Neurolin (DM-GRASP/SC-1) in Guidance of Motor Axons during Zebrafish Development." Developmental Biology **235**(1): 86-97.

Palaisa KA and Granato M (2007). "Analysis of zebrafish sidetracked mutants reveals a novel role for Plexin A3 in intraspinal motor axon guidance." Development

134(18): 3251-7.

Park H-C, Mehta A, Richardson JS and Appel B (2002). "olig2 Is Required for Zebrafish Primary Motor Neuron and Oligodendrocyte Development." Developmental Biology **248**(2): 356-368.

Park H-C, Shin J and Appel B (2004). "Spatial and temporal regulation of ventral spinal cord precursor specification by Hedgehog signaling." Development **131**(23): 5959-5969.

Persson M, Stamataki D, te Welscher P, Andersson E, Bose J, Ruther U, Ericson J and Briscoe J (2002). "Dorsal-ventral patterning of the spinal cord requires Gli3 transcriptional repressor activity." Genes Dev **16**(22): 2865-78.

Pfaff SL, Mendelsohn M, Stewart CL, Edlund T and Jessell TM (1996). "Requirement for LIM homeobox gene Isl1 in motor neuron generation reveals a motor neuron-dependent step in interneuron differentiation." Cell **84**: 309 - 320.

Placzek M, Yamada T, Tessier-Lavigne M, Jessell T and Dodd J (1991). "Control of dorsoventral pattern in vertebrate neural development: induction and polarizing properties of the floor plate." Development **Suppl 2**: 105-22.

Ramesh T, Lyon AN, Pineda RH, Wang C, Janssen PML, Canan BD, Burghes AHM and Beattie CE (2010). "A genetic model of amyotrophic lateral sclerosis in zebrafish displays phenotypic hallmarks of motoneuron disease." Disease Models & Mechanisms **3**(9-10): 652-662.

Reimer MM, Sorensen I, Kuscha V, Frank RE, Liu C, Becker CG and Becker T (2008). "Motor Neuron Regeneration in Adult Zebrafish." The Journal of Neuroscience **28**(34): 8510-8516.

Retaux S and Bachy I (2002). "A short history of LIM domains (1993-2002): from protein interaction to degradation." Mol Neurobiol **26**(2-3): 269-81.

Rodino-Klapac LR and Beattie CE (2004). "Zebrafish topped is required for ventral motor axon guidance." Developmental Biology **273**(2): 308-320.

Roos M, Schachner M and Bernhardt RR (1999). "Zebrafish semaphorin Z1b inhibits growing motor axons in vivo." Mech Dev **87**(1-2): 103-17.

Rossoll W, Jablonka S, Andreassi C, Kroning AK, Karle K, Monani UR and Sendtner M (2003). "Smn, the spinal muscular atrophy-determining gene product, modulates axon growth and localization of beta-actin mRNA in growth cones of motoneurons." J Cell Biol **163**(4): 801-12.

Roztocil T, Matter-Sadzinski L, Alliod C, Ballivet M and Matter JM (1997). "NeuroM, a neural helix-loop-helix transcription factor, defines a new transition stage in neurogenesis." Development **124**(17): 3263-3272.

Sager J, Bai Q and Burton E (2010). "Transgenic zebrafish models of neurodegenerative diseases." Brain Structure and Function **214**(2): 285-302.

Sander M (2000). "Ventral neural patterning by Nkx homeobox genes: Nkx6.1 controls somatic motor neuron and ventral interneuron fates." Genes Dev. **14**: 2134-2139.

Scardigli R, Baumer N, Gruss P, Guillemot F and Le Roux I (2003). "Direct and concentration-dependent regulation of the proneural gene Neurogenin2 by Pax6." Development **130**(14): 3269-3281.

Schmidt ERE, Pasterkamp RJ and van den Berg LH (2009). "Axon guidance proteins: Novel therapeutic targets for ALS?" Progress in Neurobiology **88**(4): 286-301.

Schneider VA and Granato M (2006). "The Myotomal diwanka (lh3) Glycosyltransferase and Type XVIII Collagen Are Critical for Motor Growth Cone Migration." Neuron **50**(5): 683-695.

Schweitzer J, Becker T, Lefebvre J, Granato M, Schachner M and Becker CG (2005). "Tenascin-C is involved in motor axon outgrowth in the trunk of developing zebrafish." Dev Dyn **234**(3): 550-66.

Segawa H, Miyashita T, Hirate Y, Higashijima S-i, Chino N, Uyemura K, Kikuchi Y and Okamoto H (2001). "Functional Repression of Islet-2 by Disruption of Complex with Ldb Impairs Peripheral Axonal Outgrowth in Embryonic Zebrafish." Neuron **30**(2): 423-436.

Sharma K (1998). "LIM homeodomain factors Lhx3 and Lhx4 assign subtype identities for motor neurons." Cell **95**: 817-828.

Sharma K, Leonard AE, Lettieri K and Pfaff SL (2000). "Genetic and epigenetic mechanisms contribute to motor neuron pathfinding." Nature **406**: 515-519.

Shirasaki R and Pfaff SL (2002). "Transcriptional codes and the control of neuronal identity." Annu Rev Neurosci **25**: 251 - 281.

Sockanathan S (2003). "Towards cracking the code: LIM protein complexes in the spinal cord." Trends in Neurosciences **26**(2): 57-59.

Sommer L, Ma Q and Anderson DJ (1996). "neurogenins,a Novel Family ofatonal-Related bHLH Transcription Factors, Are Putative Mammalian Neuronal Determination Genes That Reveal Progenitor Cell Heterogeneity in the Developing CNS and PNS." Molecular and Cellular Neuroscience **8**(4): 221-241.

Stuermer CA and Bastmeyer M (2000). "The retinal axon's pathfinding to the optic disk." Prog Neurobiol **62**(2): 197-214.

Summerton J (1999). "Morpholino antisense oligomers: the case for an RNase H-independent structural type." Biochim Biophys Acta **1489**(1): 141-58.

Takizawa F, Araki K, Ito K, Moritomo T and Nakanishi T (2007). "Expression analysis of two Eomesodermin homologues in zebrafish lymphoid tissues and cells." Mol Immunol **44**(9): 2324-31.

Tanabe Y and Jessell TM (1996). "Diversity and pattern in the developing spinal cord." Science **274**: 1115-1122.

Tanaka H, Maeda R, Shoji W, Wada H, Masai I, Shiraki T, Kobayashi M, Nakayama R and Okamoto H (2007). "Novel mutations affecting axon guidance in zebrafish and a role for plexin signalling in the guidance of trigeminal and facial nerve axons." Development **134**(18): 3259-69.

Tanaka H, Nojima Y, Shoji W, Sato M, Nakayama R, Ohshima T and Okamoto H

(2011). "Islet1 selectively promotes peripheral axon outgrowth in Rohon-Beard primary sensory neurons." Developmental Dynamics **240**(1): 9-22.

Thaler J (1999). "Active suppression of interneuron programs within developing motor neurons revealed by analysis of homeodomain factor HB9." Neuron **23**: 675-687.

Thaler JP, Lee S-K, Jurata LW, Gill GN and Pfaff SL (2002). "LIM Factor Lhx3 Contributes to the Specification of Motor Neuron and Interneuron Identity through Cell-Type-Specific Protein-Protein Interactions." Cell **110**(2): 237-249.

Thor S, Andersson SGE, Tomlinson A and Thomas JB (1999). "A LIM-homeodomain combinatorial code for motor-neuron pathway selection." Nature **397**(6714): 76-80.

Thor S and Thomas JB (1997). "The Drosophila islet gene governs axon pathfinding and neurotransmitter identity." Neuron **18**: 397 - 409.

Tokumoto M, Gong Z, Tsubokawa T, Hew CL, Uyemura K, Hotta Y and Okamoto H (1995). "Molecular Heterogeneity among Primary Motoneurons and within Myotomes Revealed by the Differential mRNA Expression of Novel Islet-1 Homologs in Embryonic Zebrafish." Developmental Biology **171**(2): 578-589.

Torigoi E, Bennani-Baiti IM, Rosen C, Gonzalez K, Morcillo P, Ptashne M and Dorsett D (2000). "Chip interacts with diverse homeodomain proteins and potentiates bicoid activity in vivo." Proc Natl Acad Sci U S A **97**(6): 2686-91.

Tsuchida T (1994). "Topographic organization of embryonic motor neurons defined by expression of LIM homeobox genes." Cell **79**: 957-970.

Tsuchida T, Ensini M, Morton SB, Baldassare M, Edlund T, Jessell TM and Pfaff SL (1994). "Topographic organization of embryonic motor neurons defined by expression of LIM homeobox genes." Cell **79**(6): 957-70.

Urasaki A, Asakawa K and Kawakami K (2008). "Efficient transposition of the Tol2 transposable element from a single-copy donor in zebrafish." Proceedings of the National Academy of Sciences **105**(50): 19827-19832.

Vallstedt A (2001). "Different levels of repressor activity assign redundant and specific roles to nkx6 genes in motor neuron and interneuron specification." Neuron **31**: 743-755.

van Meyel DJ, Thomas JB and Agulnick AD (2003). "Ssdp proteins bind to LIM-interacting co-factors and regulate the activity of LIM-homeodomain protein complexes in vivo." Development **130**(9): 1915-1925.

Vock VM, Ponomareva ON and Rimer M (2008). "Evidence for muscle-dependent neuromuscular synaptic site determination in mammals." J Neurosci **28**(12): 3123-30.

Wang Y, Klumpp S, Amin HM, Liang H, Li J, Estrov Z, Zweidler-McKay P, Brandt SJ, Agulnick A and Nagarajan L (2010). "SSBP2 is an in vivo tumor suppressor and regulator of LDB1 stability." Oncogene **29**(21): 3044-53.

Wienholds E, van Eeden F, Kosters M, Mudde J, Plasterk RHA and Cuppen E (2003). "Efficient Target-Selected Mutagenesis in Zebrafish." Genome Research **13**(12): 2700-2707.

Wijgerde M, McMahon JA, Rule M and McMahon AP (2002). "A direct requirement for Hedgehog signaling for normal specification of all ventral progenitor domains in the presumptive mammalian spinal cord." Genes Dev **16**(22): 2849-64.

Williams JA, Barrios A, Gatchalian C, Rubin L, Wilson SW and Holder N (2000). "Programmed Cell Death in Zebrafish Rohon Beard Neurons Is Influenced by TrkC1/NT-3 Signaling." Developmental Biology **226**(2): 220-230.

Windle JJ, Weiner RI and Mellon PL (1990). "Cell lines of the pituitary gonadotrope lineage derived by targeted oncogenesis in transgenic mice." Mol Endocrinol **4**(4): 597-603.

Wolpert L (1996). "One hundred years of positional information." Trends Genet **12**(9): 359-64.

Wu L (2006). "Structure and functional characterization of single-strand DNA binding protein SSDP1: Carboxyl-terminal of SSDP1 has transcription activity." Biochemical and Biophysical Research Communications **339**(3): 977-984.

Xu Z, Meng X, Cai Y, Liang H, Nagarajan L and Brandt SJ (2007). "Single-stranded DNA-binding proteins regulate the abundance of LIM domain and LIM domain-binding proteins." Genes Dev. **21**(8): 942-955.

Yaden BC, Savage JJ, Hunter CS and Rhodes SJ (2005). "DNA recognition properties of the LHX3b LIM homeodomain transcription factor." Molecular Biology Reports **32**(1): 1-6.

Yeo S-Y, Miyashita T, Fricke C, Little MH, Yamada T, Kuwada JY, Huh T-L, Chien C-B and Okamoto H (2004). "Involvement of Islet-2 in the Slit signaling for axonal branching and defasciculation of the sensory neurons in embryonic zebrafish." Mechanisms of Development **121**(4): 315-324.

Zeller J and Granato M (1999). "The zebrafish diwanka gene controls an early step of motor growth cone migration." Development **126**: 3461-3472.

Zenvirt S, Nevo-Caspi Y, Rencus-Lazar S and Segal D (2008). "Drosophila LIM-Only Is a Positive Regulator of Transcription During Thoracic Bristle Development." Genetics **179**(4): 1989-1999.

Zhang J and Granato M (2000). "The zebrafish unplugged gene controls motor axon pathway selection." Development **127**: 2099-2111.

Zhang J, Lefebvre JL, Zhao S and Granato M (2004). "Zebrafish unplugged reveals a role for muscle-specific kinase homologs in axonal pathway choice." Nat Neurosci **7**(12): 1303-1309.

Zhang J, Malayaman S, Davis C and Granato M (2001). "A dual role for the zebrafish unplugged gene in motor axon pathfinding and pharyngeal development." Dev. Biol. **240**: 560-573.

Zhang Z, Lotti F, Dittmar K, Younis I, Wan L, Kasim M and Dreyfuss G (2008). "SMN deficiency causes tissue-specific perturbations in the repertoire of snRNAs and widespread defects in splicing." Cell **133**(4): 585-600.

Zhong Z, Ma H, Taniguchi-Ishigaki N, Nagarajan L, Becker CG, Bach I and Becker T (2011). "SSDP cofactors regulate neural patterning and differentiation of specific axonal projections." Developmental Biology **349**(2): 213-224.

Zon LI and Peterson RT (2005). "In vivo drug discovery in the zebrafish." Nat Rev Drug Discov **4**(1): 35-44.

Zou Y, Stoeckli E, Chen H and Tessier-Lavigne M (2000). "Squeezing Axons Out of the Gray Matter: A Role for Slit and Semaphorin Proteins from Midline and Ventral Spinal Cord." Cell **102**(3): 363-375.

Acknowledgements

I would like to begin by thanking my referee Dr. Qilong Ying as well as Prof. Stephen Hillier and Prof. Jeremy Bradshaw, who opened the door towards my PhD journey at my PhD interview.

I would like to thank my supervisor Dr. Catherina G Becker for allowing me the opportunity to pursue this scientific endeavor. She is not only my PhD supervisor, but also a great mentor for daily life. During the last four years, she has taught me how to have a great attitude in scientific work as well as in other walks of life. Her passion and optimism always inspired me to work to my full potential. She led by example, and gave me the confidence to expand my boundaries and to be the best that I can be.

I would also like to show my gratitude to my supervisor Dr. Thomas Becker. He has guided me through the highs and lows of academic research during my projects. I enjoyed the times when I discussed my work with him, not only because of his sense of humour but also because of his scientific outlook when analysing data, resolving problems as well as presenting results.

I would like to thank my PhD committee (Prof. Peter Brophy, Prof. Andrew Jarman and Dr. John Mason) for their patience and advice. They always managed to suggest good solutions to address my issues. Special thanks are also warranted for my co-authors of my published paper (Hong Ma, Naoko Taniguchi-Ishigaki, Lalitha Nagarajan, and Ingolf Bach).

I am indebted to all my colleagues that supported me whenever I need help. To Michell M. Reimer and Cameron Wyatt, many thanks are warranted for their guidance when I was just starting my PhD. Tatyana B. Dias and Veronika Kuscha, you both are my most important companions as you were always understanding and supportive in every situation during my PhD study. To our post-doc Angela L. Scott, I add special thanks here for her endless encouragement in pursuit of excellence. I

appreciate her contribution to lab management and environment building, which made lab work systematic and orderly. I have had the happiest hours with Anneliese Norris together, which dispelled my pressure and refilled me with energy to begin one task after another. Thanks to Jochen Ohnmacht and Jolanda Münzel for their support in molecular biology techniques and Western-blots, respectively. I am also indebted to Sudeh Riahi and Maria Rubio for their excellent fish care. I would also like to thank Jan Soetaert and Trudi Gillespie for their help in confocal facility and thank Jon Moulton for his replying to my morpholino technology questions.

I would like to thank all my Chinese friends in UK. Especially thanks to Dorothy Tse for her sweetest friendship and strongest support. This thesis would not have been possible without Lee Tan's advice in molecular cloning and Wenqi Yu's proofreading. I owe my deep gratitude to Jian Yang for his everlasting patience, repeated encouragement, and unwavering support.

Finally, I would like to finish by showing my deepest thanks to my family. Their pride in what I have achieved encouraged me to continue my pursuit with persistence. Their respect made me follow my own heart in each crossing of life with confidence. Their worry also let me realize that I will bear more responsibility in the future.